WASHINGTON UNIVERSITY

SEVER INSTITUTE OF TECHNOLOGY

EFFICIENCY OF STATIC MIXERS AS GAS / LIQUID CONTACTORS

by

JOHN W. WESTON

Prepared under the direction of Professor M. Dudukovic

A thesis presented to the Sever Institute of Washington University in partial fulfillment of the requirements for the degree of

MASTER OF SCIENCE

May, 1982

Saint Louis, Missouri

WASHINGTON UNIVERSITY
SEVER INSTITUTE OF TECHNOLOGY

ABSTRACT

EFFICIENCY OF STATIC MIXERS AS GAS / LIQUID CONTACTORS

by JOHN W. WESTON

ADVISOR: Professor M. Dudukovic

May, 1982

Saint Louis, Missouri

Gas-liquid interfacial areas and liquid side mass transfer coefficients were measured in three types of static mixers. Carbon dioxide absorption catalyzed by arsenite was used as a test reaction. The liquid and gas velocities were varied from 0.19 m/s to 0.63 m/s and from 0.07 m/s to 0.32 m/s, respectively. Holdup and pressure drops were also determined and correlated.

The mass transfer coefficient was constant at 1.84×10^{-4} m/s. The Koch CY mixer was superior to the Kenics and Ross LLPD mixers and competitive with traditional two phase contactors in producing interfacial area per unit dissipated power.

TABLE OF CONTENTS

LIST OF TABLES

LIST OF FIGURES

EFFICIENCY OF STATIC MIXERS AS GAS / LIQUID CONTACTORS

1. INTRODUCTION

1.1 GENERAL

Static mixers are stationary baffle-like units which effect the mixing of flowing materials with the aid of the fluid's own kinetic energy. These mixers are not an innovation but are simply a practical engineering design that has worked in many mixing situations and are now becoming a technology. Today, there are many companies which are producing different types of static mixers and providing technical literature.

The advantages which these static mixers boast over dynamic mixers are the following:

1) Narrow residence time distribution;

2) Use of a wide range of viscosities (gases to highly viscous polymer melts) as well as use for varied continuous to dispersed phase viscosity ratios from 10^{-2} to 10^{6});

3) Ready adaptation to existing pipe systems;

4) Smaller space requirements;

5) Negligible maintainance and wear, due to the absence of moving parts;

6) Low capital investments, operating costs and energy requirements;

7) Availability in many types of materials from aluminum to teflon.

They also have shown the ability to be used in industry for a multitude of applications. The main mixing applications include blending, dispersion and homogenization. The following section describes these applications and cites specific examples.

1.1.1 Industrial Applications of Static Mixers.

Blending is the process of mixing two soluble fluids together. This includes gas/gas blending, liquid/liquid blending, and solid/solid blending. Companies are using static mixers to:

1) Dilute 50% caustic solution by blending with water;

2) Blend various gasoline stocks as well as different lubricating oils in the petroleum industry;

3) Blend fertilizers, cement, and feed grains.

The unique advantages of static mixers in blending were demonstrated by a plant in France which had to blend three hot and explosive gases (1)*. The solution was a 16 inch

* The numbers in parentheses in the text indicate references in the Bibliography.

diameter, 15 foot long static mixer. They achieved a uniform temperature and composition with the following advantages:

1) Elimination of leak hazard with explosive gases;

2) No explosion risk due to hot spots generated by by moving parts;

3) No moving parts, hence no part replacement;

4) No external power other than gas pressure; and

5) Reduced space requirements.

Dispersions occur when two immiscible fluids are combined and droplets, bubbles or particles of one phase are formed within the other continuous phase, where the two phases could be gas/liquid, liquid/liquid, solid/liquid. Some examples of this application include:

1) Soapstock acidulation for the production of high quality fatty acids by dispersing H_2SO_4 in soapstock;

2) Dispersion of CO_2 into soft drinks; and

3) Elimination of Na_2SO_3 by dispersing oxygen into the mainstream to produce Na_2SO_4.

A subcase of dispersions is the application of static mixers for high viscosity polymer melts intended for fiber, film or bulk plastic production. Some examples include:

1) Dispersion of immiscible droplets of anti-static or anti-soiling agents of much lower viscosity;

2) Break up and dispersion of unwanted immiscible gel structures of high viscosity polymers resulting from cross-linking or polymer degradation;

3) Blending of immiscible polymer systems to form controlled two phase structures of unique physical, optical or electrical properties.

The last major application is homogenization. Homogenization of polymers to eliminate radial temperature profiles is important for processing, spinning and extruding. This application is also important for the proper thermal control for many reactions. Fluids which have a tendency to separate in transfer lines before they are processed or before sampling by an on-line instrument can be homogenized by static mixers. Since the homogenization occurs in the radial direction the fluid flow approaches ideal plug flow which is also valuable for many reactions in which the desired product is an intermediate.

These are the basic uses for static mixers. There are many other more imaginative applications in the literature such as catalyst support or as a pressure reducing device to throttle superheated steam to a precise temperature and pressure (as opposed to a simple throttling valve that wears out after use). It is apparent from this brief list that the applications of static mixers are numerous and that the differences in fluid properties cover an extremely wide range.

This laboratory was particularly interested in the use of static mixers as a gas/liquid reactor. The benefits of plug flow charateristics, easier thermal control for the reactor and a design that permits easier scale up made the

idea of static mixers as chemical reactors appealing. However, there are over 20 types of static mixers currently available each with their own distinct designs. Moreover, it is not known which is the optimal design. The next section briefly describes the three static mixer designs that were studied by this laboratory.

1.1.2 Static Mixer Designs

This study was only involved with three different static mixer designs from the following three companies:

1) Charles Ross and Son Co. (Ross LLPD mixer)

2) Chemineer/Kenics (Kenics mixer)

3) Koch Engineer Co. (Koch CY mixer)

The Ross LLPD Mixer is constructed of semi-elliptical panels. Two panels are connected together in the middle at a 120° angle and this is called one element (Figure 1). Each element is fitted in a pipe with each neighboring element reversed and rotated 90° along the linear axis.

The Kenics Mixer is constructed of a series of 180° twisted helical elements (Figure 2), alternating right hand twist and left hand twist, enclosed in a tube with each element rotated 90° relative to its neighbor. The interesting feature of this mixer is the radial mixing caused by the twist of each element. The flow in each channel circulates around its own hydraulic center causing radial mixing. Since for each element the rotation is in the opposite direction than in the previous element the shear forces at the interface of the two becomes great.

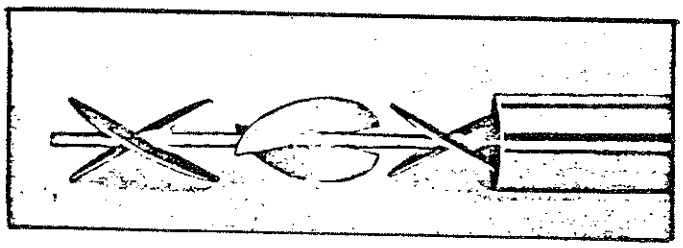

Figure 1. The LLPD Ross Mixer

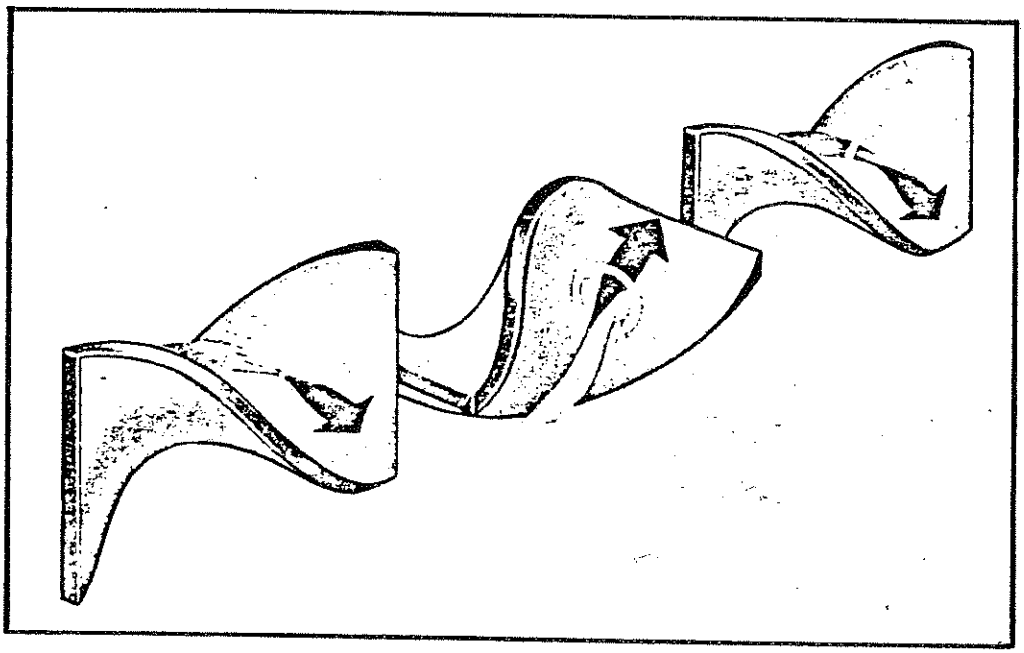

Figure 2. The Kenics Mixer

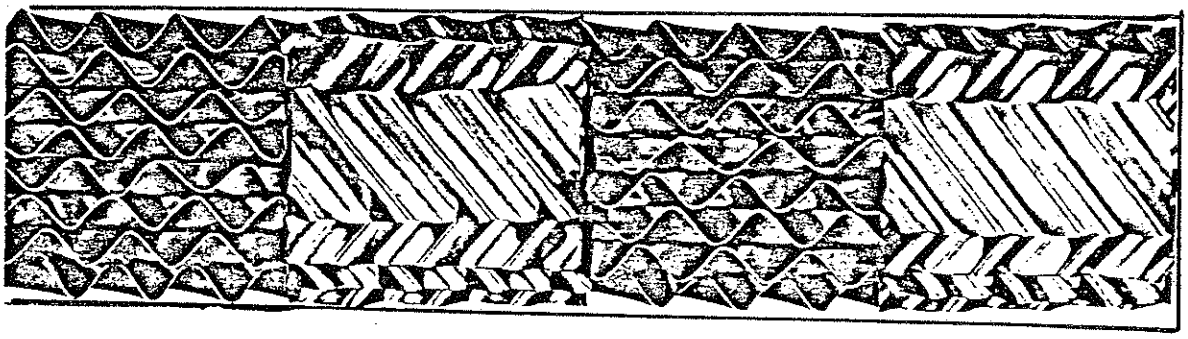

Figure 3. The Koch Mixer

The Koch Mixer is constructed of corrugated panels with the corrugations at a 45° angle to the linear axis. Separate panels, all one diameter long, are welded together lengthwise, with each panel having the corrugations running in a perpendicular direction to its neighbor (Figure 3). This set of panels, defined as one element, cause a two dimensional mixing pattern. Successive elements are rotated 90° forming one long unit as well as a third mixing dimension. The CY mixer is the second most compact type made by Koch. Each corrugation layer is 1/8 inch thick. The mixer has a hydraulic diameter of 0.15 inches and a void fraction of 0.72.

The Koch mixer comes in several sizes besides the CY mixer. The Koch AY mixer, which is most often studied in the literature, has corrugation layers that are 1/2 inch thick. This mixer has a hydraulic diameter of 0.66 inches and a void fraction of 0.92.

1.2 RESEARCH OBJECTIVES AND SCOPE

The primary goal of this study was to evaluate the efficiency of static mixers as gas/liquid contactors. Their efficiency will be defined by the amount of surface area per unit reaction volume per power input necessary to create this surface area. By using this definition comparisons between three different brands of static mixers at various flow conditions as well as other conventional gas/liquid contactors can be made. Another goal was to evaluate the static mixers' efficiency in eliminating the resistance to mass transfer in the liquid phase through the simultaneous evaluation of the liquid mass transfer coefficient.

The general objectives of this study were

1) To experimentally determine liquid holdup and total pressure drop at various liquid and gas flowrates for three different vertical static mixers.

2) To experimentally determine simultaneous values for interfacial area per unit liquid volume, a (m^2/m^3), and the liquid side mass transfer coefficient, k_L (m/s), at various gas and liquid flowrates for the same three static mixers.

3) To compare the experimental efficiencies of the three static mixers to each other and to the efficiencies of other conventional gas/liquid contactors extracted from the literature.

1.3 LITERATURE SURVEY

The literature is fairly scarce on gas/liquid contacting in static mixers and especially on the measurement

of interfacial area in static mixers. Up to now most of the research has been concerned mainly with measuring pressure drops, residence times, and holdup for gas/liquid systems (2, 3, 4, 5). The Kenics Company (6) has done some studies on gas dispersion and bubble sizes with the use of photographic techniques and found that the data can be correlated with the following equation for the Kenics Mixer:

$$\frac{d_B}{d} = 0.39\ We^{-0.43} \qquad (1)$$

where d_B = Sauter mean drop size, (m);

d = Inside diameter of the mixer, (m);

We = Weber number.

F. Strieff (7) published a study in the Sulzer Technical Review in which he reported a similar drop size correlation for Sulzer (Koch) mixers in a horizontal pipe:

$$\frac{d_B}{d_h} = 0.21\ We^{-0.50}\ Re^{0.15} \qquad (2)$$

where d_h = Mixing element hydraulic diameter, (m);

We = Weber No. = $\rho_L V_L^2 d_h / \sigma$

Re = Reynolds No. = $\rho_L V_L d_h / \mu_L$

ρ_L = Density of the liquid phase, (kg/m^3);

V_L = Liquid phase superficial velocity, (m/s);

σ = Surface tension, (N/m);

μ_L = Liquid viscosity, (Pa·s).

This result was based on the measurement of drop size by photographic methods for different liquid/liquid systems and

one gas/liquid system.

Although no work has been done to evaluate surface area in static mixers, there have been some studies of the overall mass transfer coefficients in static mixers. In 1977, K. B. Wang and L. T. Fan published a paper in Chemical Engineering Science in which they measured the volumetric liquid mass transfer coefficient, ($k_L a$), for the absorption of pure oxygen into water in a bubble column packed with Koch AY mixers (8). They presented how $k_L a$ and gas holdup, ϵ, were affected by superficial gas and liquid velocity and also the affect of adding spacers in between the Koch mixers in the column. The spacers had a negligible affect and representative correlations for $k_L a$ and ϵ are as follows:

$$k_L a = 4.35 \times 10^{-3} V_L^{0.631} V_g^{0.589} \quad (3)$$

$$\epsilon = 5.16 \times 10^{-2} V_L^{-0.102} V_g^{0.588} \quad (4)$$

where V_L and V_G have units cm/s.
Their results also showed a significant increase in $k_L a$ with the mixers as opposed to without the mixers.

J. C. Middleton is currently conducting studies of liquid mass transfer coefficients in an oxygen/water system for several static mixers, including Kenics and Sulzer mixers (3). His preliminary results suggest that all static mixers as well as some other conventional gas/liquid

contactors can be correlated by one single correlation given below:

$$k_L a = 1.74 \times 10^{-4} \left(\frac{E}{V_R}\right)^{0.8} \quad (5)$$

where E/V_R (W/m^3) is the rate of energy dissapation per unit mixer volume. The final results are yet unpublished.

A recent report by Holmes and Chen of the Koch Engineering Company based on data obtained from oxygen absorption in water experiments in a horizontal pipe filled with AY Koch mixers presented a method to predict mass transfer coefficients, $k_L a$, in such systems (9).

These equations, their sources and the conditions from which they were derived are given in Table 1. This concludes the literature survey related to the determination of a or $k_L a$ in static mixers.

Table 1

Equations for Prediction of Volumetric Mass Transfer Coefficients, $k_L a$, for Koch Static Mixers

(2)	$d_B = 5330\, d_h (We)^{-0.5} (Re)^{0.17}$	Strieff (1977)	Horizontal bubble flow, liquid/liquid and gas/liquid
(4)	$\epsilon = 0.0516\, V_L^{-0.102}\, V_G^{0.588}$	Wang and Fan (1978)	Bubble flow in vertical pipe filled with Koch A Y mixers
(6)	$k_L = \frac{2}{\sqrt{\pi}} \frac{D_A \Delta V}{d_B}$	Cichy and Russell (1969)	Bubble flow in empty pipe using penetration theory
(7)	$a = \frac{6\,\epsilon}{d_B}$	Sauter	Spherically shaped bubbles
(8)	$\Delta V = 692.8\, d_B^{1.5284}$ $100\ \mu m < d_B < 500\ \mu m$ $\Delta V = 89.3\, d_B^{0.8457}$ $500\ \mu m < d_B < 2000\ \mu m$	Motarjemi and Jameson (1978)	Bubble flow in vertical empty pipe with stagnant liquid phase

2. METHODOLOGY

2.1 LIQUID HOLDUP AND POWER INPUT

Liquid holdup is defined as the volume of liquid per unit volume of total reactor. In this study, the liquid holdup is determined experimentally by quickly closing shut off valves to the reactor at various gas and liquid rates and then measuring the remaining volume of liquid in the column.

The dissipated power density is defined by the following expression:

$$P_\omega = \frac{\Delta P_k \cdot Q_L}{V_R \cdot (1-\epsilon)} \tag{9}$$

where ΔP_k = The pressure drop across the reactor due to kinetic energy loss, (N/m^2);

Q_L = Liquid volumetric flow rate, (m^3/s);

V_R = Volume of the total reactor, (m^3);

$(1-\epsilon)$ = Liquid holdup.

The kinetic pressure drop is calculated from the difference of the experimentally measured total pressure drop across the length of the reactor and the static pressure drop

$$\Delta P_s = [\rho_g \epsilon + \rho_L (1-\epsilon)] \cdot g \cdot H \tag{10}$$

where ρ_g = Density of the gas, (kg/m^3);

ρ_L = Density of the liquid, (kg/m^3);

ϵ = Gas holdup;

g = Acceleration of gravity, (m/s^2);

H = Height difference of the inlet and outlet of the reactor, (m).

It is important to realize not only that the static pressure drop has been subtracted off but that the power needed to push the gas through the reactor has been neglected.

2.2 DETERMINATION OF THE MASS TRANSFER COEFFICIENT AND INTERFACIAL AREA

The following text is a brief description of the options open to the experimenter wanting to determine the liquid side mass transfer coefficient, k_L and interfacial area, a.

2.2.1 Measurement of Interfacial Area

There are a few methods and procedures to choose from in order to determine droplet or bubble size, or interfacial surface area, such as photography, light scattering and various chemical means. Photography and light scattering are physical methods which can be used readily and that introduce no foreign matter such as electrolytes. A good article by Landau, et al. (10) compares these methods.

Photography not only gives data for bubble size but also yeilds information about bubble size distribution and bubble shape. However, the information obtained pertains to the hydrodynamics at the wall at a particular part of the reactor and is not necessarily representative of the entire reactor or of a particular whole cross section. Also the analysis of the photographs is very time consuming and can

produce misleading results if the photographs are not properly done.

The light scattering technique avoids the long analysis of results and provides good data with adequate instrumentation. However, this technique involves placing a probe in the reactor which can cause mixing effects of its own. It also is a technique that gives point values for holdup and bubble size, not averages for the whole reactor. In addition the techniques has problems evaluating high magnitudes of surface areas above 800 m^{-1}. (10)

Chemical methods have the advantage of giving results that are a representative of averages for the total reactor, although the results can be interpreted only for a particular system and cannot be accurately extrapolated to gas/liquid systems having different physical characteristics such as viscosity and surface tension. The experiments are often more complex and time consuming than when dealing with physical methods.

2.2.2 Determination of Volumetric Liquid Side Mass Transfer Coefficient

The liquid side mass transfer coefficient, k_L, is determined usually by measuring the interfacial area, a, by the methods presented above and then can dividing an experimentally determined k_La by a. The volumetric coefficient, k_La, can basically be determined in two ways: physical absorption and chemically enhanced absorption. Just as in the case of the determination of the interfacial

area, both have disadvantages and advantages. The physical method is easier and quicker experimentally, while the chemical method can often be much more complicated due to the increase of electrolytes in solution. However, there is a fundamental advantage that the chemical method has over the physical methods (11).

The rate of absorption for a gas A being physically absorbed into a liquid B with no mass transfer resistance in the gas phase can be represented by:

$$N_A a = k_L a \, (C_{A_i} - C_{A_b}) \qquad (11)$$

where $N_A a$ = Volumetric rate of absorption of A, $(mole/m^3 s)$;

C_{A_i} = Concentration of A at the A/B interface, $(mole/m^3)$;

C_{A_b} = Bulk concentration of A in B, $(mole/m^3)$;

This equation relates $k_L a$ to several experimentally measurable quantities. In efficient contacting devices the two phases approach equilibrium conditions so C_{A_b} approaches C_{A_i}. Since the value of $k_L a$ depends on the difference of C_{A_b} and C_{A_i}, extremely accurate measurements of C_{A_b} and C_{A_i} are required in order to avoid a large error for efficient contacting devices. With chemical methods, the reaction regime is controlled so that C_{A_b} approaches zero and this fundamental problem is avoided. At this point, it would be beneficial to introduce some background for these chemical methods.

2.2.3 Chemical Methods

Briefly, for gas/liquid systems of any kind there are three different models used today to describe the physical action at a gas-liquid interface:

1) Two Film Model.

2) Higbie's Surface Renewal Model.

3) Danckwerts' Surface Renewal Model.

The descriptions of the models can be found in any good reaction engineering text book involving gas/liquid reactions (12, 13).

The main differences that these models, have besides their conceptual differences, are the definition of the liquid-side mass transfer coefficient, k_L. Two film theory leads to

$$k_L = \frac{D_A}{\delta_L} \tag{12}$$

where δ_L is the width of the liquid film, while Danckwerts' theory gives

$$k_L = (D_A \cdot s)^{1/2} \tag{13}$$

where s is the surface renewal frequency or the frequency at which the interface is renewed with an element of unreacted liquid. Higbie's theory, the least used of the three, gives

$$k_L = 2\ (D_A/\theta)^{1/2} \tag{14}$$

where θ is the exposure time of a fluid element at the interface. The important point from the above is that in film theory k_L varies with D_A but in the surface renewal

theories k_L varies with $D_A^{1/2}$. The surface renewal theories predict the experimentally determined dependence of k_L on D_A.

Although the three models are different conceptually and give different absorption rate equations, the numerical values for absorption rates of a particular single reaction gas/liquid chemical system are quite similar regardless of model used. In fact, in some cases the models can be interchanged depending on which model is more convienient.

For studies involving the evaluation of the mass transfer parameters the most common type of chemical system used is one in which a pure gas A undergoes an irreversible second-order reaction with a liquid or component in the liquid phase, B, that has the following stoichiometry:

$$A + zB \longrightarrow \text{Products}$$

and rate equation:

$$-R_A = r' C_A C_B \qquad (15)$$

An exact analytical solution for the rate of absorption, N_A, for this system is not possible. However, there are approximate solutions which are summarized by the following simple equation:

$$N_A = E_L k_L C_{A_i} \qquad (16)$$

The enhancement factor, E_L, is a not so simple function of various physical dimensionless parameters, the Hatta number

$$Ha = (D_A r' C_{B_b})^{1/2} / k_L \qquad (17)$$

the instantaneous enhancement factor

$$E_i = 1 + D_B C_{B_b} / z\, D_A C_{A_i} \qquad (18)$$

and the ratio between the volume of liquid associated with unit interface area and the film thickness parameter

$$Z = (\epsilon k_L)/(a\, D_A) \qquad (19)$$

Figure 4 presents the plot of the enhancement factor versus the Hatta number with E_i and Z as parameters (14). Basically, the magnitude of the Hatta number is an indication of the speed of the reaction relative to the speed of physical absorption. The higher the Hatta number is the faster the reaction progresses, and, therefore, the shorter the distance away from the interface the reactant A can travel before it is used up by the reaction.

Figure 4 is broken up into four basic reaction regions. In each region, the reaction occurs at a different speed, relative to diffusion, and consequently at different places in the liquid. Figure 5, based on the two film model, displays the concentration profiles in each region (14). In region A, the reaction rate is slow and nearly all the reaction occurs in the bulk. In region D, the reaction rate is fast and all the reaction occurs in the film. The other two regions have rates in between these two extremes.

In each reaction region, the enhancement factor is a different function of the physical parameters. Because of this fact, the information that can be extracted by

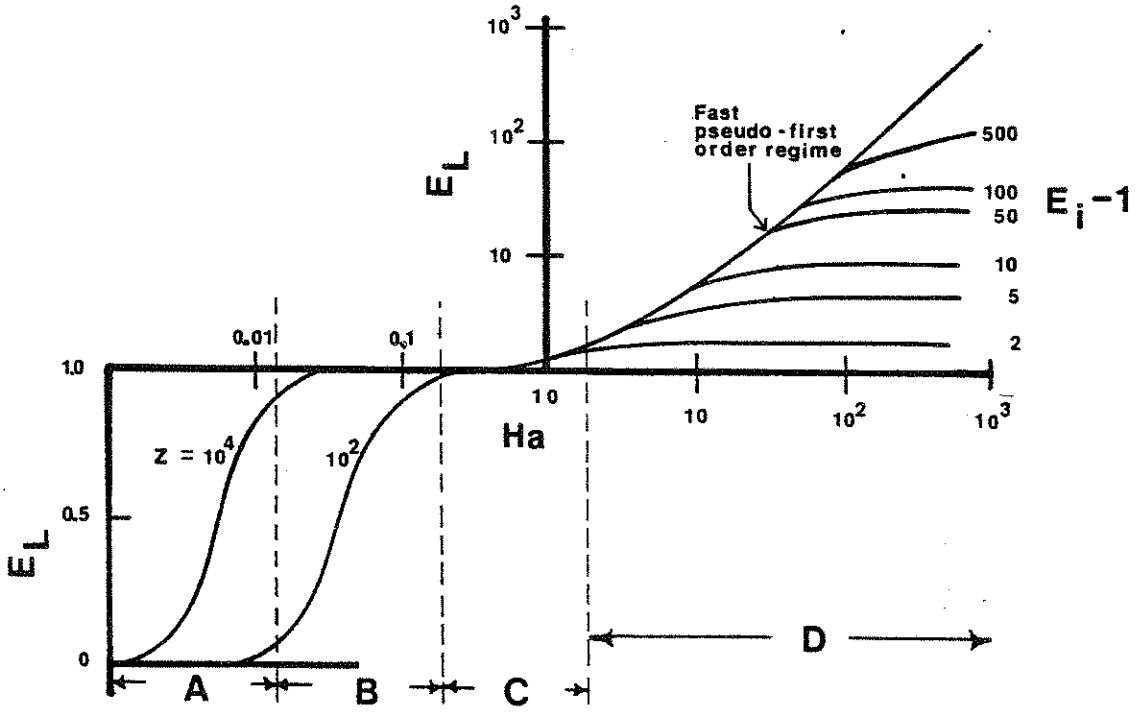

Figure 4. Enhancement Factor for Second Order Reaction

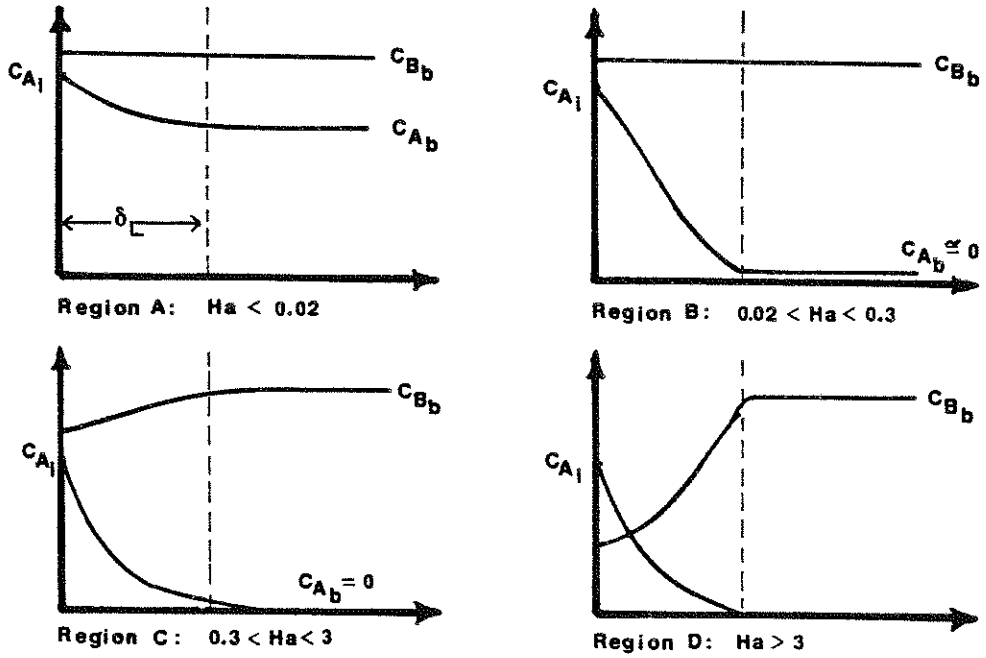

Figure 5. Liquid Phase Concentration Profiles at Various Hatta Numbers

absorption experiments is different for each region. For example, if an experimenter does absorption experiments in region B and Z >10,000 then $E_L = 1$ and the measured overall reaction rate is given by the following equation:

$$N_A a = k_L a \, C_{A_i} \tag{20}$$

Therefore, $k_L a$ can be evaluated directly if C_{A_i} is known. If however, the experimenter has a reaction system that can be operated in region D and if $E_i/2 \gg Ha$ (in the pseudo-first order reaction regime) then

$$E_L = \sqrt{1 + Ha^2} \tag{21}$$

and

$$N_A a = k_L a \, C_{A_i} \sqrt{1 + Ha^2} \tag{22}$$

By substituting for Ha and rearranging terms the following equation is obtained:

$$N_A a = a \, C_{A_i} \sqrt{k_L^2 + D_A r} \tag{23}$$

or

$$(N_A a)^2 = a^2 \, C_{A_i}^2 \, (k_L^2 + D_A r) \tag{24}$$

It is apparent from this equation that for known values of D_A and C_{A_i}, $(N_A a)^2$ can be plotted versus r on linear paper to obtain $(k_L a)^2$ from the intercept and a^2 from the slope. Such a plot is referred to as a Danckwerts' plot. This chemical

method is very powerful since the interfacial area and mass transfer coefficient can be obtained jointly.

The above examples are just two examples of the various chemical methods used to evaluate mass transfer parameters. In fact, every parameter (a, k_La, k_Ga, k_L, k_G) can be evaluated by selecting the proper chemical system. Charpentier gives a complete synopsis of all the methods, the information that can be obtained for each method as well as the parameters needed, and the requirements that need to be met for the various dimensionless parameters (12).

This study uses the above mentioned Danckwerts' type plot to determine k_La and a simultaneously. The advantage of this method is that a and k_La are measured under the same physical and chemical constraints, so that the final value of k_L will be accurate or meaningful for that chemical system. The reason that it is beneficial to measure a and k_La under the same conditions, as explained by Charpentier (14), is that those experimental quantities can be affected by the means of evaluation. For instance, if k_La is measured by physical absorption and a is measured by chemically enhanced absorption the resulting k_L will not necessarily be correct.

Appendix 7.1 gives a complete derivation of the mathematics of the method, the assumptions made and the necessary requirements for Ha and E_i.

2.3 THE CHEMICAL SYSTEM

A suitable chemical system for the method of simultaneous measurement of k_L and a must satisfy the required restraints on E_i and Ha as given in Appendix 7.1. Generally, the chemical system involves a chemical absorption in which the gas undergoes an irreversible pseudo-first order reaction preferably promoted by a catalyst in the liquid phase. The catalyst should be sufficiently powerful so that the reaction rate can be varied over a wide range without substantially altering the physical characteristics of the solution. Also, the system should have a negligible gas phase mass transfer resistance.

Charpentier lists a few candidates in Table XI from his review article. (14) Of the four systems listed, the two most popular are the following:

a) Oxygen absorption into a sodium sulphite solution with a cobalt sulphate catalyst.

b) Carbon dioxide absorption in a sodium carbonate bicarbonate buffer solution with a sodium arsenite catalyst.

Both systems have been studied extensively in the literature as well as been used successfully to evaluate the mass transfer parameters in packed columns and other conventional contacting devices.

System a) has been reviewed very completely by Linek and Vacek (15). The benefits of this system include:

1) Economy of the solutions;

2) Lack of toxicity;

3) Fire safety; and

4) Small concentrations of catalyst needed ($<10^{-4}$M).

However, as pointed out in Linek's review, this system lacks clear and accurate kinetic data. The kinetics of the reaction

$$SO_3^{=} + 1/2\ O_2 \xrightarrow{Co^{2+}} SO_4^{=} \qquad (25)$$

change significantly with reactant concentrations and catalyst concentrations. Also many of the studies done with this system are in error according to Linek because they did not properly account for these changes in kinetics.

System b) has the following benefits:

1) Substantiated kinetics and kinetic data as well as experimental results on a wetted-wall column (16) and jet apparatus (17);

2) Process is being used industrially;

3) Carbon dioxide can be used safely; and

4) Possibility of determining the rate through analysis of changes in carbon dioxide concentration in the gas phase (or simply to close the mass balance).

The detrements of the system include:

1) Large concentrations of catalyst needed (up to 0.5 M);

2) Analysis of absorbed carbon dioxide in the liquid phase with arsenite catalyst is complicated; and

3) Sodium arsenite is highly poisonous and expensive. This system was chosen for this study, because of the relatively uncomplicated kinetics and the confidence in the kinetic parameters and physical constants presented in the literature. Also, the problem of economics was partially overcome by reusing the solutions.

The fundamental overall reaction of the system is (12):

$$CO_2(g) + CO_3^{=} + H_2O \xrightarrow{H_2A_sO_3^-} 2\ HCO_3^- \qquad (26)$$

The rate of absorption of carbon dioxide could be determined from measuring inlet and outlet flowrates of the pure gas stream or by determining the change of concentration of bicarbonate in the solution. Experimentally, it seemed more feasible to measure the liquid side absorption because the experimental setup and flowrates chosen complicated the measurement of the outlet gas flowrate. Also due to the expense of the arsenite catalyst, the solutions were reused so the work necessary to determine the final concentrations had to be done whether the rate was measured from the gas side or the liquid side.

The only practical method for determining the concentration of bicarbonate was by titration, similar to a method suggested by Vogel (18). Generally, a known excess amount, v1, of NaOH is added to a sample of reaction solution which converts all of the HCO_3^- to $CO_3^=$. Then an excess amount of $BaCl_2$ is added to precipitate out all the $CO_3^=$ as $BaCO_3$ leaving only the excess NaOH in solution. Finally the NaOH is titrated to an endpoint with HCl, v2, using a mixed indicator of cresol red and thymol blue. The concentration of the HCO_3^- equals (v1 x [NaOH])- (v2 x [HCl]), where [ ] indicates concentrations. Modifications of this method had to be developed due to the fact that the presence of the arsenite broadened the titration end point. A complete description of the titration method is given in Appendix 7.2.

Once the type of chemical system had been selected, it was still necessary to determine the particular concentrations of all the species of the system. Only a few sets of concentrations had been studied in the literature and had all the physical constants evaluated. This study used the concentration set that had the most available literature values for the constants as well as the one that allowed the highest concentration range for the catalyst (17). The

concentrations for the chosen system are given as follows:

$[CO_3^{=}] = 0.6$ M — Buffer system maintains

$[HCO_3^{-}] = 0.2$ M — pH = 10.0

$0.0 \text{ M} < [\text{Arsenite}] < 0.5 \text{ M}$

$0.0 \text{ M} < [Na^+Cl^-] < 0.5 \text{ M}$

$[\text{Arsenite}] + [Na^+Cl^-] = 0.5 \text{ M}$

The sodium chloride concentration is changed as the catalyst concentration is changed in order to maintain a constant ionic strength of 2.5. It is important to keep the ionic strength of the system constant, because the physical constants for this system are affected more by the ionic strength (19)

$$I = 1/2 \sum C_j z_j^2 \qquad (27)$$

where C_j = Concentration of the jth species, (mole/m^3);

z_j = The ionic charge of the jth species;

than by the buffer ratio, $[CO_3^{=}]/[HCO_3^{-}]$ (20).

The constants for this system came from two sources. From Danckwerts and Sharma (17), the constants $C_{A_i}\sqrt{D_A}$ and r are obtained as:

$$C_{A_i}\sqrt{D_A} = 7.7 \times 10^{-8} \text{ (gmole/cm}^2\text{s}^{1/2}\text{)}$$

at T = 25°C and

$$r = 2.2 + 224.5 \times [\text{Arsenite}] \quad (s^{-1})$$

From Danckwerts and Kennedy (20), the diffusivity of carbon dioxide in solution was obtained as:

$$D_A = 1.38 \times 10^{-5} \quad (cm^2/s).$$

After some preliminary experiments with the selected system, it was determined that the reaction had to be run in a semi-batch mode in order to get a significant bicarbonate concentration change. Therefore, the overall rate of absorption was calculated by the following equation:

$$N_A a = \frac{\Delta[HCO_3^-] \cdot V_b}{2 \cdot V_R \cdot (1-\epsilon) \cdot t} \qquad (28)$$

where V_b = Total volume of the batch solution, (m^3);

$V_R(1-\epsilon)$ = Volume of the liquid in the reactor, (m^3);

t = Total time of operation, (s);

$\Delta[HCO_3^-]$ = Change in bicarbonate ion concentration during time t, ($gmole/m^3$).

The final topic for the methodology of the experimental study is that of how much absorption of carbon dioxide can be tolerated. A significant change in the bicarbonate concentration is neccessary to ensure low analytical errors in titration. However as carbon dioxide is absorbed into solution, everything changes, i.e. the buffer ratio and the ionic strength. As the buffer ratio changes the pH changes and because the actual catalyst is the dissociated arsenite ion, the concentration of the active catalyst changes. As the ionic strength changes, the physical constants are

changed. The magnitudes of these changes are presented in Table 2 along with the possible errors in titration. This table shows that in order for the total error to be less than 15% each run should not exceed a bicarbonate concentration of 0.4 M. This total error is not the actual error for each data point but is an approximate deviation from the optimal conditions or the conditions at the start of each run. When this is done, Figure 6 displays that although things seem to be changing the overall reaction rate stays constant, as it should.

For economy reasons, the solutions are reused and the amount of absorption will depend on the next desired catalyst concentration. For example, the experiment may be started with the following conditions:

$[CO_3^{=}]$ = 0.6 M $[HCO_3^{-}]$ = 0.2 M

[catalyst] = 0.5 M [NaCl] = 0.0 M

and the desired conditions to run the second experiment are as follows:

$[CO_3^{=}]$ = 0.6 M $[HCO_3^{-}]$ = 0.2 M

[catalyst] = 0.4 M [NaCl] = 0.1 M

All that can be done to reuse the solution after the end of the first run is dilution of the total mixture and addition of any of the solutes with the exception of the expensive catalyst. This implies that the maximum final concentration of bicarbonate for the first experiment is 0.25 M. This is

Table 2

Changes in Parameters with Time due to the Absorption of Carbon Dioxide into a Buffer Solution

Time (min)	$[CO_2]$ Absorbed (moles/ℓ)	%	$[HCO_3^-]$ moles/ℓ	$\left(\frac{[CO_3^=]}{[HCO_3^-]}\right)$	$[A_{rs}^-]$ moles/ℓ	%	I	%	Total % Deviation
0	0	—	0.18	2.89	0.193	0	2.24	0	—
3	0.03	10	0.24	2.80	0.193	0	2.24	0	10
11	0.045	7	0.27	1.76	0.190	2	2.20	2	11
15	0.040	8	0.26	1.76	0.190	2	2.20	2	12
20	0.095	3	0.37	1.15	0.185	5	2.14	5	13
30	0.105	3	0.39	1.06	0.184	5	2.14	5	13
60	0.240	1	0.65	0.45	0.165	15	2.05	9	25
90	0.381	1	0.78	0.18	0.127	34	2.00	11	46

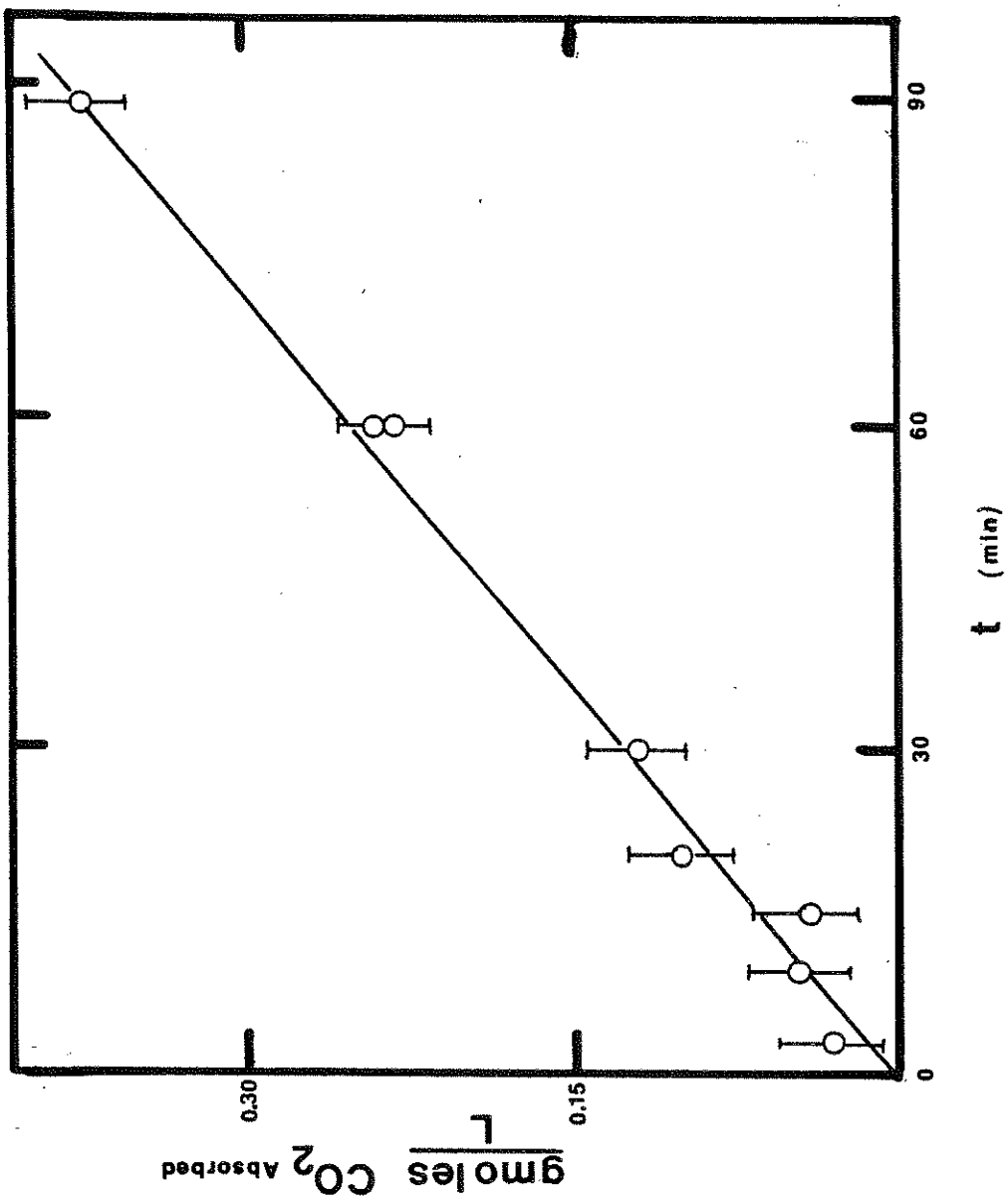

Figure 6. Carbon Dioxide Absorption Versus Time

a more limiting requirement than the requirement to keep the pH and ionic strength constant. Therefore the idea for each run was to get enough change in the bicarbonate concentration to have small titration errors while at the same time limiting the change so that a significant amount of solution was not wasted in diluting it to the next concentration.

3. EQUIPMENT AND PROCEDURE

3.1 EQUIPMENT AND PROCESS FLOW DISCRIPTIONS

Figure 7 is a general schematic for the experimental equipment used in this study. The absorbing solution is pumped from a 15 liter container through 3/4 inch garden hose, a liquid rotameter and two control valves (v1 and v2) to the bottom of the reactor where the gas and liquid initially come into contact. The gas/liquid mixture travels upward through the 1 inch diameter reactor to the separator where the gas and liquid are separated simply by density differences. From the separator, the solution returns through a smaller 1/2 inch tube by gravity flow to the bucket where it is recycled.

The gas rotameters have a maximum capacity of 2.2×10^{-4} m^3/s for nitrogen and 1.6×10^{-4} m^3/s for carbon dioxide. The liquid rotameter has a maximum capacity of 3.2×10^{-4} m^3/s. These capacities translate into the following superficial velocities in the reactor:

V_G from 0.074 to 0.32 m/s; and

V_L from 0.193 to 0.63 m/s.

The calibration charts are given in Appendix 7.3.

The gas, either carbon dioxide or nitrogen, flows from pressurized gas cylinders with regulators through a 1/4 inch gas line, a gas flowmeter with a control valve and a solenoid on/off valve to the bottom of the reactor. The long gas lines before and after the flowmeters have been

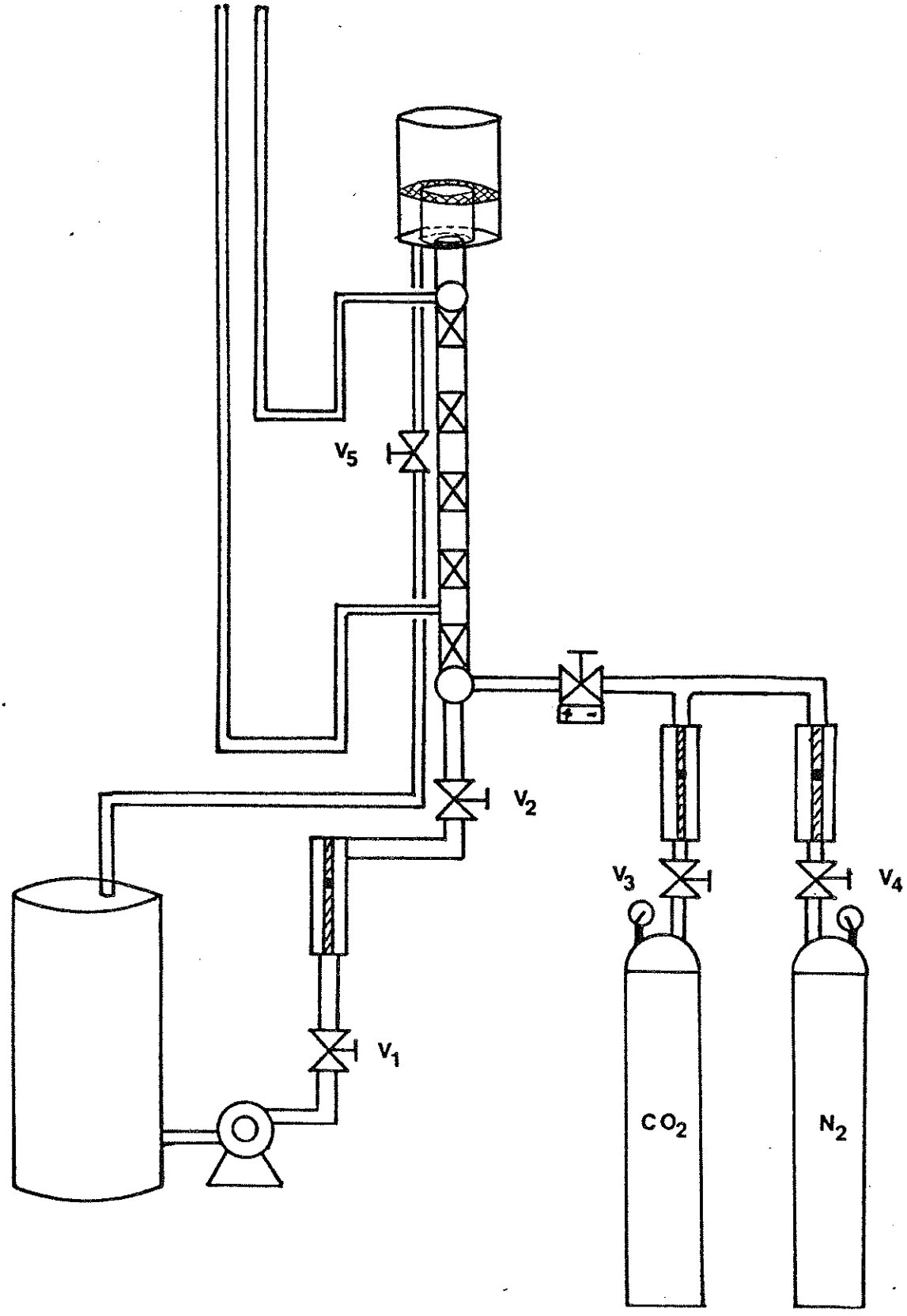

Figure 7. Schematic of the General Equipment

coiled in order to assure the inlet gas to the reactor is at room temperature. From the separator, the gas is released to the atmosphere. The gas solenoid valve and the liquid shut off valve, v2, can be closed quickly and simultaneously for the holdup measurements.

Two 1/4 inch pressure tap lines, one near the bottom of the reactor but still away from the gas inlet and the other at the top of the reactor just below the separator, are connected to two separate water/air manometers used for the total pressure drop measurements.

Figure 8 gives a more complete picture of the pressure drop measurement equipment. It shows that the monometers can be connected to a water supply with a control valve and flowmeter in between. This additional feature was added in order to properly assure that all the pressure lines are constantly filled with water by supplying a small water purge stream. For the pressure measurements for the Koch mixer, the water manometers were substituted by an accurate Helicoid pressure gauge.

Figure 9 shows specifically how the gas is sparged into the liquid mainstream. The gas is injected perpendicularly into the center of the liquid mainstream less than 1 pipe diameter from the first mixing element of the reactor. This method is suggested by the Kenics and Koch Companies.

Figure 10 displays the gas/liquid separator in detail. The separator has a doughnut-shaped wire screen at the top

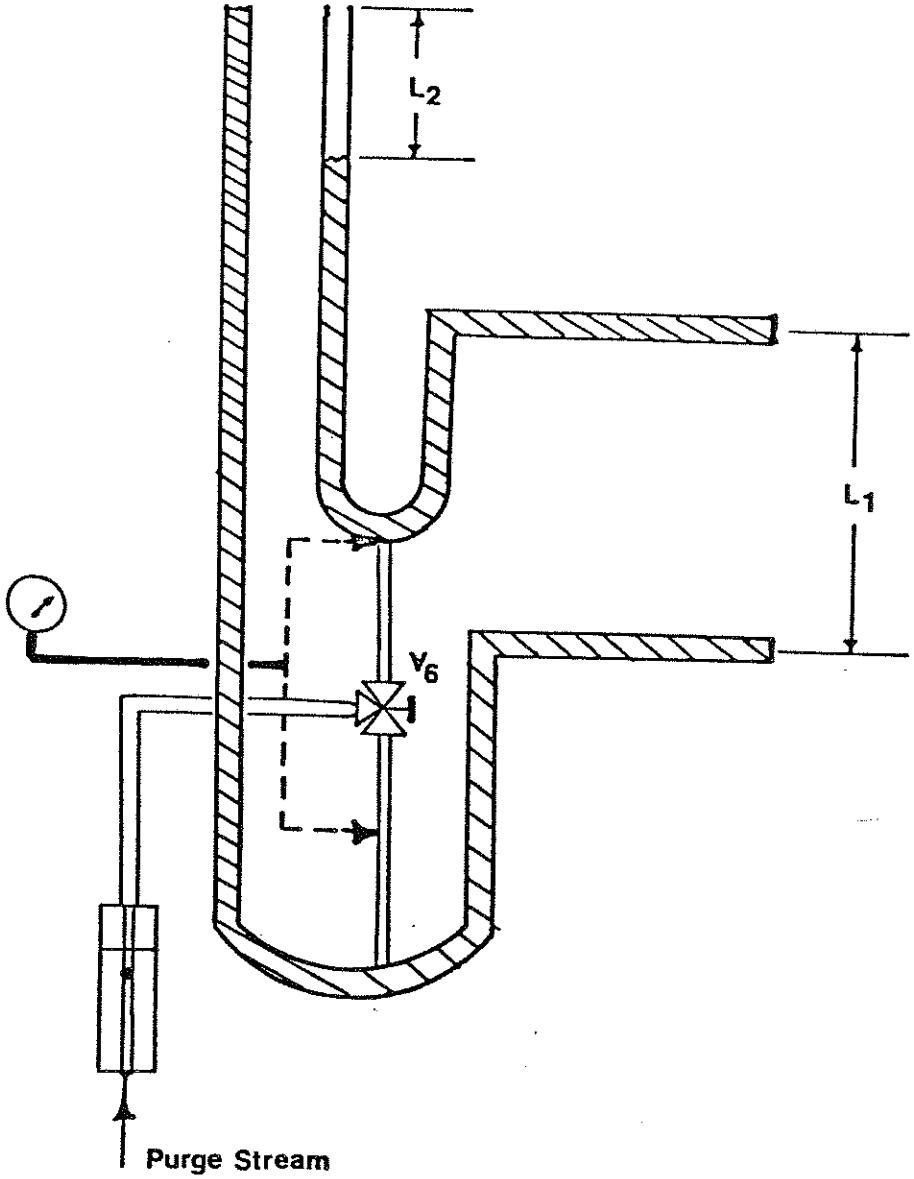

Figure 8. Pressure Measurement Apparatus

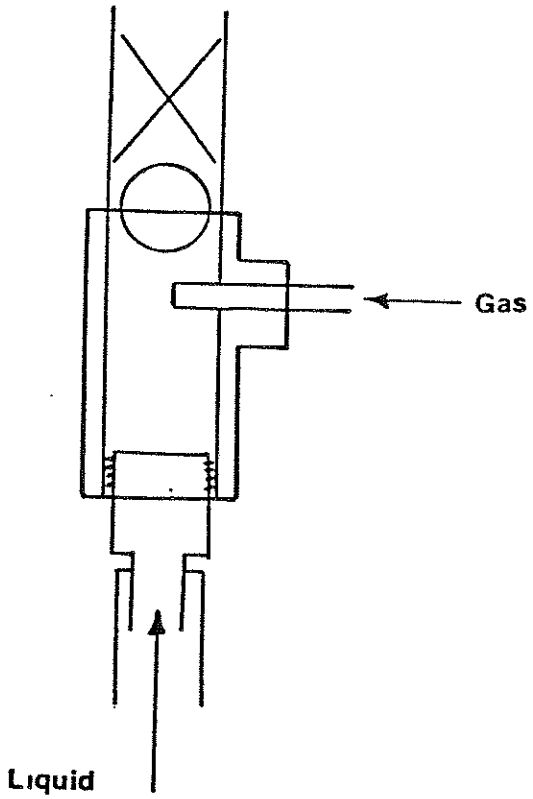

Figure 9. Schematic of Gas Injection into the Liquid Mainstream

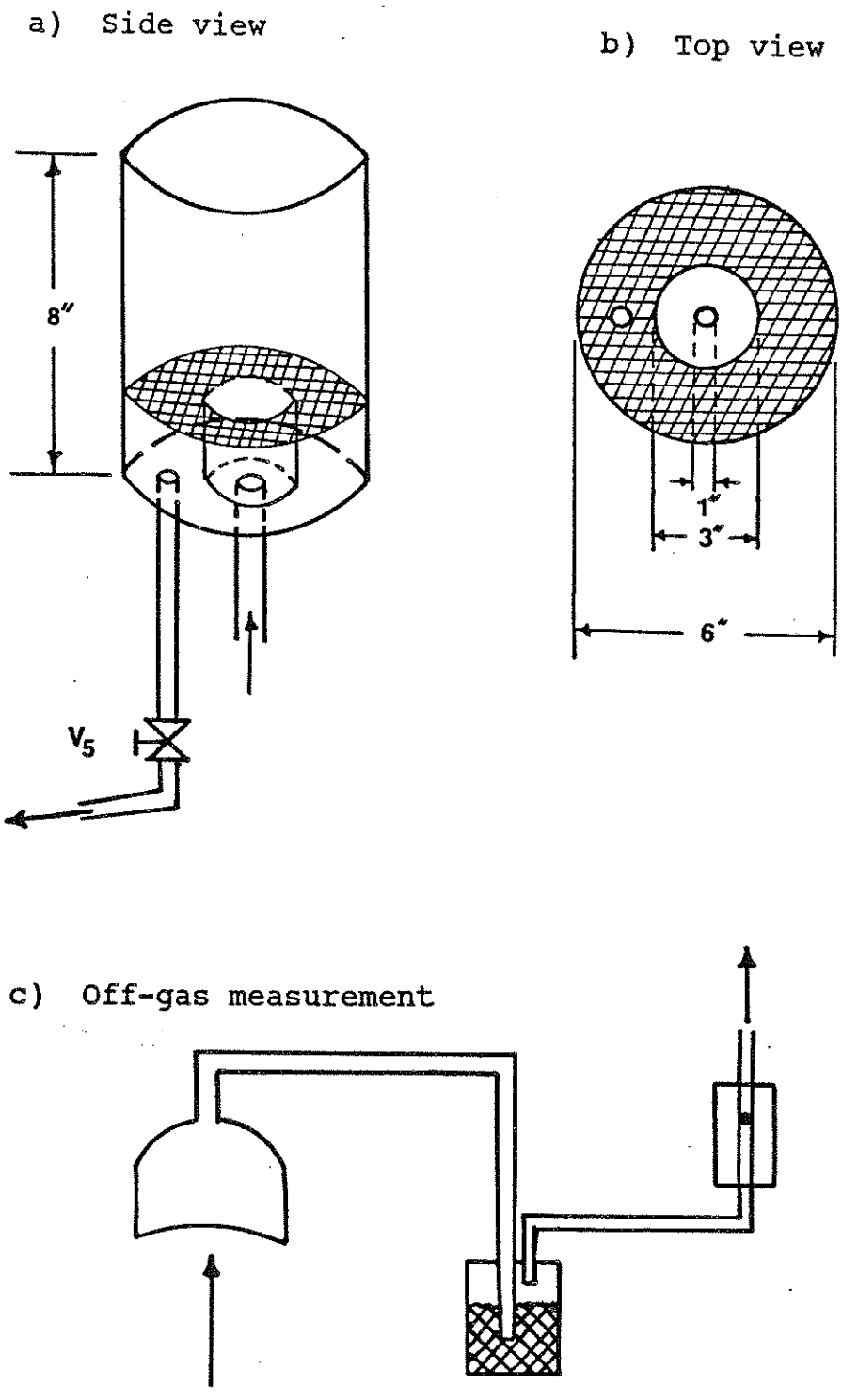

Figure 10. Diagram of the Gas/Liquid Separator

of the liquid outlet to help prevent localized down currents of the liquid that tend to pull gas bubbles down. Valve 5 is simply a pinch valve to control the flowrate out of the separator.

The separator can be fitted with a air tight top in order to capture the off gas, if desired. Experimental problems measuring the off gas flowrate occured with this design. The gas flows from a six inch diameter separator to a 1/4 inch tubing to the outlet flowmeter. Any fluctuation in the liquid rate, changes the liquid height in the separator which causes tremendous fluctuations in the outlet gas flowrate measurement. Also, the outlet gas passes through a water vapor absorption chamber before going to the outlet rotameter. This chamber causes a significant backpressure on the system that affects the sensitivity of the valves. In other words, the backpressure makes it more difficult to maintain steady state in the separator.

Figure 11 is a schematic of the electrical set up for the apparatus. The laboratory power source is split into two branches. The first branch is connected to the pump motor through a variac with an on-off switch. The liquid flowrate is adjusted mainly by this variac, and secondarily by the liquid control valve, v1. The second branch is connected to the following:

1) A timer;

2) The gas solenoid on-off valve;

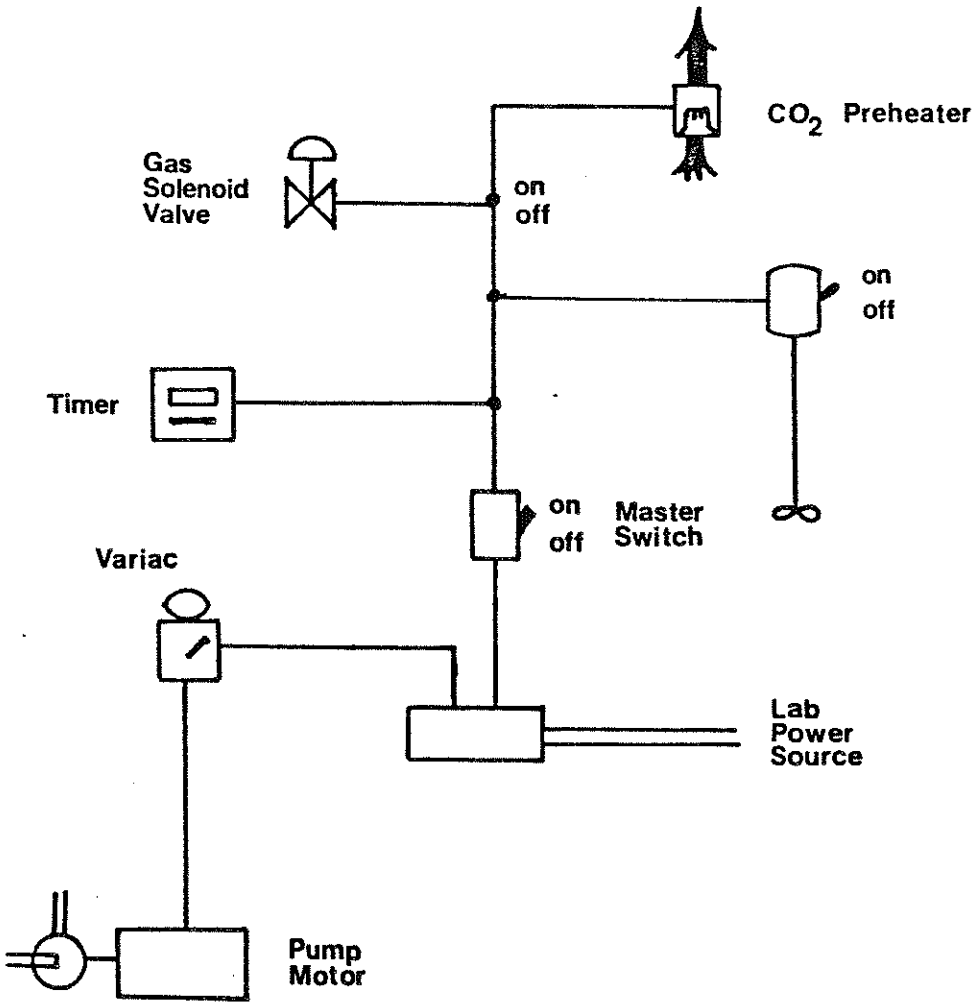

Figure 11. Schematic of the Electrical Connections

3) An electric stirrer to mix solutions in the 15 liter container; and

4) The CO_2 preheater connected between the cylinder and the regulator.

In this configuration, the gas flow can be turned off (by switching the master switch off) without affecting the liquid flow. For holdup measurements the pump can be connected to the second branch in order to stop both flows simultaneously.

The static mixers, in the case of the Kenics and Ross mixers, filled the entire length of the reactor pipe from the gas inlet to the throat of the separator. For the Koch mixer, however, the packing configuration was different. Each Koch segment, which was comprised of two elements rotated 90° to each other, was separated by a spacer of equal length. The spacer was constructed of a thick wire to provide support for the space so that the Koch segments would remain separated even under the highest pressures drops. Since the Koch mixing elements used were significantly denser, this configuration was used in order to obtain the same voidage or the same usable reactor volume per unit length as with the other two mixers.

3.2 EXPERIMENTAL PROCEDURES

The following sections present a general description of the various procedures. Step by step detailed procedures are given in Appendix 7.2.

3.2.1 Holdup and Total Pressure Drop Procedures

The liquid holdup, $1-\epsilon$, and the total pressure drop, ΔP_T, were measured for each reactor type at various gas and liquid flowrates that spanned the capacities of the flowmeters. The procedures to accomplish these measurements are straight forward. Liquid holdup was measured by shuting off the gas and liquid flows into the reactor quickly and simultaneously with the shut-off valves and then measuring the volume of the liquid remaining in the reactor. The liquid holdup was then calculated as the ratio of the volume of liquid remaining and the total volume of liquid the reactor can contain.

The total pressure drop across the column was measured with the use of water manometers or a pressure guage. When carbon dioxide and the buffer solution were used to measure the pressure drop instead of nitrogen and water, the water purge apparatus was used to insure that all the pressure tap lines were filled with only water. With the gas and liquid flowing through the reactor at a constant rate, the total pressure drop is determined from the difference in height of the two water manometers or from the gauge pressure

readings. Refering to Figure 8, the total pressure drop was calculated by one of the following equation:

$$\Delta P_T = (L_1 + L_2)\, g\, \rho_{H_2O} \quad (29)$$

or

$$\Delta P_T = (\Delta P_{guage}) + L_2\, g\, \rho_{H_2O} \quad (30)$$

where L_1 = The liquid level difference of the two manometers, (m); and

L_2 = The height difference of the two pressure taps, (m).

Holdup and pressure drop measurements were performed for nitrogen/water system and for carbon dioxide/buffer system. The two systems gave slightly different results because of their different physical properties and because of the absorption of the carbon dioxide in the latter system. Section 4.1 and 4.2 present the data for the nitrogen/water system while the results by the carbon dioxide/buffer system were used for the absorption calculations and power calculations.

3.2.2 Mass Transfer Procedure

The basic procedure for the evaluation of a and k_L depends on the determination of the rate of absorption of carbon dioxide at various catalyst concentrations. The rate of absorption of carbon dioxide can be directly related to the rate of appearance of bicarbonate in the solution through stoichiometry. The rate of appearance of bicarbonate can be determined by titrating for the bicarbonate

concentration change in the buffer solution after a certain contact time with carbon dioxide gas. Therefore, the basic procedure is to titrate for the bicarbonate concentration change of a solution after a certain reaction time for various solutions of different catalyst concentrations. This procedure is then repeated for various gas and liquid flowrates that span the capacities of the flowmeters and for the three different reactors.

This procedure is complicated by the desire to reuse the solutions in order to reduce the expense of the catalyst. Since, there are no practical separation methods only the operations of dilution and addition of the less costly compounds are available to readjust the concentrations of all species to the desired levels. The required concentrations of all species at the beginning of any run are as follows:

1) The concentration of bicarbonate equals 0.2 M;

2) The concentration of carbonate equals 0.6 M; and

3) The concentrations of catalyst and salt should always be less than or equal to 0.5 M and their sum should always equal 0.5 M.

The readjustment procedure begins after a run is completed. The concentration of bicarbonate is determined by titration. The total solution is then diluted by removing a specific volume of the solution and replacing that volume by water. The quantity of solution to be replaced by water is determined by the amount of dilution

necessary to change the concentration of bicarbonate from the evaluated final concentration of the previous run to 0.2 M. Once the dilution is accomplished the concentrations of the other species have been diminished. The concentration of the catalyst has been reduced which is desired in order to get another point on the Danckwerts' plot. The only thing left to do before starting the new run is to add carbonate in order to get its concentration back up to 0.6 M and to add enough salt in order to reestablish the ionic strength at 2.5.

Figure 12 is a flowsheet that displays a simplified procedure to determine the points necessary for one Danckwerts' plot. The procedure begins by making a buffer solution with the maximum concentration of catalyst and no salt. As the procedure progresses and dilutions are made the concentration of catalyst decreases.

Two major points need to be made concerning this procedure. The first item is that the amount of bicarbonate produced due to the absorption of the carbon dioxide determines the amount of dilution necessary and thereby regulates the next catalyst concentration level. If, for example in the first run in Figure 12, the concentrations after the absorption phase were 0.3 M, 0.55 M and 0.5 M for bicarbonate, carbonate and arsenite, respectively, then the amount of dilution would be 2/3 instead of 1/2 and the final arsenite concentration would be 0.33 M instead of 0.25 M. So by decreasing the absorption time or the amount of carbon

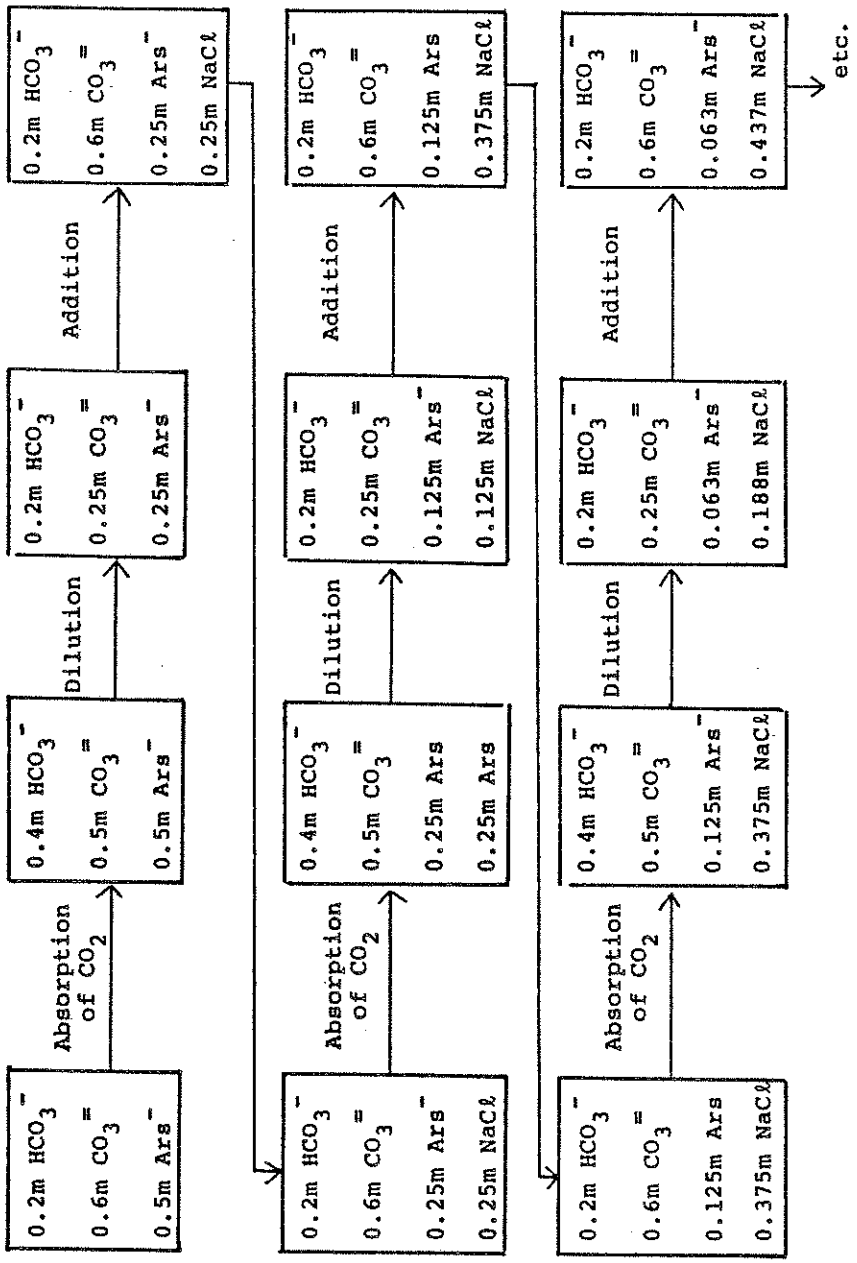

Figure 12. Absorption Procedure Flowsheet

dioxide absorption, more points for one Danckwerts' plot can be obtained. However, since the amount of the absorption is measured by difference the bicarbonate concentrations, the smaller this difference the larger the error for each point. Therefore a trade-off between having many points with large errors for each plot or having a few points with small errors needed to be resolved. It was decided to obtain bicarbonate concentrations of approximately 0.3 M. This gave five to six data points for each Danckwerts' plot with an error of about 15% for each point. The reaction time necessary to obtain this concentration was determined for each run by educated guessing.

The other important point to discuss is the way of keeping track of all the concentrations at the end of every step. This was important because any error would propogate throughout the rest of the procedure.

The tools available to help the bookkeeping of all the concentrations are two different titrations, an accurate balance, the experimentally verified stoichiometry and knowing that there is no depletion of the catalyst during the absorption phase.

The two titrations determine the concentrations of different species. The first titration, which will be refered to as the TBC titration, determines the total base concentration and is extremely accurate and simple. It requires titrating a sample of solution with HCl to a blue to yellow bromophenol blue end point. The second titration,

which determines the concentration of bicarbonate plus the concentration to the catalyst and will be refered to as the BI titration, is difficult and can be accompanied by a significant amount of error. This titration procedure is described fully in Appendix 7.2. So the best overall procedure was to use the TBC titration preferentially over the BI titration.

Refering to Figure 12, bicarbonate and carbonate are accurately weighed and added to pure water in the 15 liter container. Since there may be some water in the process lines, the exact starting volume is unknown. But by using the TBC titration and knowing exactly how much bicarbonate and carbonate is added then the exact volume can be determined. The catalyst can then be added and the TBC titration can be performed again. The difference between the two titrations gives the exact starting concentration of the catalyst. After the absorption, the BI titration must be preformed. The new bicarbonate concentration is now determined by subtracting the known catalyst concentration from the results of this titration. The concentration of carbonate can be evaluated from the stoiciometry. The next step to be performed is the dilution. Once the dilution is performed the exact dilution ratio can be verified by doing th TBC titration and comparing it to the last TBC titration. The knowledge of the exact dilution ratio allows the calculation of all the reduced concentrations. After the dilution, the volume will not exactly be the same as the

original volume due to volumetric measurement errors, so the addition phase can be used to determine the new exact volume by a similar method as the determination of the original volume. This bookkeeping procedure is repeated for each step.

4. RESULTS AND DISCUSSION

4.1 HOLDUP

Liquid holdup, $1-\epsilon$, and gas holdup, ϵ, in a gas/liquid contactor are dependent upon the relative velocities of the gas and liquid phases. For the ideal situation of homogeneous flow, the two phases travel at the same relative velocities or

$$\frac{V_L}{1-\epsilon} = \frac{V_G}{\epsilon} \tag{31}$$

However because of density and viscosity differences, the gas phase often travels faster than the liquid phase and consequently the liquid holdup is larger than it should be ideally. The velocity of the gas relative to the liquid is called the slip velocity, ΔV, and is defined by Wallis (21) in the following equation:

$$\Delta V = \frac{V_G}{\epsilon} - \frac{V_L}{1-\epsilon} \tag{32}$$

Since the two-phase flow is often not homogeneous, some theories and correlations have been developed to predict holdup and other flow parameters. One of the most popular correlations is the Lockhart-Martinelli correlation. For air/water systems, Butterworth (22) gives the following form of this well known correlation:

$$\frac{1-\epsilon}{\epsilon} = 2.4 \left(\frac{V_L}{V_G}\right)^{0.64} \tag{33}$$

Figure 13, 14, 15 show the results of the holdup experiments for the Kenics, Ross, and Koch mixers in a vertical arrangement, respectively, with a nitrogen/water system. Also displayed on these plots for comparison are the homogeneous flow model and the Lockhart-Martinelli correlation. The Kenics and Koch mixer are similar in their plot charateristics. Both mixers have a family of lines of constant liquid superficial velocity that are parallel to and approach the homogeneous flow model line as the liquid superficial velocity increases. This interesting result is contrasted by the characteristics of the plot of the Ross mixer data. Figure 14 shows essentially that all the lines of constant liquid velocity overlap into one line with that line still parallel to the homogeneous line.

Appendix 7.4 analyzes the reason for the differences between the Ross mixer and the other two mixers. Briefly, as the liquid superficial velocity is increased, the slip velocity increases with the Ross mixer but decreases in the case of the Koch and Kenics mixers. This is a revealing difference between the reactor types. The slip velocity will decrease with increased liquid rate if the radial mixing is increased. This is definitely a beneficial characteristic for a static mixer, since increasing the liquid rate is the major way to increasing the turbulence in the mixer.

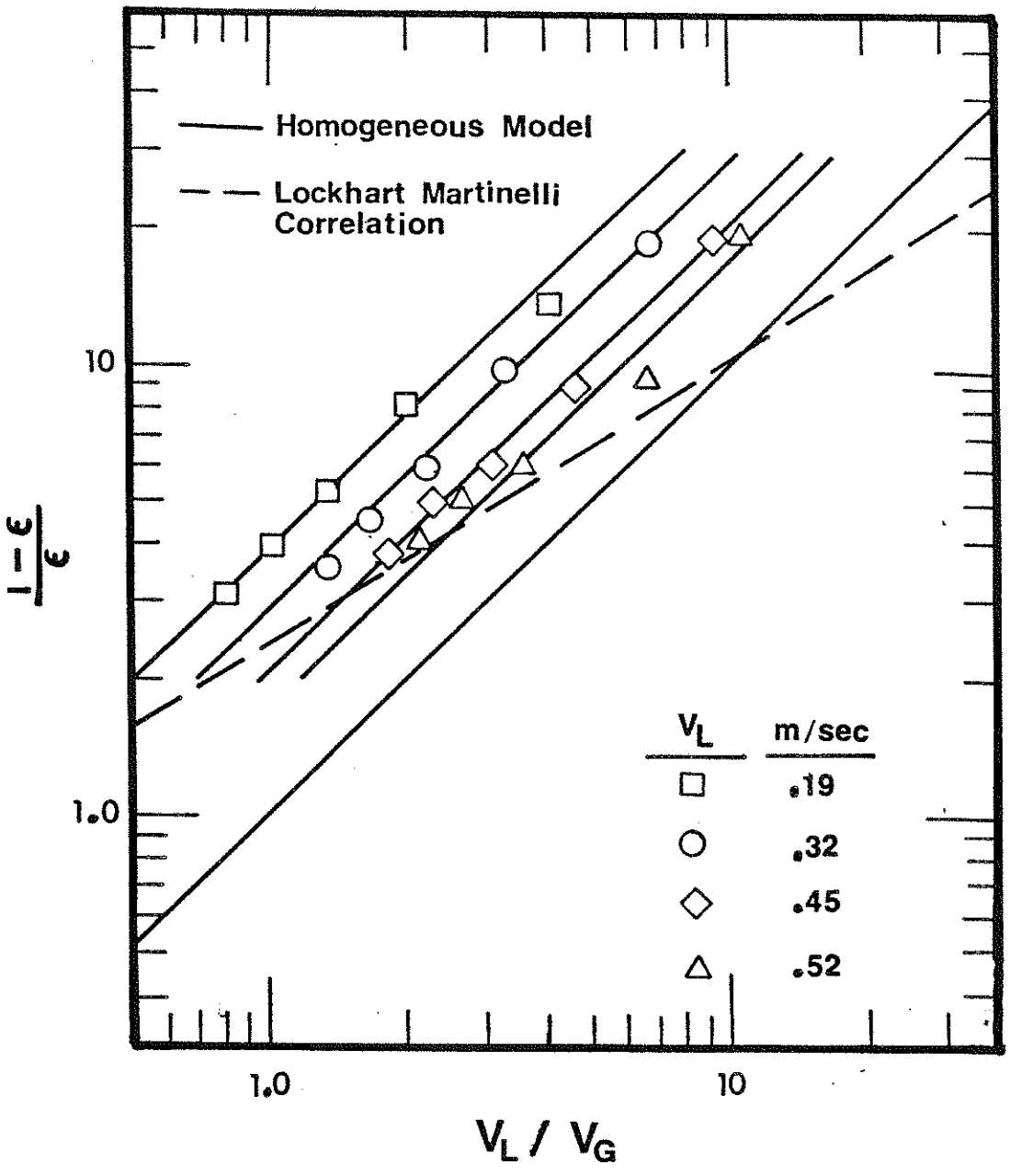

Figure 13. Effect of Fluid Velocity Ratio on the Holdup Ratio in the Kenics Mixer (Vertical)

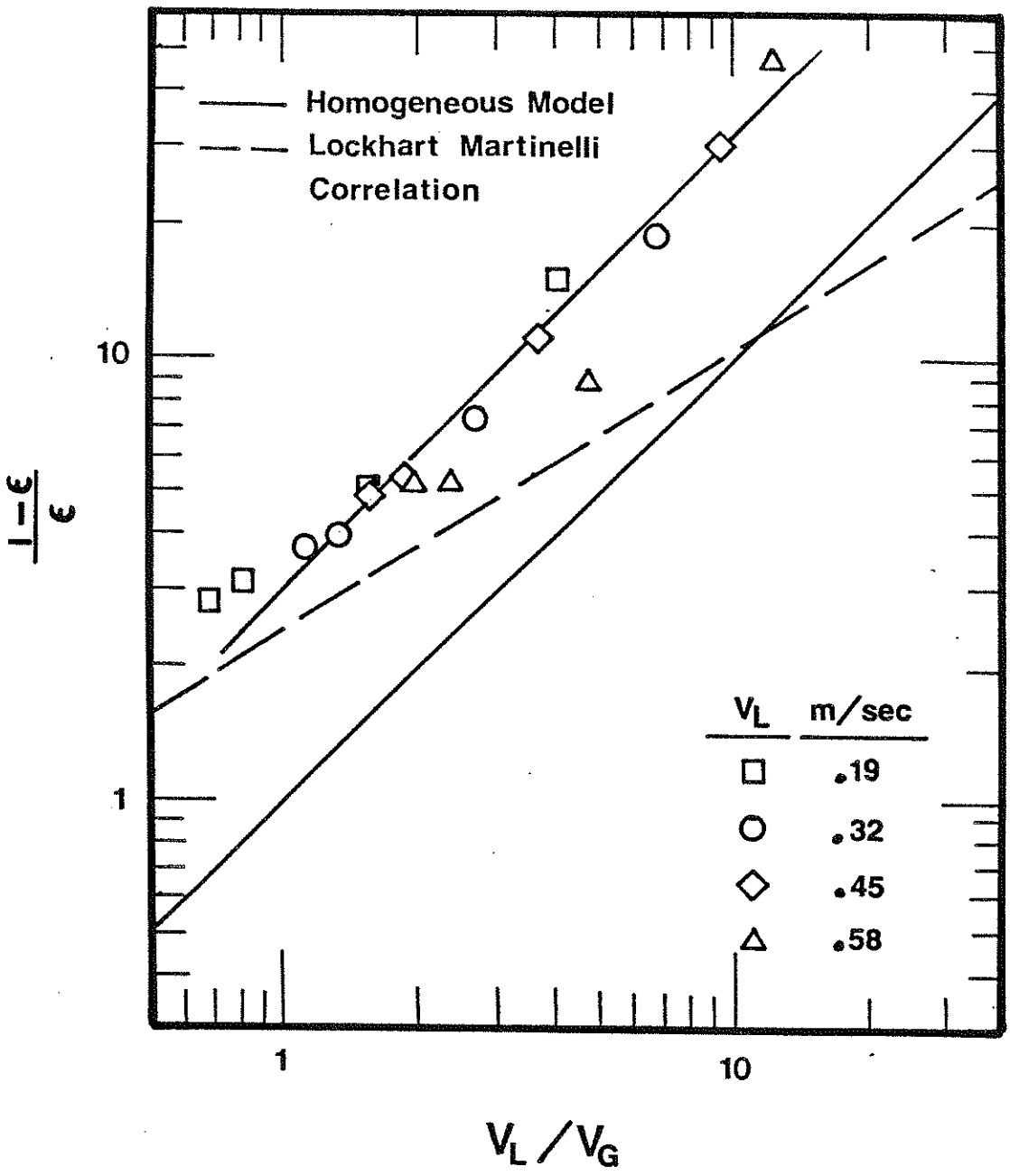

Figure 14. Effect of Fluid Velocity Ratio on the Holdup Ratio in the Ross LLPD Mixer

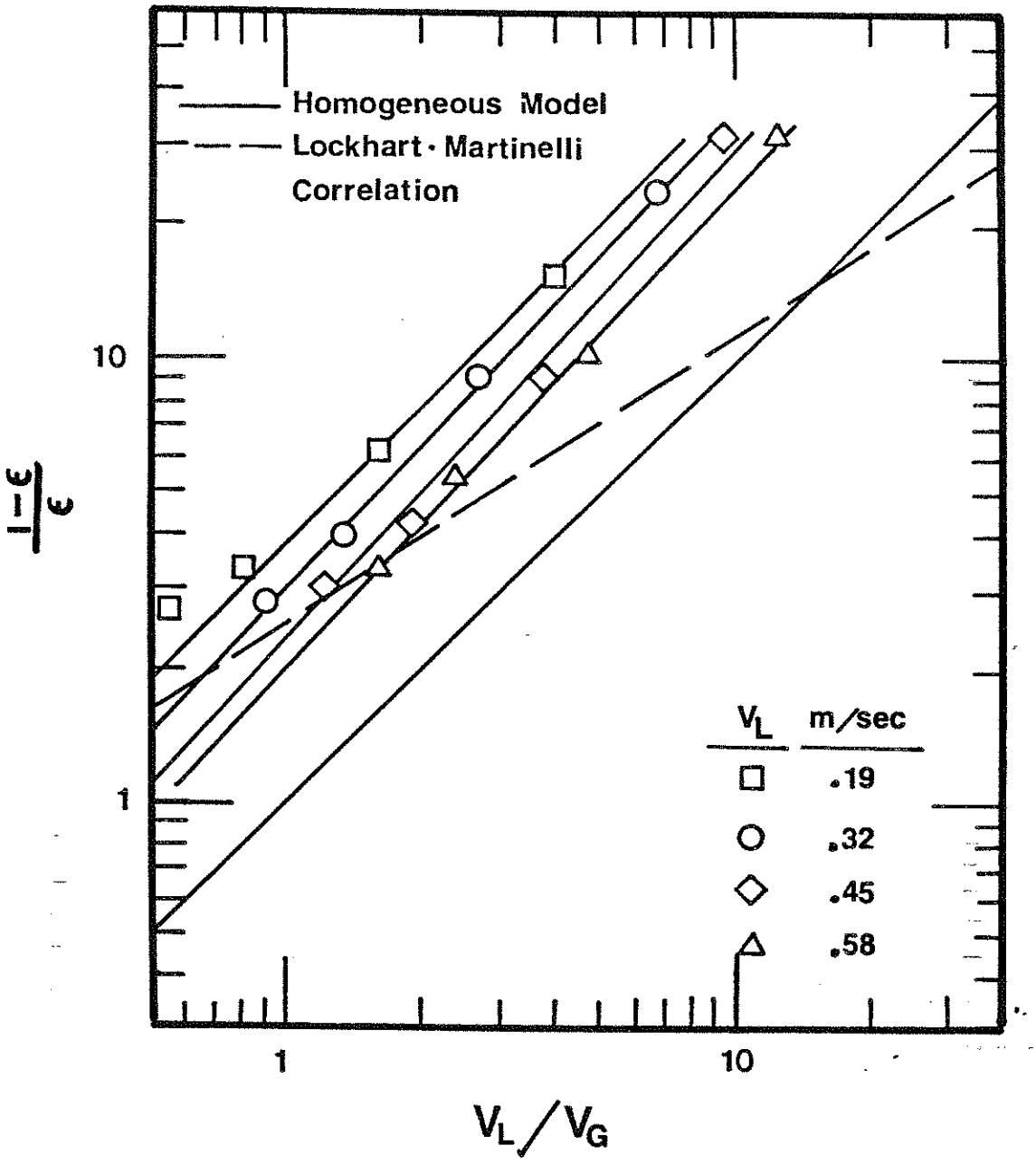

Figure 15. Effect of Fluid Velocity Ratio on the Holdup Ratio in the Koch CY Mixer

The effect of the slip velocity on mass transfer is not as clear cut. Cichy and Russell (23) showed from penetration theory that the liquid side mass transfer coefficient can be estimated from the following equation:

$$k_L = \frac{2}{\sqrt{\pi}} \sqrt{\frac{D_A \, \Delta V}{d_B}} \qquad (6)$$

This equation suggests that the mass transfer is increased by an increase in slip velocity. However, this formula was derived for bubble flow in empty pipes where the shear caused by the velocity differences is a main cause of turbulent effects on the gas/liquid interface. In static mixers, this shear could be insignificant compared to the turbulence induced by the surfaces of the mixer elements.

Horizontal flow in the Kenics mixer is different than upflow. Figure 16 shows that this flow seems to act more like the flow predicted by the Lockhart-Martenilli correlation, although not exactly. Also the family of lines are not as distinct as in the vertical flow. The reason for this difference between vertical and horizontal flow is not immediately clear.

Generally, the gas holdup is larger in the horizontal flow and is caused by the the absence of any static pressure across the reactor. In the vertical flow case, the larger total pressure drop provides a larger driving force in the axial direction which tends to magnify the viscosity and

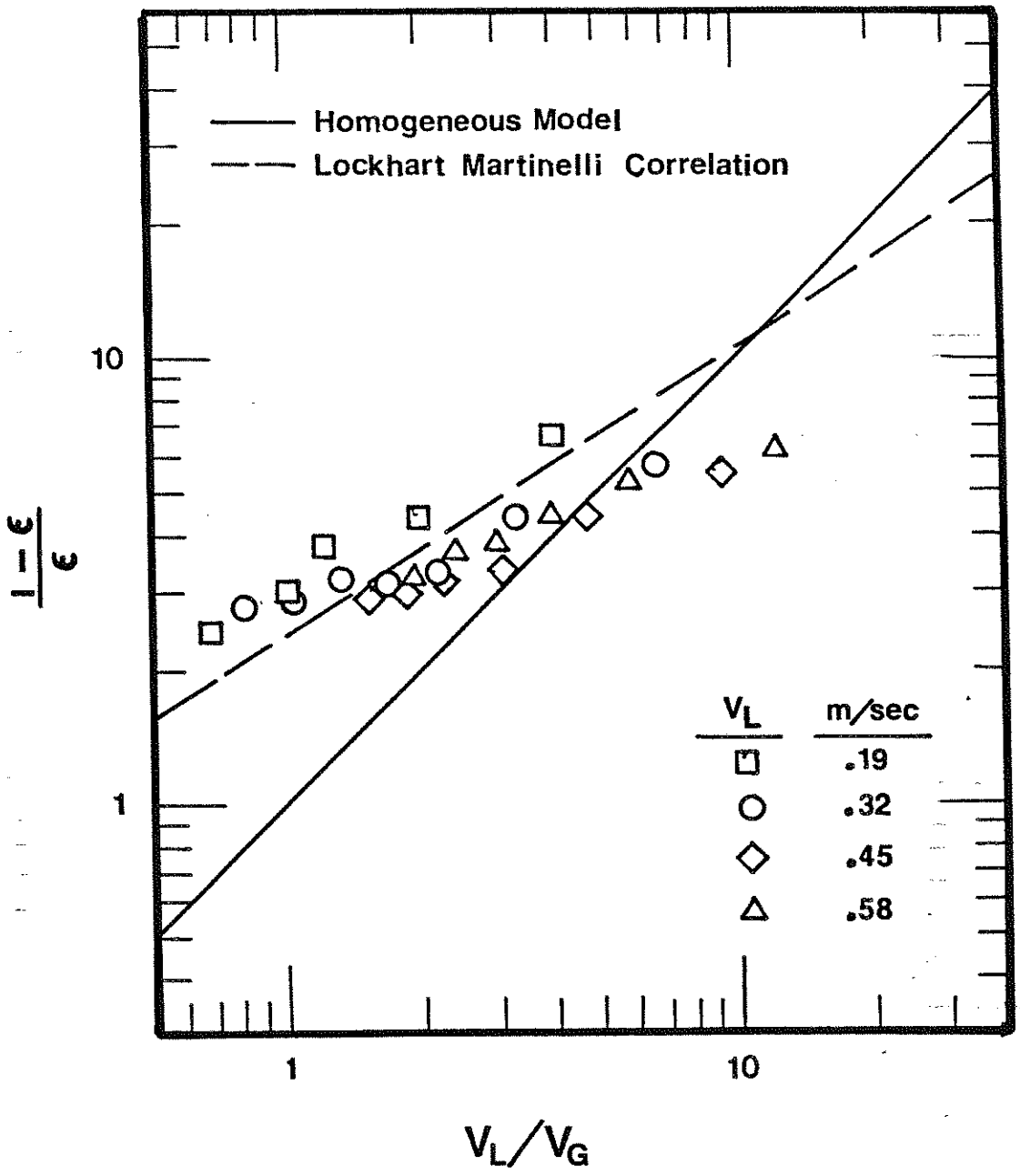

Figure 16. Effect of Fluid Velocity Ratio on the Holdup Ratio in the Kenics Mixer (Horizontal)

density differences of the two fluids. The gas travels faster and consequently the gas holdup decreases in vertical flow.

The family of lines found in Figures 13 and 15 were also seen by Yung Hsu in his investigation of the gas-lift reactor (24). In his doctoral thesis, he suggested a revised model described by the following equation:

$$\frac{1-\epsilon}{\epsilon} = D \left(\frac{V_L}{V_G}\right)^m \qquad (34)$$

where $D = f(V_L, \rho_L, \mu_L, \sigma \ldots)$

He also showed that D1 can be correlated with the two phase Reynolds, Froude, and Weber numbers. It is possible that this type of correlation could be beneficial when discussing the holdups for co-current gas/liquid upflow in the Koch and Kenics mixers. Appendix 7.8 gives this correlation attempt.

4.2 PRESSURE DROP

The accurate prediction of pressure drop across a gas/liquid reactor is essential for the proper design and selection of a suitable in-line mixer. Each commercial static mixer studied has a method to predict the kinetic pressure drop of two phase flow per unit length of the reactor. These methods are all based on the Lockhart-Martinelli correlations, which were derived from the results of two-phase horizontal flow experiments. Based on the evidence in the last section, this method does not necessarily apply when considering upflow. This statement is

substantiated by a study done by John Smith (2), who studied holdup and pressure drops in two phase co-current vertical pipes filled with Kenics mixer. He found "that over the whole range of these experiments the relative increase in pressure drop in the two-phase system is about half that which would be expected in a horizontal straight pipe", [as predicted by the Lockhart-Martinelli correlation].

From the last section, the vertical flow is more closely related to the homogeneous flow model although not too closely. The kinetic pressure drop using the homogeneous model can be predicted from the following equation:

$$\frac{\Delta P_K}{L} = \frac{4\ f_H}{2\ d}\ \rho_H\ V_H^{\ 2} \qquad (35)$$

where f_H = Homogeneous friction factor;
V_H = Velocity of homogeneous fluid; and
ρ_H = Density of homogeneous fluid.

The homogeneous velocity can be closely approximated by the liquid superficial velocity and for a constant gas flowrate the homogeneous density can be considered fairly constant. Considering these two approximations, a plot of kinetic pressure drop per unit reactor length versus liquid velocity on log-log paper should give some information in a concise manner. Figure 17 provides this plot using data from the

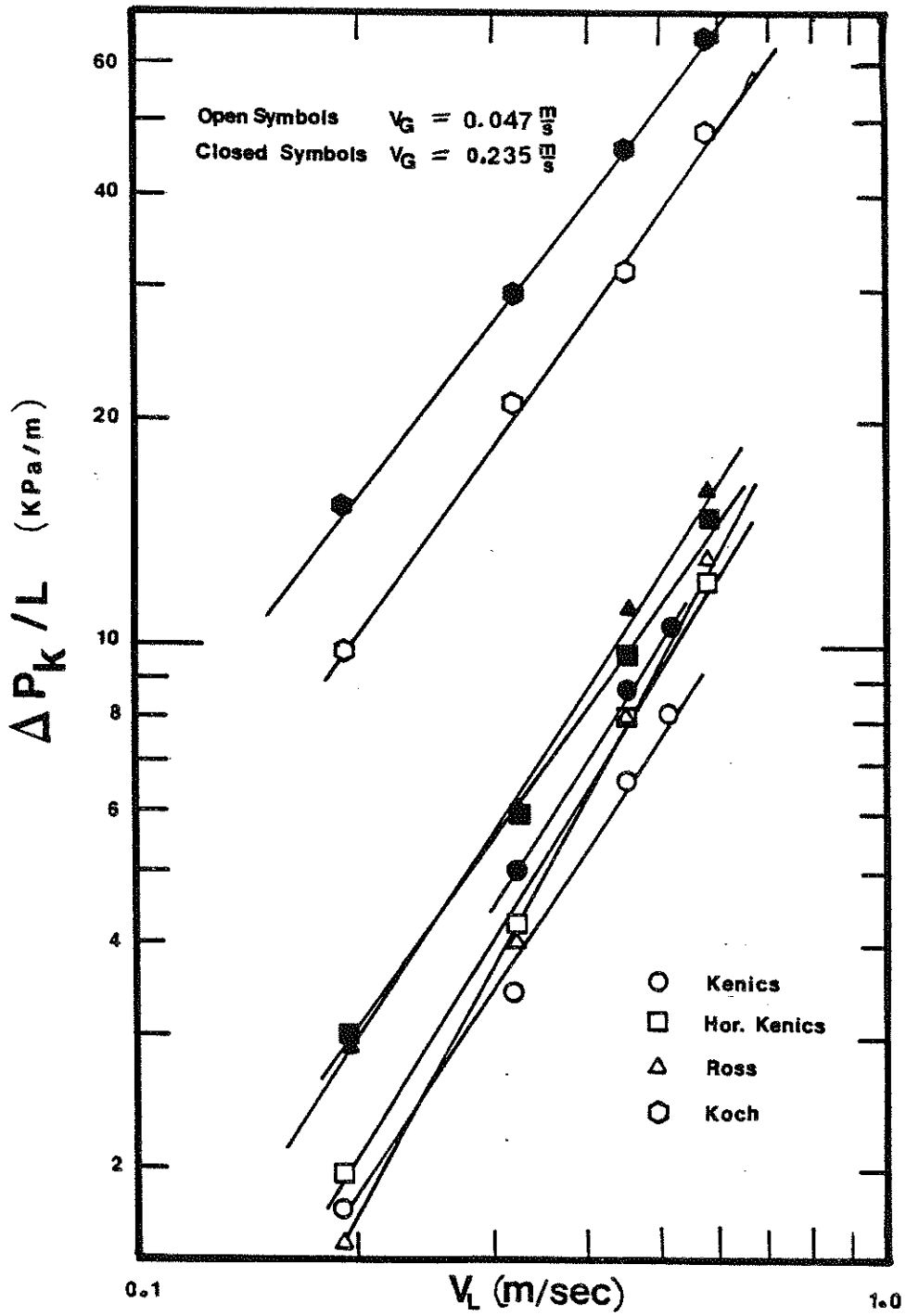

Figure 17. Effect of Fluid Velocities on Pressure Drop Per Unit Length for All Mixers

Kenics, Koch, Ross mixers at a high and low gas velocity for a nitrogen/water system.

Although an in depth analysis of the pressure drop data of this experiment is beyond the scope of this paper, some general comments can be made. 1) The Koch mixer has a significantly higher pressure drop than the other two mixers. 2) The kinetic pressure drop is slightly greater for horizontal flow than vertical flow in the Kenics mixer. 3) The slopes of the constant gas velocity lines are around 1.5 and less than 2.0 which is predicted from the homogeneous model. These slopes are affected by the change in gas velocity but only slightly. 4) By increasing this the superficial gas velocity, the kinetic pressure drop is increased. This phenomenon was also discovered by Smith in his paper (2).

4.3 INTERFACIAL AREA AND MASS TRANSFER COEFFICIENT

Before the results of these experiments can be presented some assumptions and corrections needed to be devised to compensate for some problems that arose during the experimentation. These two corrections are the separator/sparger correction and the correction to compensate for the uptake of the pure carbon dioxide gas.

4.3.1 Separator and Sparger Correction

Since the separator had a significant volume compared to the volume of the reactor, some mass transfer occured in the separator. Also, the initial creation of interfacial

area at the gas inlet, which is not a result of the mixer, has some associated mass transfer. These two effects were orginally assumed to be significantly less than in the reactor since the gas bubbles should be coalescing in the separator and the actual volume around the sparger is small. However, by bypassing the reactor and sparging the gas just below the entrance to the separator at the top pressure tap location and measuring the rate of absorption, it was determined that the absorption from these two effects were significant. Unfortunately, these two effects were experimentally inseparable and could only be measured together.

Appendix 7.5 gives the details of the results of those experiments, their interpretation and the derivation of some correction schemes. Briefly those results showed that the effect of the separator and sparger can be approximated by extending the defined volume of the reactor by the same amount as the product of the distance between the top of the reactor and the liquid level in the separator and cross sectional area of the tubular reactor. In other words, the total reactor volume includes the volume of the 0.0254 m diameter cylinder down the center of the separator. Visually, the bubbles maintain their integrity and do not spread radially as they pass through the separator to the liquid surface. So this approximation also makes practical sense.

4.3.2 Gas Phase Depletion Correction

Since the gas used was pure carbon dioxide, the molar flowrate of the gas stream constantly decreased with increasing distance up the reactor. As the gas was absorbed, the interfacial area also decreased. One possible solution could have been to label the interfacial surface area experimentally determined as an average area for the mean of the inlet and outlet gas flowrate. Unfortunately, this simple minded approach fails because of the way that the interfacial area is evaluated. The interfacial area is extracted from the slope of a line comprised of experimental points evaluated at different catalyst concentrations. Since the rate of absorption is different at each catalyst concentration, the outlet gas flowrate, and thereby the average gas flowrate, would be different for each point.

Appendix 7.6 shows the development of a correction scheme to correct the measured rate of absorption to account for the changing molar gas rate. Once the rate of absorption is corrected for each catalyst concentration then those points are plotted as originally planned.

Figure 18 shows the original data and correlating straight lines based on the volume of the physical reactor (line A). It also shows the subsequent effect of the separator and sparger correction (line B) and finally the effect of the gas depletion correction scheme (line C). Table 3 shows the resulting interfacial area, a, and mass transfer coefficient, k_L, that are calculated from the

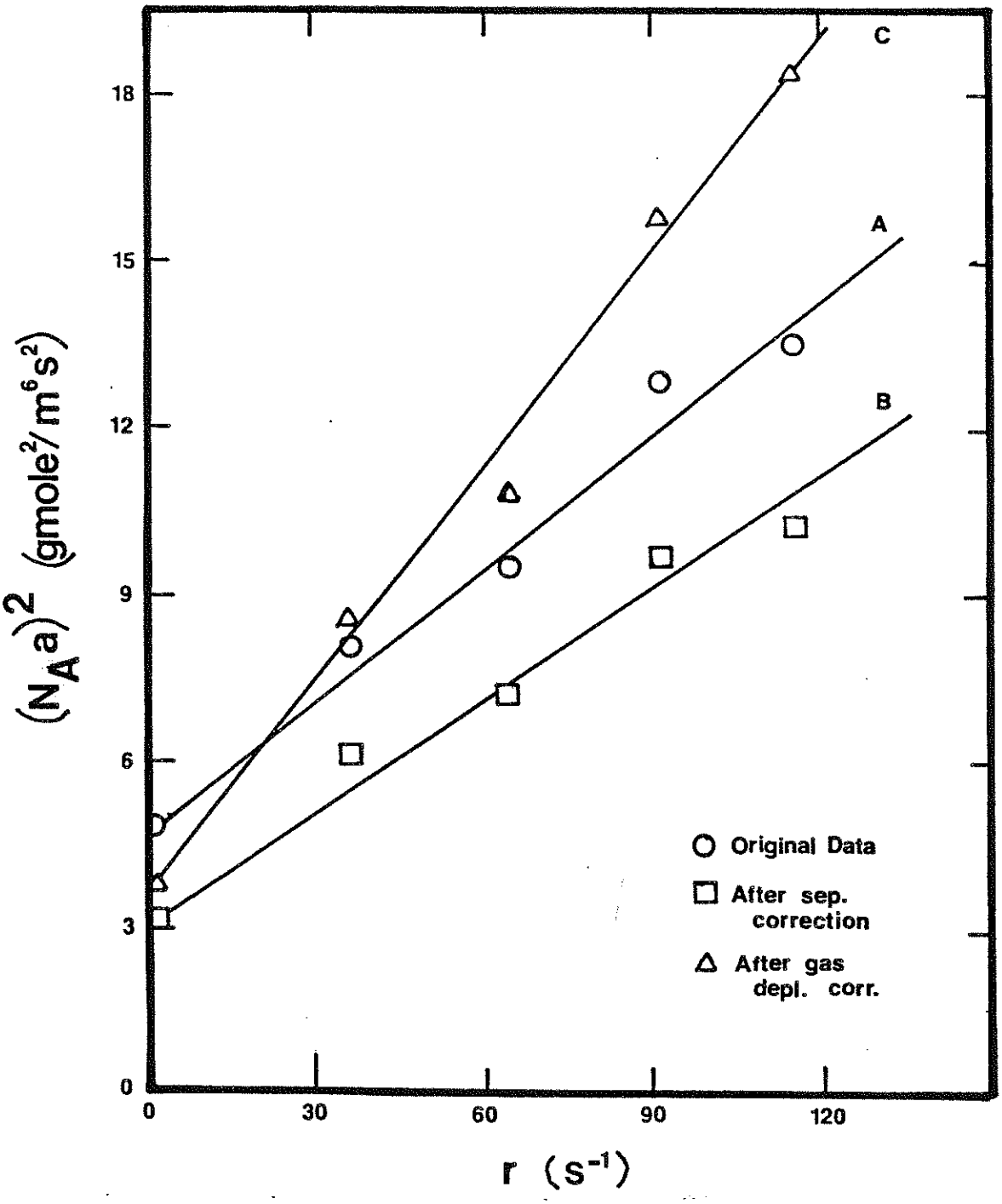

Figure 18. Effect of the Correction Schemes on the Danckwerts' Plot

Table 3

Effect of Correction Factors on the Experimental Values of the Mass Transfer Coefficient and Interfacial Area

Line	Intercept	Slope	a	k_L
	$mole^2/m^6 s^2$	$mole^2/m^6 s$	m^{-1}	m/s
		x 10^2		x 10^4
A	4.6	8.15	371	2.8
B	3.1	7.36	352	2.4
C	3.4	13.7	472	1.8

slopes and intercepts of each of the lines. In review, a and k_L are calculated from the following equations:

$$a = \frac{\sqrt{\text{slope}}}{C_{A_i}\sqrt{D_A}} \tag{36}$$

$$k_L = \sqrt{D_A\left(\frac{\text{intercept}}{\text{slope}}\right)} \tag{37}$$

The gas depletion in the Koch mixer was extreme, such that the "correction" became more significant than the actual measured rate of absorption. In fact, at medium and high catalyst concentrations the gas was almost completely absorbed. Therefore, it became impractical with the current experimental apparatus and procedure to obtain a Danckwerts' plot in order to evaluate a and k_L separately in this mixer. However, it was still practical to measure the rate of absorption with no arsenite and to evaluate k_La by the following formula:

$$N_Aa = k_La\ C_{A_i} \tag{20}$$

So k_La can be measured experimentally and a can be evaluated from the assumption that k_L in the Koch mixer is equal to the k_L that was experimentally measured in the Kenics and Ross mixers. The foundations for this assumption will be supplied in the following sections.

4.3.3 True Mass Transfer Coefficient

Based on the experimental results for the Kenics and Ross mixers, the true mass transfer coefficient, k_L, was found to be constant within experimental error for the gas and liquid flowrates studied. These results are presented in Table 4. The average value for k_L is 1.84×10^{-4} m/s with a standard deviation of 0.27×10^{-4} m/s. Also included in Table 4 are the predicted values of k_L from equation (6) from experimental values of d_B and ΔV. Comparison shows that the predicted values for k_L are up to 10 times larger than the experimental values and also that the predicted values vary with the flow conditions while the experimental values are essentially constant.

This analysis shows that the flow conditions and turbulence in the experimental system do not match the conditions for which equation (6) was derived. It also casts doubt on any proposed method using this equation to predict values of k_L or k_La for static mixers in a vertical configuration, i.e. the method described in Section 1.3 by Holmes and Chen.

Interestingly, the situation for which equation (6) was derived is less turbulent than the situation from which the experimental values were determined and yet the experimental mass transfer coefficients are smaller. This result as well as the constancy of k_L with changes in bubble diameter is verified by Figure 19; a plot presented by Calderbank and

Table 4

Comparison of Experimentally Determined Mass Transfer Coefficients and Values Predicted by Equation (6)

V_L	V_G	$1-\epsilon$	ΔV	d_B	eq. (6) k_L	exp. k_L
m/s	m/s		m/s	m	m/s	m/s
				$x10^4$	$x10^{-4}$	$x10^{-4}$
0.630	0.146	0.93	1.41	3.13	28.1	1.64
0.450	0.146	0.90	0.96	7.96	14.6	1.81
0.193	0.146	0.88	1.00	18.27	9.8	1.92
0.450	0.219	0.87	1.17	7.58	16.5	1.70
0.450	0.073	0.95	0.99	6.20	16.7	2.13
0.630	0.146	0.93	1.41	5.41	21.4	2.28
0.450	0.146	0.91	1.13	11.23	13.3	1.85
0.193	0.146	0.85	0.746	31.58	6.4	1.83

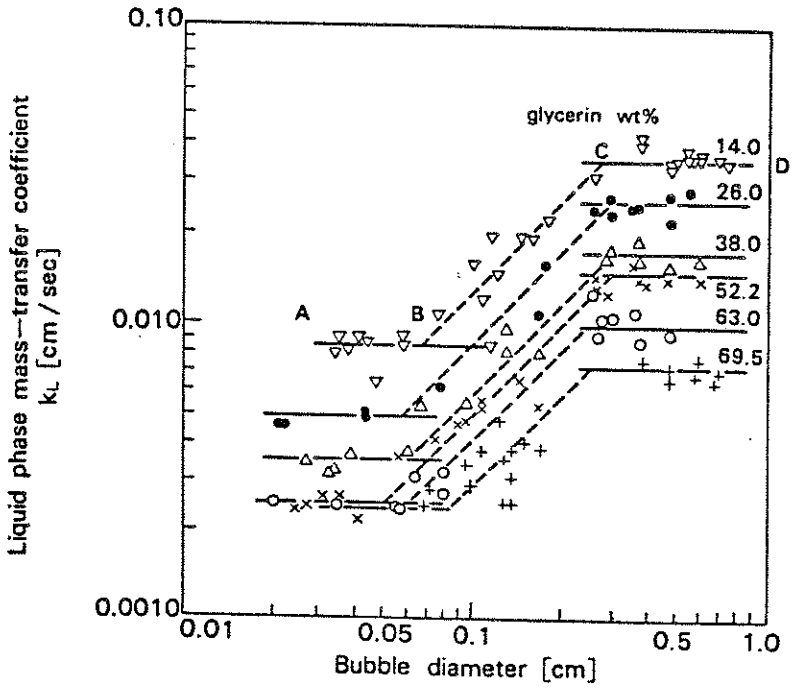

Figure 19. Effect of Bubble Diameter on the Mass Transfer Coefficient (25)

Moo-Young for carbon dioxide absorption into various glycerin solutions at 25°C in agitated vessels (25).

The abscissa of Figure 19 is the bubble diameter which is indirectly related to the turbulence created by the impeller. The figure shows that k_L goes through a decreasing transition range as the turbulence is increased. It also shows that at either end of the transition range, k_L remains constant. Most of the results of this study fall in the high turbulence range. Therefore a constant experimental value of k_L is comprehendable.

Since the degree of turbulence is higher (the bubble diameter is smaller) in the Koch mixer and the experimental k_L for the Kenics and Ross mixers was constant, then the assumption that k_L would be the same in the Koch mixer seems reasonable for the same fluids.

Wang and Fan (8) in their study of mass transfer in bubble columns filled with AY Koch mixers, suggest that:

$$k_L \propto V_L^{0.733} V_G^{0.01} \tag{38}$$

This finding definitely contradicts the above statement. Their conclusion is based on experimental correlations of k_La and ϵ given below:

$$k_La = C_1 V_L^{0.631} V_G^{0.589} \tag{3}$$

$$\epsilon = C_2 V_L^{-0.102} V_G^{0.588} \tag{4}$$

Equation (38) was derived on values of holdup correlated by equation (4), values of volumetric mass transfer coefficient correlated by equation (3), and on the assumption that area, a, is proportional to gas holdup, ϵ. Unfortunately they seemed to have missed one point. From equation (6) a is proportional to ϵ, but it is also inversely proportional to d_B, which is also a function of flowrates. The equation developed by Streiff for d_B can be written in the crude form:

$$d_B = C_3 \, V_L^{-0.85} \tag{39}$$

Since

$$a = \frac{6 \, \epsilon}{d_B} \tag{6}$$

then

$$a = C_4 \, V_L^{0.748} \, V_G^{0.588} \tag{40}$$

and therfore from (3) and (40)

$$k_L \propto V_L^{-0.117} \, V_G^{0.001} \tag{41}$$

This is now a more reasonable correlation for k_L, showing that it is a very weak function of flow conditions and showing an overall weak decrease as the turbulence, caused by increased liquid velocity.

Mangartz and Pilhofer (26) studied mass transfer coefficients in bubble columns with a similar system; air/water/carbon dioxide. They compared their results with a few correlations. These correlations are as follows:

Calderbank and Moo-Young (25)

$$k_L = 0.31 \left(\frac{\rho_L D_A}{\mu_L}\right)^{2/3} \left[\frac{(\rho_L - \rho_G)\mu_L g}{\rho_L}\right]^{1/3} \quad d_B < 2.5\text{mm} \qquad (42)$$

$$k_L = 0.42 \left(\frac{\rho_L D_A}{\mu_L}\right)^{1/2} \left[\frac{(\rho_L - \rho_G)\mu_L g}{\rho_L}\right]^{1/3} \quad d_B > 2.5\text{mm} \qquad (43)$$

Hughmark (27)

$$\frac{k_L d_B}{D_A} = 2 + 0.0187 \left[\left(\frac{d_B \Delta V}{\mu_L}\right)^{0.484} \left(\frac{\mu_L}{D_A}\right)^{0.339} \left(\frac{d_B g^{1/3}}{D_A^{2/3}}\right)^{0.072}\right]^{1.61} \qquad (44)$$

and Higbie (28)

$$k_L = 1.31\sqrt{\frac{D_A \Delta V}{d_B}} \qquad (6)$$

Of these three correlations, they found that the correlation by Calderbank and Moo-Young provided the best fit. Their measured k_L value was about constant for various gas and liquid rates and averaged around 1.0×10^{-4} m/s.

This study's value for k_L, 1.84×10^{-4} m/s is approximately 80% higher than their value. This discrepancy can be partly explained by the effect of a chemical reaction on k_L. Linek (15) in his comprehensive article mentions an experiment done using oxygen and argon as different

absorbing gases into sulphite solution with no catalyst. The argon absorption is a physical process while the oxygen absorption is chemically enhanced. Linek found that the oxygen transfer coefficients were about 50% higher than those of argon.

4.3.4 Interfacial Surface Area

This section is concerned with how experimental values of a and $k_L a$ are affected by the changes in superficial velocities. The next section will show the functional dependence of these experimental values on dissipatated power.

Figures 20 and 21 present interfacial area, a, versus V_L and versus V_G respectively for each reactor type. From these plots the following correlations were developed:

Kenics $$a \propto V_L^{1.0} V_G^{0.68} \quad (45)$$

Ross LLPD $$a \propto V_L^{0.85} V_G^{0.68} \quad (46)$$

Koch CY $$a \propto V_L^{0.67} V_G^{0.89} \quad (47)$$

The effect of V_G on area, a, in the Ross mixer was not evaluated, but it can be assumed to be similar to the Kenics mixer. The exponents for the Koch mixers are averaged from the different slopes on each plot.

The ordinate on the right hand side, which is accompanied by the closed symbols, refers to a redefinition of

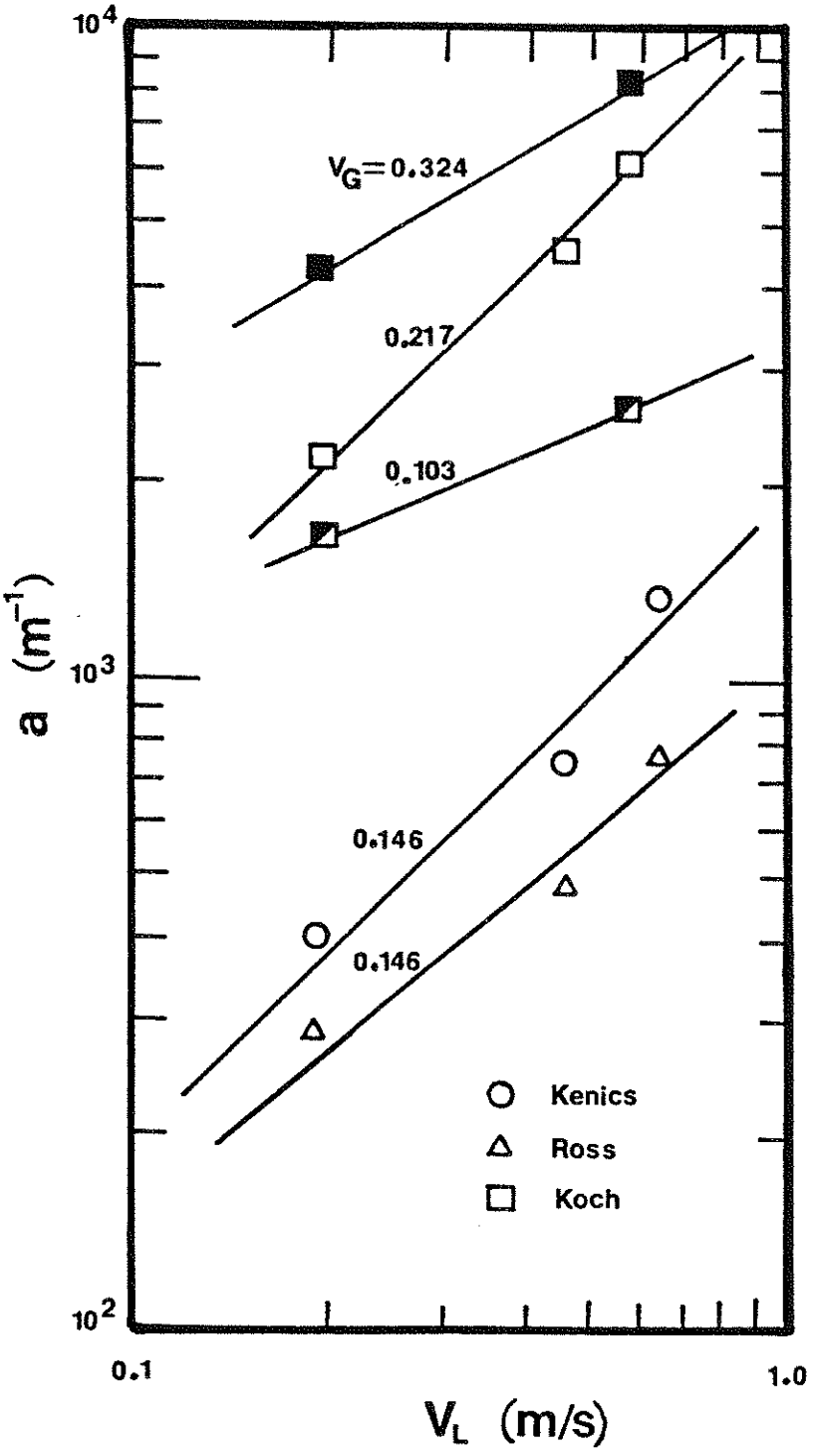

Figure 20. Effect of Liquid Velocity on Interfacial Area for All Mixers

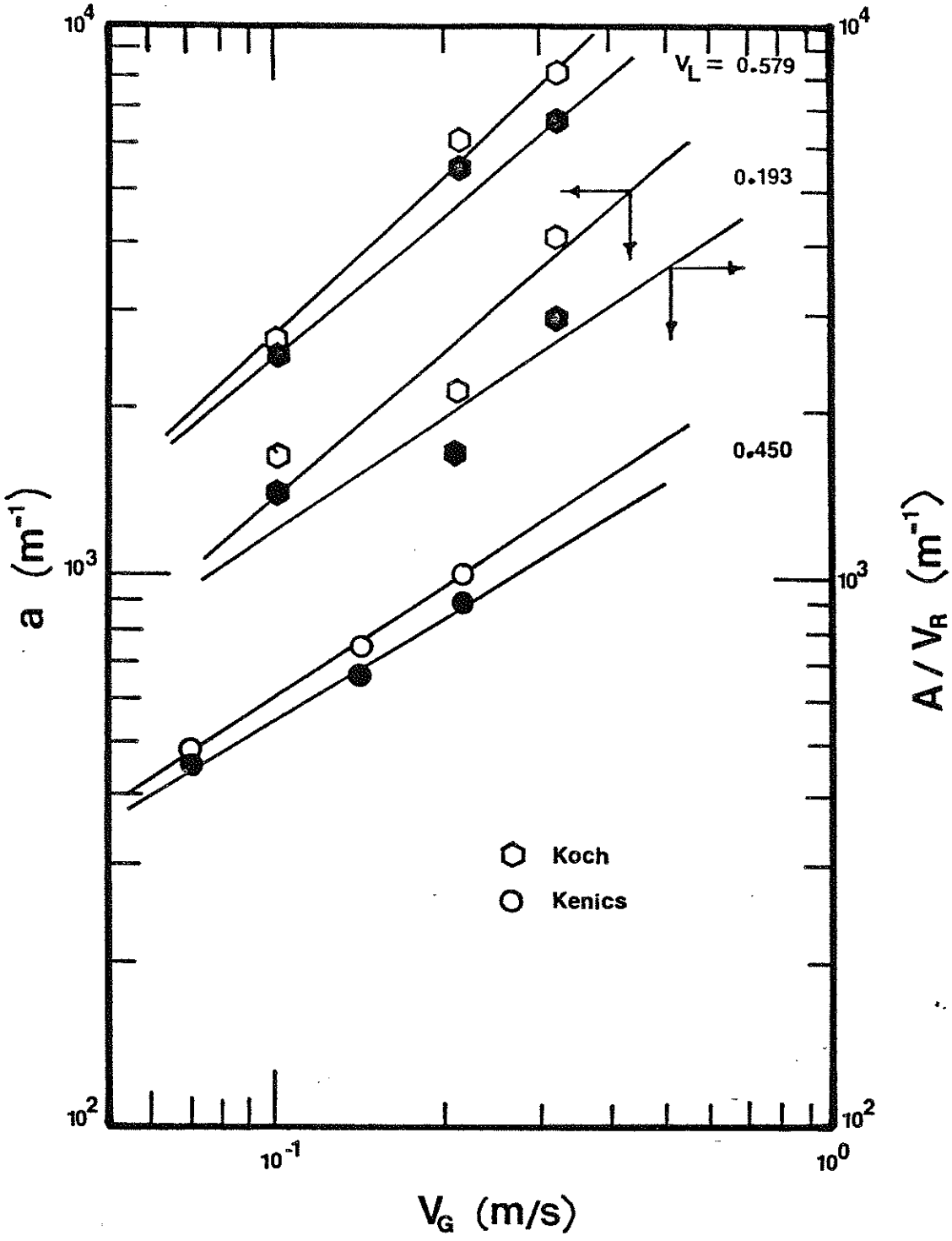

Figure 21. Effect of Gas Velocity on Interfacial Area for the Kenics and Koch Mixers

the interfacial surface area by using a basis of volume of both phases instead of volume of liquid only. This will be used in the next section.

Generally, for the same gas and liquid superficial velocities, the Kenics mixers slightly out perform the Ross LLPD mixers while the Koch CY mixer with spacers provides approximately 4 times the amount of interfacial area per unit liquid volume.

4.4 Efficiency of Static Mixers

The efficiency of a gas/liquid contactor can be found by determining the amount of interfacial area for a given dissipated power. By plotting values of interfacial area per unit volume of liquid, a, versus the dissipated power per unit liquid volume, P_w, for different gas/liquid contactors on the same figure, the efficiency of the different contactors can be compared.

Figure 22 is an efficiency plot for the results of this study for the three different static mixers. This figure shows that the Ross LLPD mixer is the least efficient and that the CY Koch mixer with spacers is the most efficient. The Koch mixer can produce up to 3 times more interfacial area for the same power input that the Kenics mixer.

One desired result of this study is to compare these efficiencies to other gas/liquid contactors. Nagel et al. (29, 30) have done studies of interfacial area in various gas/liquid contactors and presented the results for one gas

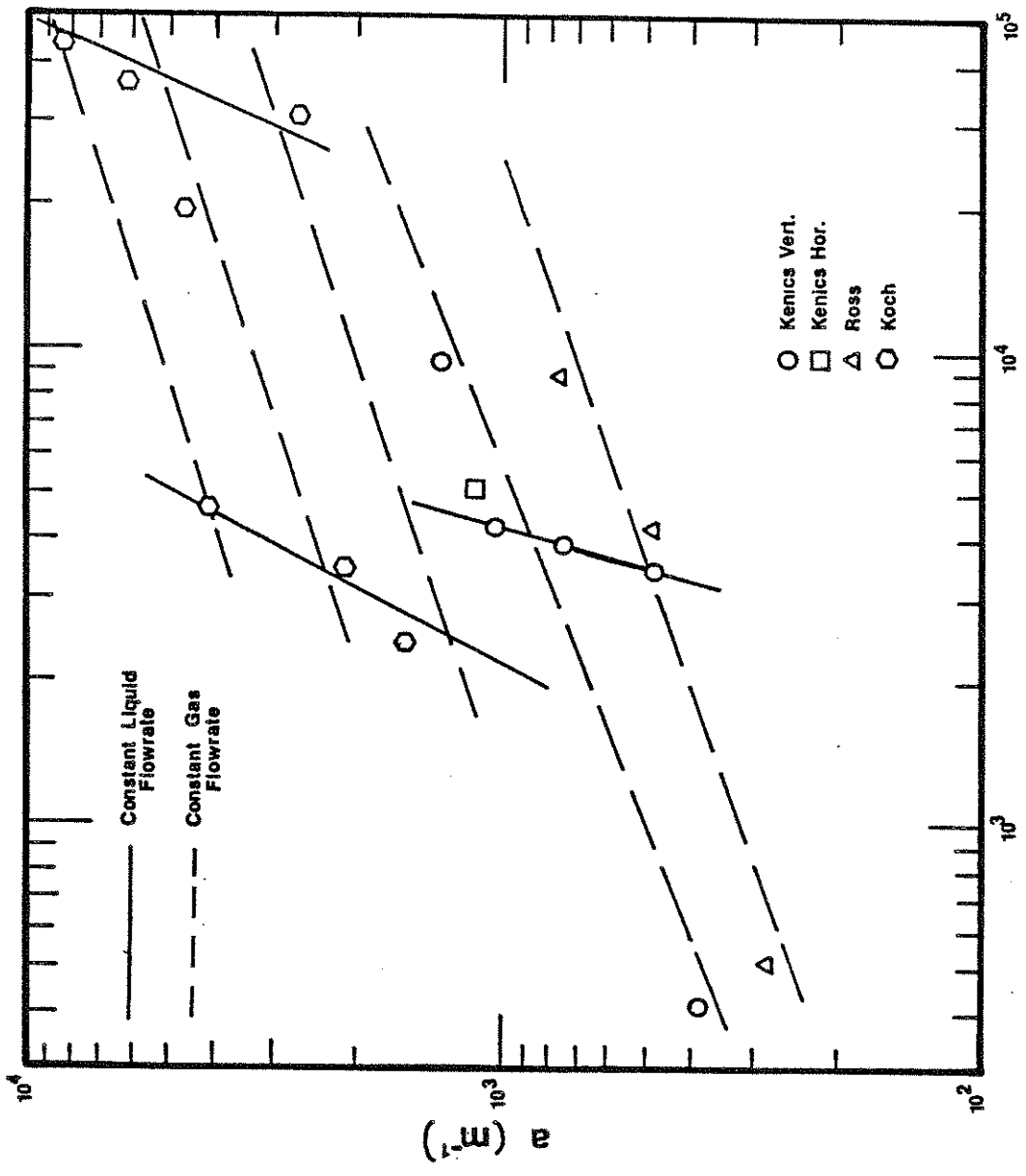

Figure 22. Comparative Efficiencies of the Static Mixers at Various Flow Conditions

flowrate versus power dissipation. Before this data is presented, some details need to be addressed.

First, Nagel's interfacial areas were also determined by a chemical method, only the chemical reaction used was the absorption of oxygen into sulphite solution. Although, his results are for a different chemical systems, Alper (31) showed experimentally that the two chemical systems (carbon dioxide absorption into carbonate/bicarbonate buffer solution with an arsenite catalyst and oxygen absorption into sulphite solution with a cobalt catalyst) give essentially the same interfacial areas.

Second, Nagel defines his interfacial area and power dissipation per unit two phase volume instead of volume of the liquid only. So all the subsequent results needed to be multiplied by the appropriate liquid holdup values.

Finally, Nagel's data is only for one gas flowrate of 0.047 m/s and undetermined liquid flowrates. Unfortunately this particular gas velocity was impratical to perform experimentally in the static mixers. Therefore, since it is apparent from Figure 22 that the gas rate does affect the efficiency of the mixers significantly, this study's results need to be adjusted to this lower gas rate before a comparison could be made.

Nagel (29) does suggest a correlation to account for the effect of the gas rate. In this study's terminology this correlation becomes:

$$\frac{A}{V_R} = C_5 \left(\frac{E}{V_R}\right)^m V_G^n \qquad (48)$$

where $\frac{A}{V_R}$ = Interfacial area per unit reactor voidage, (m^{-1}); and

$\frac{E}{V_R}$ = Power dissipation per unit reactor voidage, (W/m^3).

Plotting $((A/V_R) \cdot V_G^{-n})$ versus (E/V_R) should create a single line instead of a family of lines. The exponent on the gas velocity for the static mixer are from the previous sections analysis. Figure 23 is such a plot with each reactor. From this plot C_5 and m are calculated and the final correlations are as follows:

Kenics $$\frac{A}{V_R} = 77 \left(\frac{E}{V_R}\right)^{0.42} (V_G)^{0.59} \qquad (49)$$

Ross LLPD $$\frac{A}{V_R} = 34 \left(\frac{E}{V_R}\right)^{0.48} (V_G)^{0.59} \qquad (50)$$

Koch CY $$\frac{A}{V_R} = 344 \left(\frac{E}{V_R}\right)^{0.37} (V_G)^{0.76} \qquad (51)$$

Now that these correlations have been developed it is easy to backtrack and calculate interfacial areas at the gas velocity of 0.047 m/s for various power inputs and then plot

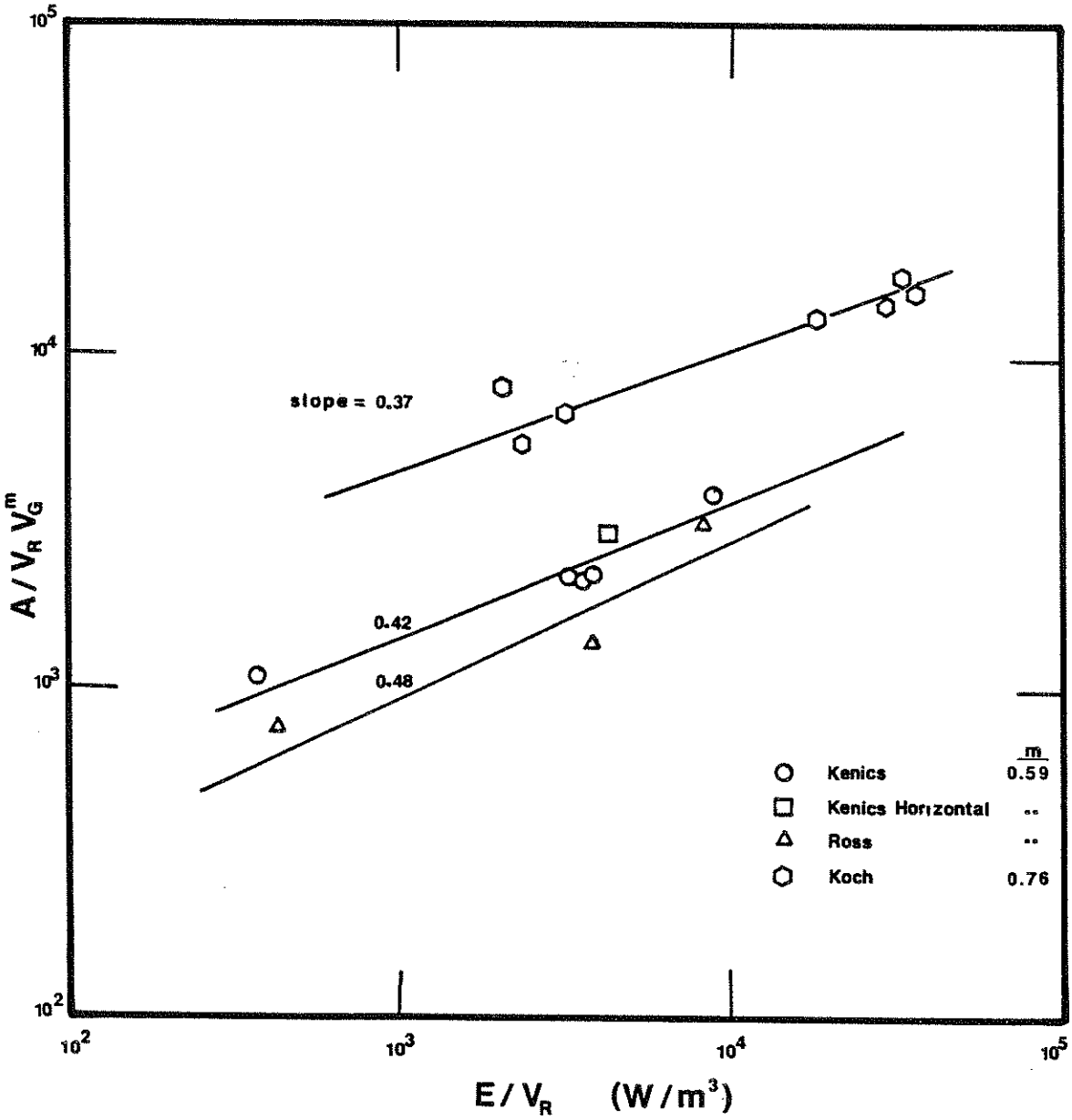

Figure 23. Efficiencies of the Static Mixers that Account for Variable Gas Flowrates

these values on Nagel's diagram (30). This was done and the final result is Figure 24. This figure shows that only the Koch mixer is competitive to the other gas/liquid contactors.

Although this plot is only valid for one gas flowrate, its validity could be extended to all gas flowrates if the other contactors have roughly the same relationship between the interfacial area and gas flowrate. This point is important since it is not recommended to operate static mixers at this gas flowrate, whereas the other devices may be well suited for this low gas rate. Refering to equation 48, the exponent n equals 0.5 and 0.7 for the packed and bubble columns, respectively (32), but less than 0.5 for a stirred tank (33). So Figure 24 would be an adequate representation of the comparative efficiences for the static mixers and the packed and unpacked bubble columns. Depending on the exact value of n for stirred tanks, the static mixers' efficiencies may become more comparable to stirred tanks at higher gas flowrates.

From the equations 49 through 51, the exponents of the power dissipation for the static mixers are around 0.4. This is the same as the exponent for packed columns and two-phase vertical and horizontal flows in empty pipes. It also corresponds to the theoretical value of 0.4 from Kolmogoroff's theory of area production (29). However, stirred tanks have a much higher exponent than these other mixers which has been shown to be of the order of 0.8.

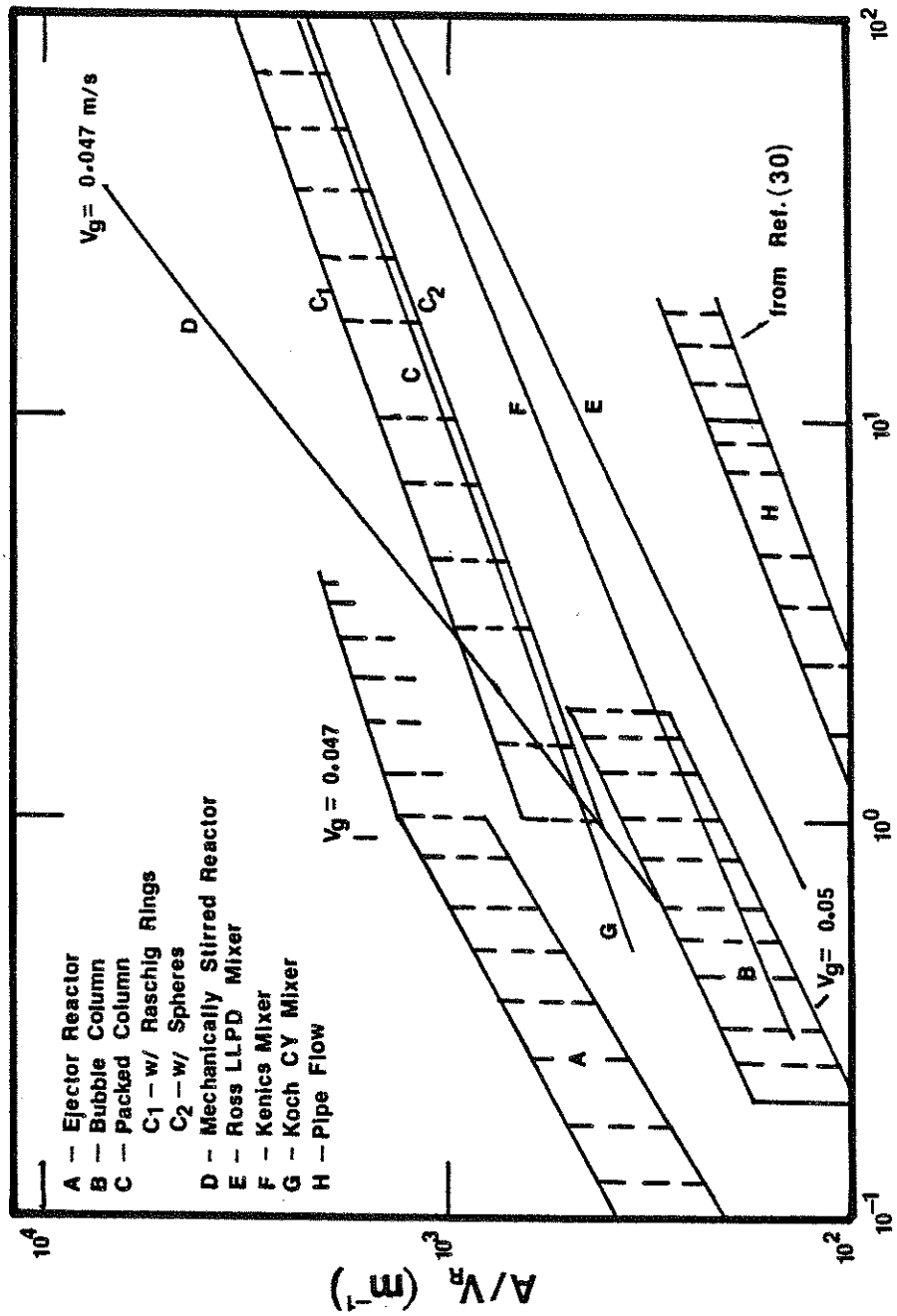

Figure 24. The Efficiencies of the Static Mixers Compared with Other Gas/Liquid Contacting Devices at One Gas Velocity

Middleton (3) reports that from k_La measurements that the exponent to which dissipated power is raised for all gas/liquid contactors including static mixers is 0.8. From the assumption that k_La and a differ only by the constant factor of k_L (providing that the power input is high enough to be past the transition range) this is equivalent to claiming that the interfacial area is proportional to the rate of energy dissipation raised to a power of 0.8. Middleton (3) arrives at that conclusion based on his interim experimental results of k_La values in gas/liquid upflow for empty tubes and tubes containing meshes, Kenics mixers, Sulzer (Koch) mixers, and Etoflo mixers.

Figure 25 is his figure for interfacial area versus power dissipation including only his Kenics and Sulzer (Koch) mixer results. Line A is the line plotted by Middleton through all his data based on which his conclusion is formulated. The raw data is unquestionable but the analysis seems incorrect. In light of this study it would seem more appropriate to construct two separate lines; one line correlating the Sulzer (Koch) data (line C) and one line passing through the Kenics data (line B). If this is done, the exponents for the dissipated power are 0.48 for the Kenics mixer and 0.47 for the Sulzer (Koch) mixers which are more consistant with the findings of this study.

No information about which type of Sulzer (Koch) mixer was used, nor about the specific gas and liquid rates was reported by Middleton. However, the data of this study

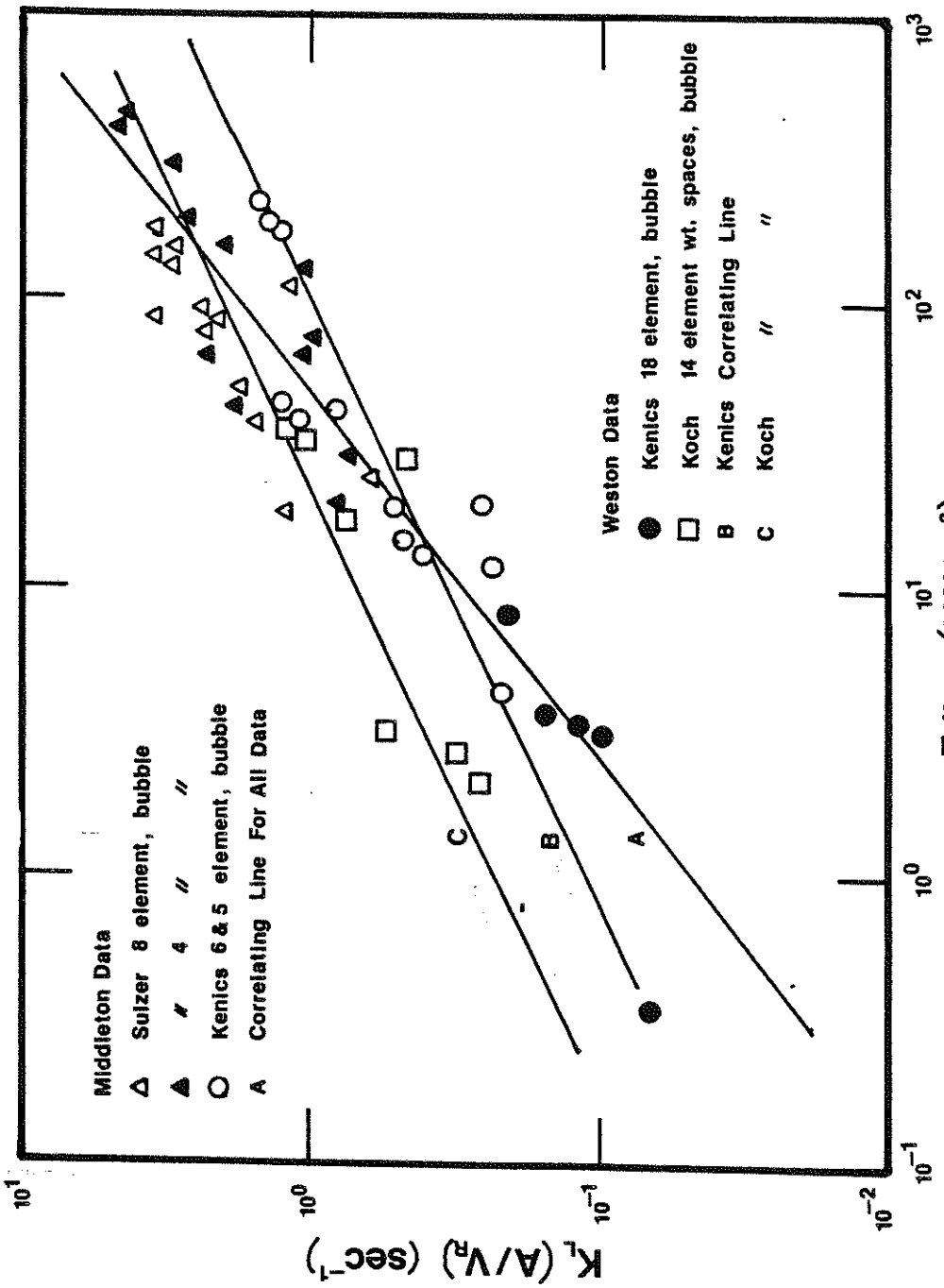

Figure 25. Interfacial Area versus Power Dissipation Containing This Study's Results and Middleton's Results (3)

plotted on Figure 25 seems to correlate well with Middleton's results and to extend them to a broader range.

4.5 COMMENTS

4.5.1 Spacing

The reason for spacing the Koch CY mixers in the pipe was an attempt to get the same reactor length. Since Wang and Fan found that the use of spacers did not significantly reduce the mass transfer, and since it did reduce the pressure drop across the reactor, it made sense to use the spacers. It may even be the only reason why the Koch mixer was as efficient as it was found to be.

This does raise an interesting question. If the same reactor was used, but the spacers were doubled in length, would the reactor be more efficient? Unfortunately, no studies were done specifically to answer this question. However it seems logical that there should be an optimal spacing to maximize the efficiency of the reactor which may occur when the average time required for to bubbles to coelesce equals the travel time of a fluid element containing those two bubbles to travel between two mixer elements.

Since the Kenics mixers are more efficient than an empty pipe, it also raises the possibility that a combination of Koch and Kenics mixers, where the Kenics mixer replaces the spacer, might be a very efficient mixer.

4.5.2 Horizontal Mixers

This study was basically involved with static mixers in a vertical position. The reason for doing the experiments

in that configuration was that the holdup measurements were easier to accomplish and that there was positively no layer separation.

Since industrial users potentially are more interested in these mixers in a horizontal configuration, one absorption run was done in a horizontal Kenics mixer. The results showed that the horizontal mixer was just as efficient as the vertical mixer. In fact, the amount of interfacial area created was greater than that in a vertical mixer. The reason for this is because of the larger gas holdup in the horizontal reactor. From the holdup measurements, the horizontal mixer always has a larger holdup. Therefore, it is reasonable to assume that for nearly all flow conditions, the amount of interfacial area produced in a horizontal reactor will be greater than in the vertical reactor.

4.5.3 Chemical Method Usefulness

One of the underlying goals of the project was to test the usefulness of the carbon dioxide absorption chemical method for the determination of k_L and a separately. Also, another equally important purpose was to develop or refine the titration methods necessary to properly measure the amount of absorption. Some overall comments, more than just an error analysis, need to be presented.

The liquid side evaluation of absorption through titrations should be avoided if possible. If the measurements can be accomplished on the gas side either by

flowrate measurements or gas chromatography without causing experimental difficulties such as excessive pressure requirements or sophisticated sampling equipements then this should be prefered. This statement arises form the complexity, heavy time requirements and significant errors of the titrations.

If gas side measurement is definitely not feasible, then to reduce the time and error of the titrations, the experimentor should try to operate at low concentrations of the catalyst. The reduced concentration of the arsenite makes the titrations more accurate and somewhat easier.

Dr. Ashok Gokarn (34) is currently working on a project in which gas side measurements are impractical and is therefore utilizing the titration methods developed by this study. He is using catalyst concentrations up to 0.25 M and his preliminary comments suggest that the method is useful and the results from the experiments are satisfactory.

If the experimenter needs to use high concentrations of the catalyst for any reason (i.e. higher rates of absoption or higher Hatta numbers) then another system like oxygen absorption into sulphite solution using a cobalt catalyst should be seriously considered.

Concerning the usefulness of measuring k_L and a separately, it should be mentioned that since k_L was found to be a constant, a definite value for k_L was measured and it seems to be reasonable with respect to what is currently reported in the literature. Since k_L is a parameter that is

very dependent on a particular chemical system, it is valuable to experimentally determine a value for it.

When a value for k_L is obtained it is no longer necessary to measure area, a from a Danckwerts' plot. All that is required is to measure k_La and divide by the known value of k_L. The measurement of k_La and the subsequent titrations are an order of magnitude easier and more accurate, since this measurement relies on the titration of the solution with no arsenite. Remember that the although the buffer solution does not contain arsenite the absorption is still chemically enhanced and the k_L measured from the Danckwerts' plot is the appropriate value.

If future experiments were to be done regarding the optimal Koch mixer spacing, only k_La needs to be determined, as long as the same solution (i.e. concentrations and ionic strengths) were used.

4.5.4 Error Analysis

A simple minded error analysis was done on the calculated values of the interfacial surface area and mass transfer coefficient. The major error in the analysis was brought about by the titration errors. All other measurement errors were significantly smaller.

Each titration to determine the bicarbonate concentration before and after a run was done at least three times. From those three values an average and an error was calculated. Since the change in concentration was

the desired result, the subtraction was made and the errors added. From this, a percentage error was calculated.

One set of flow conditions was repeated once for various arsenite concentrations and the resulting deviations were within the titration error. The experimental procedure of dilution was tested also by repeating a zero catalyst concentration run at a single flow condition four times. The results were all within titration error.

After the gas correction was taken and the resulting values of $(N_A a)$ were plotted on a Danckwerts' plot, the percentage errors (now doubled because of the square) were also plotted as error bars. A sample plot is given in Appendix 7.7. Then three lines were drawn , one of high slope, one of low slope and the best eye reckoned slope through the points and error bars. From the deviations of the resulting values of a and k_L, a new percentage error was determined.

The run that was selected to present this error analysis in Appendix 7.7 was an early run when the errors were very large. Therefore this analysis should give a maximum error.

The error in the values of area, a are 15% and for k_L are 31%. In the case of the Koch mixer where no Danckwerts' plots were used the error of area, a, was equal to the titration errors which were no more than 10%.

4.5.5 Hatta Numbers

For the results to have meaning, the conditions as specified by the derivation in Appendix 7.8 for the Hatta number and the instantaneous enhancement factor must be satisfied. The Hatta numbers, depending on the catalyst concentrations, ranged from 0.3 to 2.8. The instantaneous enhancement factor was calculated and was equal to 21. So the condition:

$$E_i /2 >> Ha \qquad (52)$$

was satisfied. However, the suggested requirement (15) on the Hatta number:

$$Ha >> 3 \qquad (53)$$

was not satisfied. This is not as debilitating as it may seem at first sight. Appendix 7.8 is an analysis on the effect of low Hatta numbers on the enhancement factor. It is shown that the first criterion, equation (52), must be satisfied but that the second one, equation (53), may be unnecessary.

This analysis also shows that for all but the zero concentration points, the error due to low Hatta numbers is less than 1%. For the zero catalyst concentration points the error is less than the titration errors.

5. SUMMARY, CONCLUSIONS AND RECOMMENDATIONS

5.1 SUMMARY OF RESULTS

The primary objective of this study was to determine the relative efficiency of static mixers as gas/liquid contactors. This was accomplished through an experimental investigation of interfacial areas and mass transfer coefficients obtained per dissipated power for gas/liquid co-current upflow.

Experiments were performed on three different types of static mixers, namely:

1) Kenics;

2) Ross LLPD;

3) Koch CY with spacers;

placed in a 1 inch diameter pipe. The experimental apparatus was set up for evaluation of liquid holdup and total pressure drop as well as for the parameters necessary to evaluate interfacial areas and mass transfer coefficients.

The interfacial areas and mass transfer coefficients were determined with a chemical method and the use of Danckwerts' plots for a chemical system of carbon dioxide absorption into carbonate-bicarbonate buffer solution with arsenite catalyst. All experiments were conducted at atmospheric pressure and room temperature.

The operating variables (i.e. V_L and V_G) were chosen so that the operating flow conditions were in the bubble flow

regime. The experimental fluid velocities cover the range: V_G = 0.073 to 0.324 m/s and V_L = 0.193 to 0.630 m/s.

The liquid holdup, $1-\epsilon$, ranged from 0.97 to 0.70 and varied with gas and liquid flowrates. Each mixer type differed in how the holdup varied with these parameters. Neither the homogeneous model nor the Lockhart-Martinelli correlation accuratly predicted the holdup values.

The Koch and Kenics mixers had holdup configurations similar to those found by Yung-Hsu for gas-lift reactors. The following correlation form was suggested:

$$\frac{(1-\epsilon)}{\epsilon} = D \left(\frac{V_L}{V_G}\right)^m \qquad (34)$$

where $D = f(V_L, \rho_L, \mu_L, \sigma...)$

The same form could be used for the Ross mixer, except the leading term, D, would be a constant.

The Kenics mixer in a horizontal configuration gave liquid holdups smaller than in a vertical position at all flow conditions.

The Koch CY mixer produced the largest kinetic pressure drop per unit length of the three mixers tested. It's pressure drop ranged from 10 to 65 kPa/m which was 5 times greater than the Kenics and Ross mixers. The pressure drop, like the holdup was a function of the gas and liquid flowrates. Increased gas flowrate increased the pressure drop.

Table 4 presents the results of the absorption experiments. These results showed that k_L was not a function of flowrates and averaged out at a value of 1.84×10^{-4} m/s.

Table 4

Summary of Experimental Results

Mixer	V_L	V_G	$1-\epsilon$	a	k_L	k_La	P_w
	m/s	m/s		m^{-1}	m/s $x10^4$	s^{-1}	W/m^3 $x10^{-3}$
Kenics Vert.	0.630	0.146	0.93	1340	1.68	0.225	9.43
	0.450	0.146	0.90	754	1.81	0.136	3.90
	0.193	0.146	0.88	394	1.92	0.076	0.42
	0.450	0.219	0.87	1030	1.70	0.175	4.36
	0.450	0.073	0.95	484	2.13	0.103	3.44
Kenics Hor.	0.450	0.146	0.82	1140	1.34	0.152	5.11
Ross LLPD	0.630	0.146	0.93	776	2.28	0.177	8.84
	0.450	0.146	0.91	481	1.85	0.089	4.22
	0.193	0.146	0.85	285	1.83	0.052	0.52
Koch CY with spacers	0.193	0.324	0.70	4180	1.84	0.769	4.64
	0.193	0.217	0.79	2150	1.84	0.395	3.47
	0.193	0.103	0.88	1620	1.84	0.298	2.42
	0.450	0.217	0.89	4600	1.84	0.847	19.8
	0.579	0.217	0.83	8150	1.84	1.50	43.9
	0.579	0.217	0.91	6140	1.84	1.13	36.1
	0.579	0.103	0.96	2690	1.84	0.494	30.6

The amount of interfacial area per unit liquid volume varied with liquid and gas flowrates according to the following relationships:

Kenics $$a \propto V_L^{1.0} \; V_G^{0.68} \tag{45}$$

Ross LLPD $$a \propto V_L^{0.85} \; V_G^{0.68} \tag{46}$$

Koch CY $$a \propto V_L^{0.67} \; V_G^{0.89} \tag{47}$$

The Koch mixer produced 4 times more interfacial area at any given flow conditions than the others, while the Kenics mixer was twice as productive as the Ross mixer.

The comparative efficiencies of the static mixers are reflected in the following correlations:

Kenics $$\frac{A}{V_R} = 77 \left(\frac{E}{V_R}\right)^{0.42} (V_G)^{0.59} \tag{49}$$

Ross LLPD $$\frac{A}{V_R} = 34 \left(\frac{E}{V_R}\right)^{0.48} (V_G)^{0.59} \tag{50}$$

Koch CY $$\frac{A}{V_R} = 344 \left(\frac{E}{V_R}\right)^{0.37} (V_G)^{0.76} \tag{51}$$

The Koch CY mixer with spacers was the most efficient of the static mixers tested as gas/liquid contactors. When compared with other gas/liquid contactors, the Koch mixer was competitive with a packed bubble column reactor.

5.2 CONCLUSIONS

The main conclusion of this study is that the Koch CY mixer with spacers is a more efficient gas/liquid contactor than a Kenics or Ross LLPD static mixer.

The other conclusions of this study are as follows:

1) The Koch CY mixer with spacers provides five times more interfacial area per power dissipated than the Kenics mixer and 10 times more than the Ross mixer.

2) As a general rule for static mixers:

$$\frac{A}{V_R} \propto \left(\frac{E}{V_R}\right)^{0.4}$$

which is the same dependence as that found for packed bubble columns, bubble columns and empty pipes.

3) The Koch mixer is competitive with the packed column as a co-current gas/liquid contactor.

4) The mass transfer coefficient, k_L, is not a function of the liquid or gas velocities for gas bubble diameters less than 3.0×10^{-3}m in the static mixers.

5) The commonly used homogeneous model and Lockhart-Martinelli correlation do not adequately predict holdup and pressure drops for co-current gas/liquid upflow in static mixers.

5.3 RECOMMENDATIONS

The following are recommendations directed toward industry:

1) If the unique charateristics that a static mixer gives are prefered, (i.e. plug flow characteristics, low maintainance costs, horizontal configuration, radial thermal homogenization ...) then pack the tubular reactor with Koch CY mixers with element sized spacers.

2) If mixing is currently done in a pipe with no mixers, then better mixing efficiency can be accomplished by using static mixers.

The following recommendations are directed toward further experimentation:

3) Studies concerning the optimal spacing of the Koch CY mixers should be done.

4) Better correlations need to be devised to accurately predict pressure drop and holdup in vertical and horizontal two phase flow in static mixers.

7. ACKNOWLEDGMENTS

The author wishes to express his sincere graditude to Professor M. Dudukovic for his scientific guidance throughout this investigation as well as his commitment to reliability and completeness that are so important in scientific endeavors.

The financial support provided by the Chemical Reaction Engineering Laboratory of Washington University is gratefully acknowledged.

Thanks are also extended to Monsanto Company, Chemineer/Kenics Corporation, Koch Engineering Company and Charles Ross and Son Company for their generous equipment contributions for the study.

Finally, I wish to thank Anna-Maria, my loving wife, for her encouragement, support and optimism which were invaluable for the successful completion of this thesis.

7. APPENDICES

APPENDIX 7.1

Derivation of Rate of Absorption for Single Irreversible (Pseudo) First Order Reaction

The unsteady mass balance for gas A around a one dimensional element of liquid B with a pseudo-first order irreversible reaction can be written as:

$$\frac{\partial C_A}{\partial t} = D_A \frac{\partial^2 C_A}{\partial y^2} - rC_A \tag{54}$$

with the following boundary conditions:

$$y = 0 \qquad t > 0 \qquad C_A = C_{A_i} \tag{55}$$

$$y = \infty \qquad t > 0 \qquad C_A = 0 \tag{56}$$

and initial condition:

$$t = 0 \qquad y > 0 \qquad C_A = 0 \tag{57}$$

This partial differential equation can be solved by the method of Laplace Transforms to give:

$$\bar{C}_A = \frac{C_{A_i}}{s} \exp\left[-\sqrt{\frac{s+r}{D_A}}\, y\right] \tag{58}$$

The molar flux of A at any time, t, across the gas/liquid interface by definition is given by the following equation:

$$N_A(t) = -D_A \left.\frac{\partial C_A}{\partial y}\right|_{y=0} \tag{59}$$

Danckwerts' surface renewal theory provides the following equation for the average molar flux:

$$N_A = \int_0^\infty N_A(t)\ se^{-st}\ d\ t \tag{60}$$

Replacing Equation (59) into Equation (60), reversing the differentiation and integration and using the definition of Laplace Transforms the following equation is obtained:

$$N_A = -D_A s \left.\frac{\partial \bar{C}_A}{\partial y}\right|_{y = 0} \tag{61}$$

The molar flux can now be solved by substituting Equation (58) into the above and performing the differentiation;

$$N_A = C_{A_i} \sqrt{D_A(s+r)} \tag{62}$$

Now a relationship for s can be obtained by letting $r \to 0$ and substituting for N_A with the expression for the flux due to physical absorption in terms of the mass transfer coefficient: This gives:

$$s = \frac{k_L^2}{D_A} \tag{63}$$

By substituting equation (63) into equation (62), dividing through by k_L^2 and using the definition of the Hatta number as expressed in equation (17), the molar flux can be written as:

$$N_A = k_L a \, C_{A_i} \sqrt{1 + Ha^2} \tag{22}$$

This equation provides the definition of the enhancement factor for absorption of gas A into a liquid B with an irreversible pseudo first order reaction using Danckwerts' surface renewal theory and can be expressed as:

$$E_L = \sqrt{1 + Ha^2} \tag{21}$$

According to Linek (15), for this derivation to hold true, two conditions must be satisfied:

$$1) \quad E_{i/2} \gg H_a \tag{53}$$

$$2) \quad H_a \gg 3 \tag{54}$$

where $E_i = 1 + \frac{D_B}{D_A} \frac{C_{B_o}}{C_{A_i}}$ (18)

and $H_a = \frac{\sqrt{D_A \, r}}{k_L}$ (17)

These requirements will be discussed in Appendix 7.8.

APPENDIX 7.2

Holdup, Total Pressure Drop and Absorption Procedures

7.2.1 Hold Up Procedure

1) Disconnect the two pressure tap lines, sealing the top one and attaching a shut-off valve on the bottom tap. Also disconnect the gas line from the bottom of the reactor and attach another shut-off valve.

2) Fill column with water, including the separator.

3) Measure the volume of liquid that drains out of the bottom pressure tap. Record this volume as u1.

4) Measure the volume of the remaining liquid that drains out of the gas inlet to the reactor. Record this volume as u2.

5) Reconnect the gas line to the bottom of the reactor.

6) With the gas and liquid streams flowing at the desired rates and the liquid level in the separator stable and below the wire screen, quickly and simultaneously shut off the master switch (which controls both the gas solenoid valve and the pump in this case) and the liquid on-off valve, v2.

7) Allow liquid to settle in the reactor.

8) Measure the volume of liquid that drains from the bottom pressure tap. Record this volume as u3.

9) Calculate and record the liquid holdup:

$$\epsilon = (u3 - u2) / (u1 - u2) \qquad (64)$$

7.2.2 Total Pressure Drop Procedure

1) Measure the distance between the two pressure taps on the reactor. Record this distance as L_2.

2) Using water as the process fluid, circulate the water throughout the system allowing water to fill the pressure tap lines. For water, the purge stream apparatus is not needed.

3) Turn on gas flow and adjust to the desired rate. Maintain steady conditions.

4) Measure the difference in height of the two manometers. Record this difference as L_T.

5) Calculate and record the total pressure drop:

$$\Delta P_T = (L_1 + L_2) g \rho_{H_2O} \qquad (29)$$

7.2.3 Mass Transfer Procedure

The following sections provides a detailed procedure for one run.

7.2.3.1 Initial Solution Preparation

1) Fill container with 8 liters of water.

2) Accurately weigh out 508.8 grams of Na_2CO_3 and 134.6 grams of $NaHCO_3$ in separate weighing containers in order to make an 8 liter buffer solution of 0.6 M carbonate and 0.2 M bicarbonate.

3) Add the solids to the 8 liters and mix completely with electic stirrer.

4) With the nitrogen slightly flowing, turn on pump and circulate the solution throughout the system for a few minutes.

5) Pipet 10 ml of solution and accurately titrate with 1 N HCl for total base concentrations (TBC). See TBC procedure on page 107. Record the intital and final buret readings. Their difference will equal $\Delta 1$.

6) Calculate and record the true volume of the solution:

$$V_{b\ (true)} = 8\ (l)\ \frac{14\ (ml)}{\Delta 1\ (ml)} \qquad (65)$$

7) Add 500 grams (1 bottle) of $NaAsO_2$ to solution and mix completely.

8) Again with the nitrogen barely flowing, activate the pump and circulate the solution throughout the system for a few minutes.

9) Pipet 10 ml of activated solution and accurately titrate with 1 N HCl for TBC. Record initial and final buret readings. Their difference will equal $\Delta 2$.

10) Calculate and record true concentration of arsenite catalyst, [Ars]:

$$[Ars1] = \frac{\Delta 2\ (ml) - \Delta 1\ (ml)}{10\ (ml)} \times 1\ N \qquad (66)$$

11) Calculate and record the grams of NaCl needed to maintain the ionic strenghth of the solution at 2.5.

$$Grams_{NaCl} = (0.5 - [Ars])(V_{b(true)})(58.44) \quad (67)$$

12) Accurately weigh and add desired amount of NaCl to the solution. Again circulate solution throughout system to assure homogeneity.

7.2.3.2 Reaction Procedure

13) With the nitrogen flowing slowly, set liquid rate using pump motor variac to the desired flowrate refering to the liquid flowmeter. (It may be necessary to use the liquid control valve to help adjust the liquid flowrate especially at low levels).

14) Adjust the pinch valve on the separator outlet tubing in order to achieve and maintain the proper liquid level in the separator. The liquid level should be just above the wire screen.

15) Turn the master power switch off. This turns off the gas solenoid, but leaves the pump on. The pump should not be connected to the main power source.

16) Shut the nitrogen flow valve off, v_4, and open the CO_2 valve, v_3. Make sure that the CO_2 preheater is on.

17) Reset the timer which is connected to the main power source.

18) Collect a 50 to 75 ml sample of the initial solution from the outlet of the separator tube. Cap and label the flask "BEFORE".

19) Turn the master switch on and quickly adjust the CO_2 gas flowrate with the control valve to the desired flowrate refering to the gas inlet rotameter.

20) As the run proceeds, adjust and maintain the gas and liquid flowrates as well as the liquid level in the separator.

21) At the desired time, turn the master power switch off and quickly shut off the inlet gas control valve to assure that no CO_2 is inputed.

22) Open the separator outlet pinch valve and allow the solution to continue to circulate for a few minutes in order to assure a homogenous concentration.

23) Fill and label a second erlenmeyer flask with 50 to 75 ml of the final solution. Cap and label the flask "AFTER". Set the flask aside with "BEFORE" sample.

7.2.3.3 Dilution Procedure

24) Pipet out 10 ml of the batch solution and titrate the concentration of bicarbonate using the procedure on page 108. Record the initial and final buret readings. Their difference will equal $\Delta 3$.

25) Calculate and record the concentration of bicarbonate, $[HCO_3^-]$:

$$[HCO_3^-] = \frac{5 - (\Delta 3 \text{ (ml)} - 10 \times [Ars])}{10} \quad (68)$$

26) Calculate the volume of solution to be removed and replaced by the same volume of water in order to obtain a bicarbonate concentration of 0.2 M by the following equation:

$$V_{b_{(replace)}} = V_{b_{(true)}} \times \left[1 - \frac{0.2}{[HCO_3^-]} \right] \qquad (69)$$

27) Remove a volume of solution equal to the volume calculated above less that volume that has previously been removed for samples and titrations. Add a volume of water equal to the volume calculated in step 26) to the remaining solution and circulate the solution throughout the apparatus.

28) Pipet out 10 ml of the diluted solution and titrate for the TBC. Record both the initial and final buret readings. Their difference will be $\Delta 4$.

29) Calculate and record actual dilution ratio, D_R, in order to determine the new concentrations of all the ionic species.

$$D_R = \Delta 4 \text{ (ml)} / \Delta 2 \text{ (ml)} \qquad (70a)$$

30) Record the new concentration of asenite, [Ars2]:

$$[Ars2] = [Ars1] \times (D_R) \qquad (70b)$$

31) Calculate the quantities of carbonate and bicarbonate needed to add in order to boost their concentrations to 0.6 M and 0.2 M, respectively (based on $V_{b_{(true)}}$).

32) Add the carbonate and bicarbonate to the solution, mix and homogenize. Again pipet out 10 ml of new concentrated solution and titrate for the TBC. Record both initial and final readings. Their difference will be $\Delta 5$.

33) Calculate and record the actual volume by the following equation:

$$V'_{b\,true} = \left[\left(\Delta 4 \left(V_{b_{(true)}} \right) \right) + \left(\frac{2 \cdot Grams_{Na_2CO_3}}{106} \right) + \left(\frac{Grams_{NaHCO_3}}{84} \right) \right] \Big/ \Delta 5 \qquad (71)$$

34) Calculate and add the amount of NaCl needed to maintain the ionic strength of the system equal to 2.5. This can be determined by the following equation:

$$Grams_{NaCl} = 58.44 \times V'_{b\,(true)} \times (0.5 \times (1 - D_R)) \qquad (72)$$

35) Repeat steps 14) to 34) until [Ars] < 0.1 M.

7.2.3.5 Determination of CO_2 Absorption

1) Titrate a "BEFORE" sample for bicarbonate concentration to a color before the endpoint (light rose to orange, see section 7.2.4.2).

2) Titrate two more "BEFORE" samples and three "AFTER" samples to the same color as the first titration. Record the initial and final buret readings for all titrations.

7.2.4 Chemical Analysis Procedure

7.2.4.1 Determination of Total Base Concentration

1) Pipet 10 ml of solution into a 250 ml erylenmeyer flask. Add two drops of bromothymol blue indicator.

2) Titrate solution with 1.0 N HCl from a 50 ml buret to a blue to yellow end point. Record the initial and final buret readings. Their difference will be $\Delta 6$.

3) Calculate the total base concentration as follows:

$$[\text{Base}] = (\Delta 6(\text{ml}) / 10 (\text{ml})) \times 1.0 \text{ N} \quad (73)$$

7.2.4.2 Determination of Bicarbonate Concentration

1) Pipet 10 ml of solution into a 250 ml erylemeyer flask. Then pipet 5 ml of 1.0 N NaOH into the same flask and swirl.

2) Add 18 ml of 20% $BaCl_2$ to form the white $BaCO_3$ precipitate. Then add two drops of cresol red - thymol blue mixed indicator and swirl.

3) Immediately titrate the mixture with 1.0 N HCl from a 10 ml accurate buret to a pale orange color similar to a standard color of a previously titrated sample of known bicarbonate concentration. (The mixed indicator color changes from purple to rose to white to yellow. The end point is when the solution is white. Since the samples contain arsenite the end point is very broad and difficult to detect as well as being time consuming. The color matching is easier and more accurate.) Record the initial and final buret readings. Their difference will be $\Delta 7$.

4) The concentration of bicarbonate is determined by the following formula:

$$[HCO_3^-] = \frac{5.0 - (\Delta 7 - 10 \times [\text{Ars}])}{10} \quad (74)$$

5) The titration of samples with no arsenite in solution has a different end point than the solutions with arsenite. The end point is very distinct; a color change from purple to pink. No color matching is needed.

APPENDIX 7.3

Rotameter Calibrations

This appendix provides the calibrations for the two gas rotameters and one liquid rotameter used in this study. They are provided for the benefit of future experimenters using the apparatus.

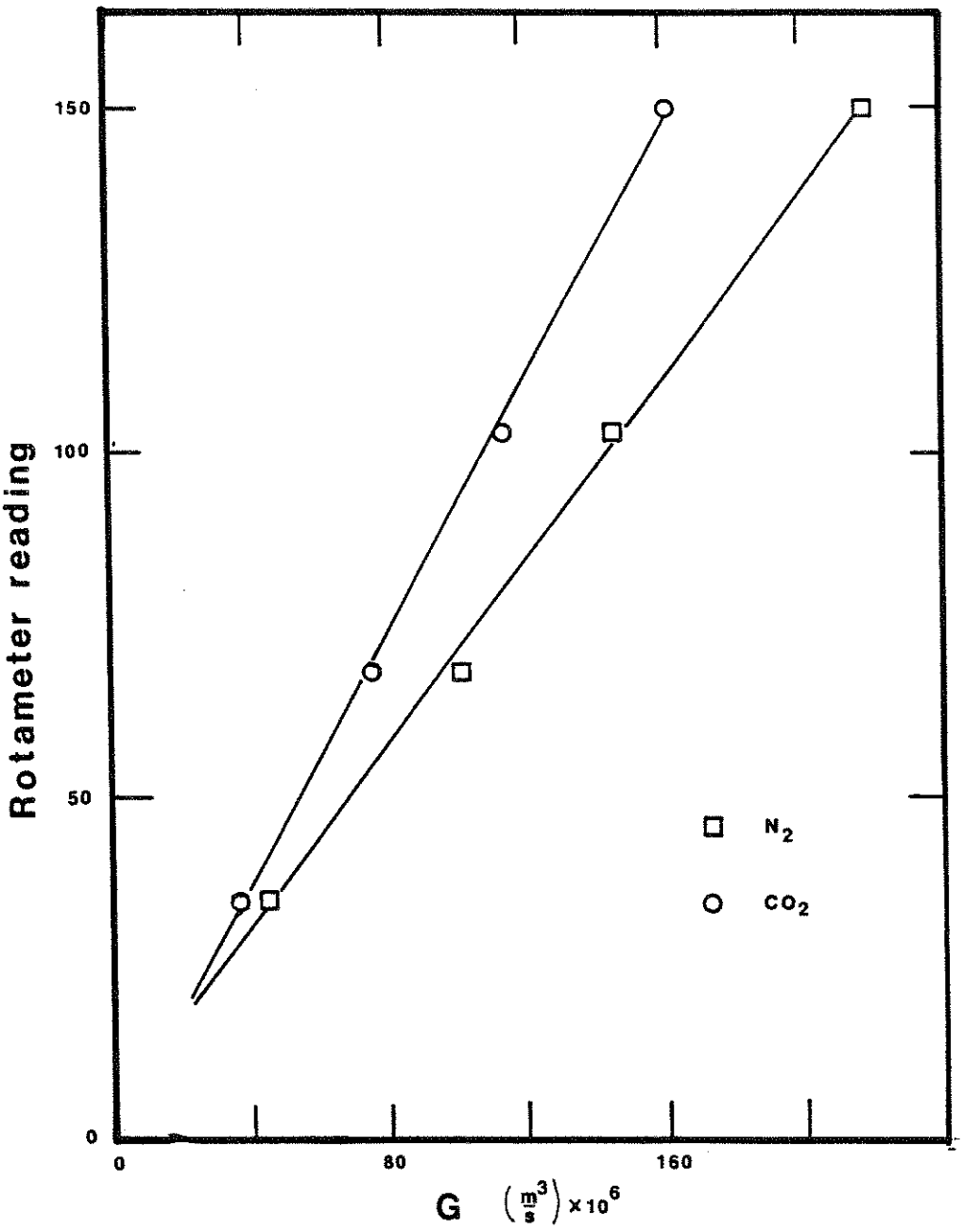

Figure 7.3.1 Inlet Gas Rotameter Calibration Curve

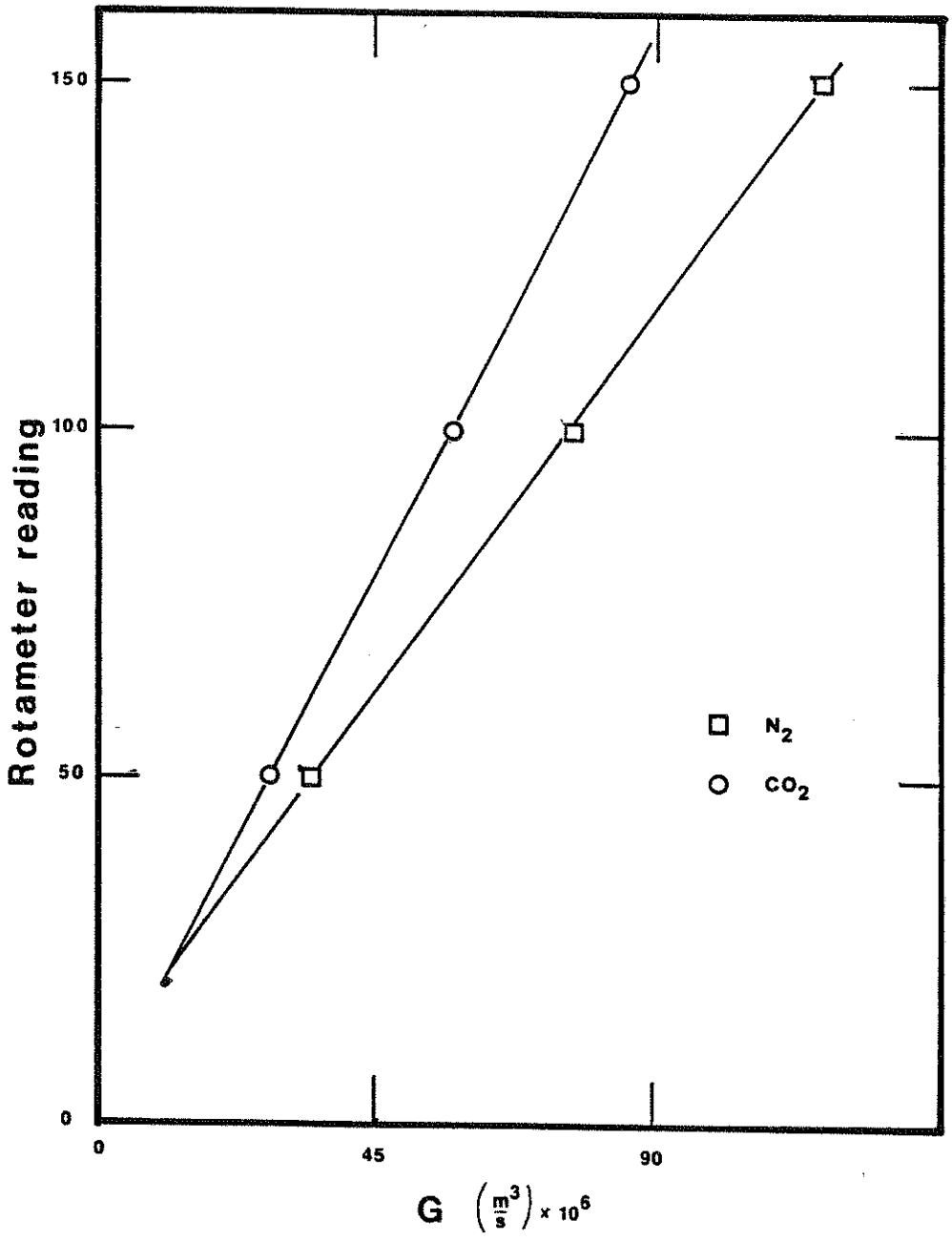

Figure 7.3.2 Outlet Gas Rotameter Calibration Curve

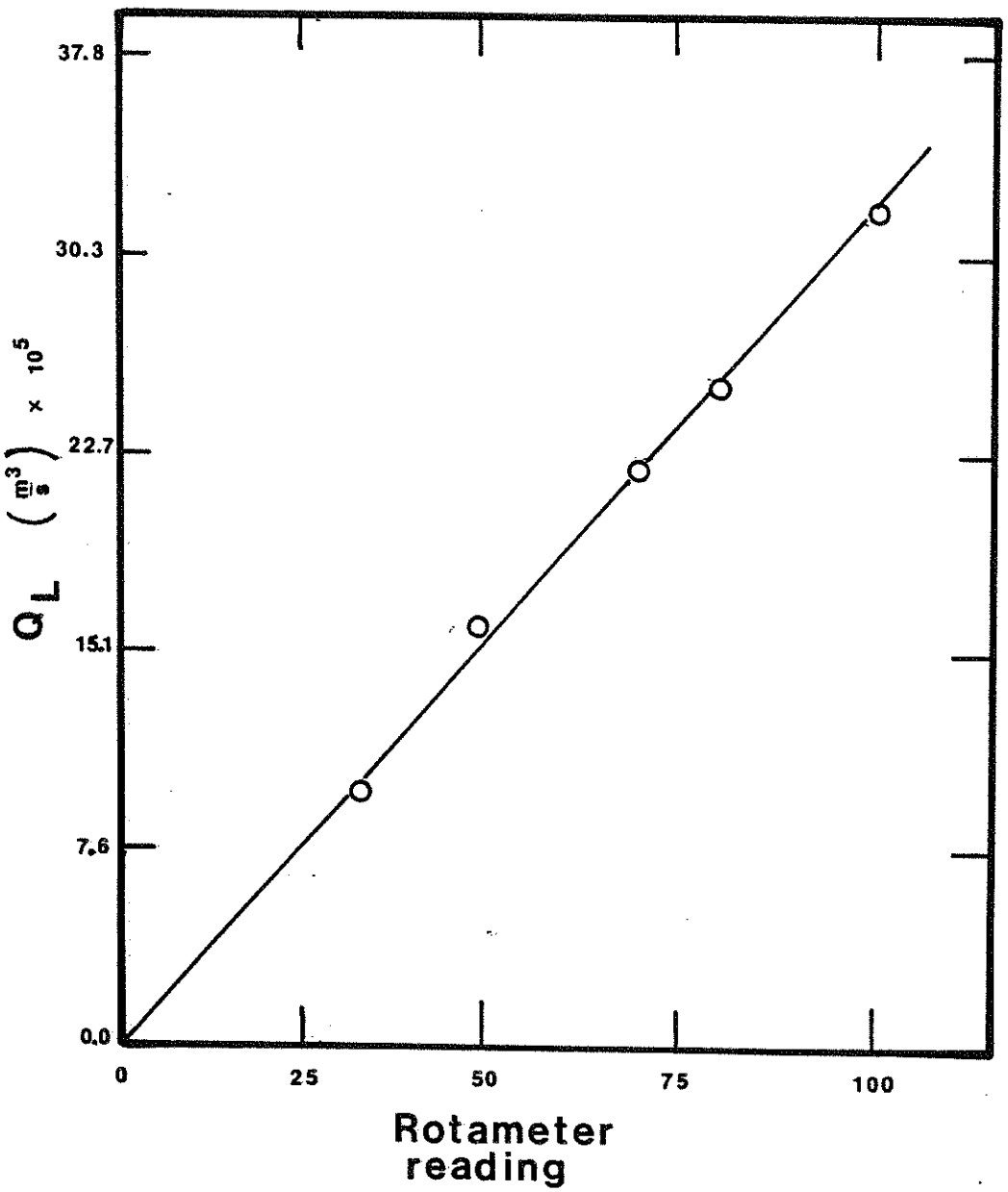

Figure 7.3.3 Liquid Rotameter Calibration Curve

APPENDIX 7.4

Holdup Analysis

This analysis has the main purpose of determining the reason why the Koch and Kenics mixer have a family of lines on the plot of $(1-\epsilon)/\epsilon$ versus V_L/V_G and the Ross mixer does not.

Assume that for the static mixers the following experimentally found relationship holds:

$$\frac{1-\epsilon}{\epsilon} = D \left(\frac{V_L}{V_G}\right)^n \tag{34}$$

where $n \approx 1$.

Starting from the definition of slip velocity (21):

$$\Delta V = \frac{V_G}{\epsilon} - \frac{V_L}{1-\epsilon} \tag{32}$$

and solving for the holdup ratio one gets:

$$\frac{1-\epsilon}{\epsilon} = \frac{1-\epsilon}{V_G} \Delta V + \frac{V_L}{V_G} \tag{75}$$

Replacing Equation (34) into Equation (75) and dividing through by V_L/V_G allows D to be determined as:

$$D = \frac{1-\epsilon}{V_L} \Delta V + 1 \tag{76}$$

For the Ross mixer, since there is only one line, D is a constant for all liquid and gas velocities. Then, the consideration of two different liquid velocities provides the following equation:

$$\frac{(1-\epsilon)_1}{V_{L_1}} \Delta V_1 + 1 = \frac{(1-\epsilon)_2}{V_{L_2}} \Delta V_2 + 1 \tag{77}$$

or by rearranging:

$$\frac{\Delta V_2}{\Delta V_1} = \frac{(1-\epsilon)_1}{(1-\epsilon)_2} \frac{V_{L_2}}{V_{L_1}} \tag{78}$$

Supposing that :

$$\frac{V_{L_2}}{V_{L_1}} > 1 \tag{79}$$

then

$$\frac{(1-\epsilon)_1}{(1-\epsilon)_2} < 1 \tag{80}$$

However, since the change in liquid holdup is not large as the change in the liquid velocities, the following is true:

$$\frac{V_{L_2}}{V_{L_1}} \frac{(1-\epsilon)_1}{(1-\epsilon)_2} > 1 \tag{81}$$

and therefore

$$\frac{\Delta V_2}{\Delta V_1} > 1 \tag{82}$$

The confirmation of the last inequality comes from a case study from the Ross mixer data.

$V_{L_1} = 0.19$ m/s $\qquad (1-\epsilon)_1 = 0.76$

$V_{L_2} = 0.45$ m/s $\qquad (1-\epsilon)_2 = 0.84$

$$V_{L_2} / V_{L_1} = 2.13$$

This shows, in the Ross mixer case, that the slip velocity increases as the liquid velocity increases.

Now for the Kenics and Koch mixer:

$$\frac{D_2}{D_1} < 1 \qquad \text{when} \qquad \frac{V_{L_2}}{V_{L_1}} > 1 \tag{83}$$

This condition provides the following inequality:

$$\frac{\Delta V_2}{\Delta V_1} < \frac{(1-\epsilon)_1}{(1-\epsilon)_2} \frac{V_{L_2}}{V_{L_1}} \tag{84}$$

Unfortunately this inequality gives no definitive statement about the slip velocity relationship except that the slip velocity must change less than in the Ross mixer case.

Considering a case study for the Kenics mixer for $V_G = 0.142$ m/s:

$V_{L_1} = 0.19$ m/s $\qquad (1-\epsilon)_1 = 0.840$

$V_{L_2} = 0.52$ m/s $\qquad (1-\epsilon)_2 = 0.863$

$D_1 = 3.9 \qquad D_2 = 1.67$

then

$$\frac{\Delta V_2}{\Delta V_1} = 0.615$$

For the Kenics and Koch mixer, the slip velocity is decreased as the liquid velocity is increased.

It also can be shown directly that the slip velocity is increased as the gas velocity is increased for all mixers.

APPENDIX 7.5

Separator/Sparger Correction

If the total volume of the apparatus is broken up into two parts, the reactor volume and the separator and sparger volume, the following equation holds for an overall mass balance:

$$(N_A a)_T \, V_T \, (1-\epsilon)_T = (N_A a)_S \, V_S \, (1-\epsilon)_S + (N_A a)_R \, V_R \, (1-\epsilon)_R \qquad (85)$$

where the subscripts mean the following:

T = Total

S = Separator/Sparger

R = Reactor

Assuming that all the liquid holdups equal the measured average liquid holdup and solving for the desired rate of absorption in equation (85) one gets:

$$(N_A a)_R = \frac{(N_A a)_T \, V_T - (N_A a)_S \, V_S}{V_R} \qquad (86)$$

Since all the volumes are known and $(N_A a)_T$ is the experimentally determined value, the value of $(N_A a)_S$ needs to be evaluated. Previous to this analysis $(N_A a)_S \, V_S$ was

assumed to be negligible. Unfortunately, this assumption was incorrect.

A few runs were performed to determine values for $(N_A a)_S$ and their variation with catalyst concentration and gas flowrate. The gas was injected through the top pressure tap in the same manner as in all the runs. The liquid flowrate was set at 70% of the maximum. Everything else was performed in the same manner as when dealing with the injection in front of the mixer. Table 7.5.1 gives the results of these experiments.

It was assumed that for a constant liquid flowrate, the following empirical power law relationship holds

$$(N_A a)_S = D\, r^b\, G^c \tag{87}$$

where G ≡ outlet gas volumetric flowrate $(\frac{cm^3}{s})$ and a, b and D are empirical constants. From the four data points D, b, and c were evaluated and averaged. The final correlation became for one liquid flowrate:

$$(N_A a)_S = 2.30 \times 10^{-8}\, r^{0.41}\, G^{0.70} \tag{88}$$

For any outlet gas flowrate and catalyst concentration, the rate of absorption can now be estimated at a liquid rate of 70% of the maximum. For regular runs, the gas flowrate out of the separator is unknown, but can be

Table 7.5.1

Separator/Sparger Absorption Results

r	G_{in}	$1-\epsilon$	$(N_A a)_S$	G_{out}
s^{-1}	cm^3/s		gmole/cm^3 s x 10^6	cm^3/s
2.92	34	0.90	3.4	32
2.92	110	0.81	8.7	105
135	34	0.90	17.6	23
135	110	0.81	38.1	88

calculated by the overall mass balance:

$$G_{out} = G_{in} - \frac{(N_A a)_T \, V_T \, (1-\epsilon)_T}{(\rho_{CO_2} / M_{\omega\ CO_2})} \qquad (89)$$

Finally $(N_A a)_R$ can be calculated from the equation (86) where $(N_A a)_S$ is calculated from equations (88) and (89).

Although the correction scheme seems logical, it is very cumbersome and does include some assumptions. This correlation is only good for one specific liquid flowrate. More experiments would have to be done at more liquid flowrates which would be very costly.

From the visual observation of the bubbles in the separator, a simpler correction scheme was devised. The bubbles from the reactor traveled straight up without any radial movement. Also the bubbles did not seem to coalesce as they traveled to the surface. Therefore, the reactor volume can be increased by an imaginary volume that extends from the liquid surface in the separator to the end of the physical reactor length through the core of the separator and having a diameter of 1 inch, the same as the tubular reactor. This volume corresponded to a value of 81 cm^3.

Table 7.5.2 gives a comparison of the two proposed correction schemes for three different initial gas rates at one liquid rate (70% of the maximum). Both correction schemes correlate well together, with an error of 10%.

The second scheme's simplicity, physical reality and consistency for all liquid rates made it the better choice of the two schemes.

Table 7.5.2

Comparison of Results from Two Separator/Sparger Correction Schemes

r	$(N_A a)_T$	G_{in}	G_{out}	eq.(88) $(N_A a)_S$	#1 eq.(86) $(N_A a)_R$	#2 $(N_A a)_R$
s^{-1}	$gmole/m^3 s$	cm^3/s		$gmole/m^3 s$		
112.4	3.55	76	24.1	2.2	4.5	5.1
111.0	3.97	76	18.0	1.9	5.5	5.7
90.5	3.20	76	29.2	2.06	4.1	4.6
52.7	2.50	76	32.0	1.77	3.9	4.3
42.4	2.51	76	39.3	1.37	3.4	3.6
34.9	2.17	76	44.3	1.25	2.9	3.1
2.9	2.05	76	46.0	0.22	3.4	3.0
138	4.67	115	49.0	3.41	5.60	6.72
104	4.97	115	44.8	2.70	6.70	7.15
79.6	4.26	115	54.8	2.18	4.42	4.98
60.9	3.46	115	66.1	2.18	4.42	4.98
31.7	3.62	115	63.9	1.36	5.30	5.21
2.92	2.41	115	81.0	0.28	3.99	3.47
137.5	1.40	38	16.4	2.17	0.82	2.01
104.1	2.00	38	7.1	1.27	2.54	2.88
79.0	1.79	38	10.4	1.22	2.21	2.57
49.2	1.99	38	7.3	0.76	2.91	2.86
32.2	1.60	38	13.3	0.72	2.25	2.30
2.93	1.31	38	17.8	0.15	2.17	1.88

APPENDIX 7.6

Gas Depletion Correction

A gas depletion correction scheme is necessary to correct an experimental value for $N_A\bar{a}$, which is an average value for the whole column, to a true value of $N_A a_o$, which is a point value at the beginning of the reactor when the gas molar flowrate is F_{go}.

The differential mass balance on the gas (assuming plug flow) can be stated as:

$$-\frac{d F_g}{dV} - N_A a = 0 \qquad (90)$$

with the boundary condition:

$$F_g = F_{go} \text{ at } V_R = 0$$

Since, the point value of the interfacial area, a is always changing in the column an average area $\bar{a}$, must be defined and can be written as:

$$\bar{a} = \frac{1}{V_R} \int_0^{V_R} a \, dV \qquad (91)$$

The experimenter measures the value $N_A\bar{a}$ not $N_A a$, so from the overall mass balance on the gas one gets:

$$F_{go} - F_{ge} = N_A \bar{a} V_R \tag{92}$$

or

$$\frac{F_{ge}}{F_{go}} = 1 - \frac{N_A \bar{a} V_R}{F_{go}} \tag{93}$$

An assumption must be made concerning the change of a with respect to F_g. This assumption is justified "a posteriori" by our findings.

$$a = D F_g^n \tag{94}$$

and

$$a_o = D F_{go}^n \tag{95}$$

By replacing equation (94) into equation (90) and integrating one gets:

$$- \int_{F_{go}}^{F_{ge}} \frac{dF_g}{F_g^n} = N_A D \int_0^{V_R} dV \tag{96}$$

for $n \neq 1$

$$(1 - \frac{F_{ge}}{F_{go}})^{(1-n)} = N_A a_o (1-n) \frac{V_R}{F_{go}} \tag{97}$$

From equation (93) and (97) one obtains:

$$N_A a_o = \frac{F_{go}}{V_R (1-n)} \left[1 - \left(1 - \frac{N_A \bar{a} V_R}{F_{go}}\right)^{(1-n)} \right] \qquad (98)$$

For known values of V_R and n and experimental values of $N_A \bar{a}$ and F_{go}, $N_A a_o$ can be found.

There are two problems with this solution. The first is that there are no reliable values for n. It is not an experimentally determinable exponent. It is expected to be around 0.7, as for packed and bubble columns, but it is not known for sure.

The second problem is with the sensitivity of the solution. When $\frac{N_A \bar{a} V_R}{F_{go}}$ approaches a value of one, any significant error in the value of $N_A \bar{a}$ or F_{go} will cause the calculated value of $N_A a_o$ to vary tremendously.

In order to handle the first problem, an assumption concerning the average area, $\bar{a}$ is made and later shown to be experimentally justified:

$$\bar{a} = D' \left(\frac{F_{go} + F_{ge}}{2} \right)^m \qquad (99)$$

$$a_o = D' F_{go}^{\ m} \qquad (100)$$

From the following equation

$$N_A = C_{A_i} \sqrt{D_A (s + r)} \qquad (101)$$

N_A is a constant for all liquid and gas rates at a particular catalyst concentration and hence:

$$N_A\bar{a} = N_A D' \left(\frac{F_{go} + F_{ge}}{2}\right)^m \tag{102}$$

Replacing for F_{ge} in equation (102) from equation (93) one gets:

$$N_A\bar{a} = N_A D' F_{go}{}^m \left(1 - \frac{N_A\bar{a} V_R}{2 F_{go}}\right)^m \tag{103}$$

With the use of equation (100), equation (103) becomes:

$$N_A\bar{a} = N_A a_o \left(1 - \frac{N_A\bar{a} V_R}{2 F_{go}}\right)^{-m} \tag{104}$$

Now m is an experimentally determined value. Figures 7.6.1 and 7.6.2 show plots for the determination of m for the Kenics and Koch mixer. The Kenics mixer shows that m is a function of r or catalyst concentration. This relationship is shown in Figure 7.6.3.

Equation (104) is preferred to equation (98) for computation of $N_A a_o$ because the exponent m can be obtained more readily.

Nevertheless equation (98) is the more realistic solution while equation (104) is only an approximation,

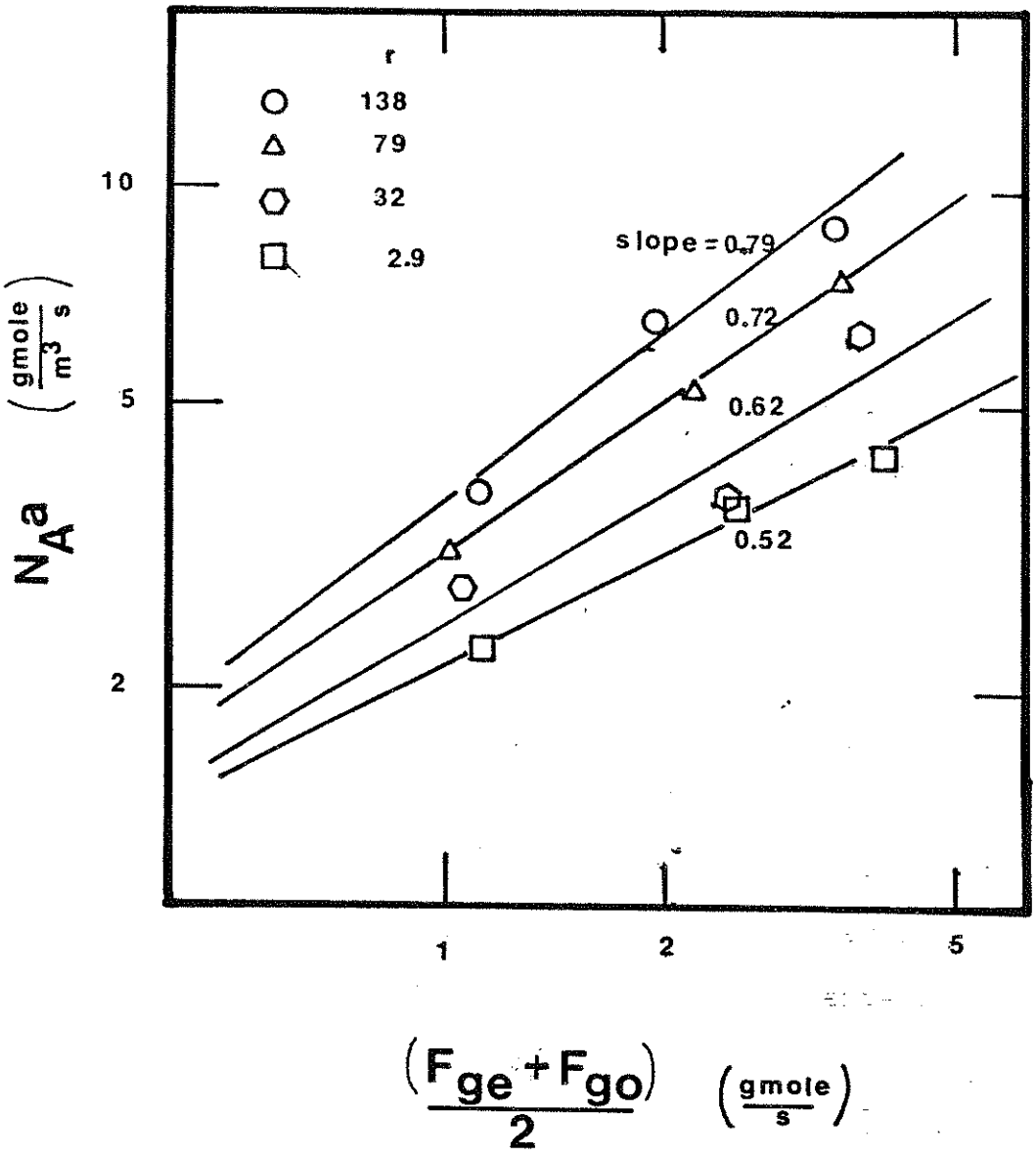

Figure 7.6.1 Relationship Between Rate of Absorption and Average Gas Flowrate in the Kenics Mixer

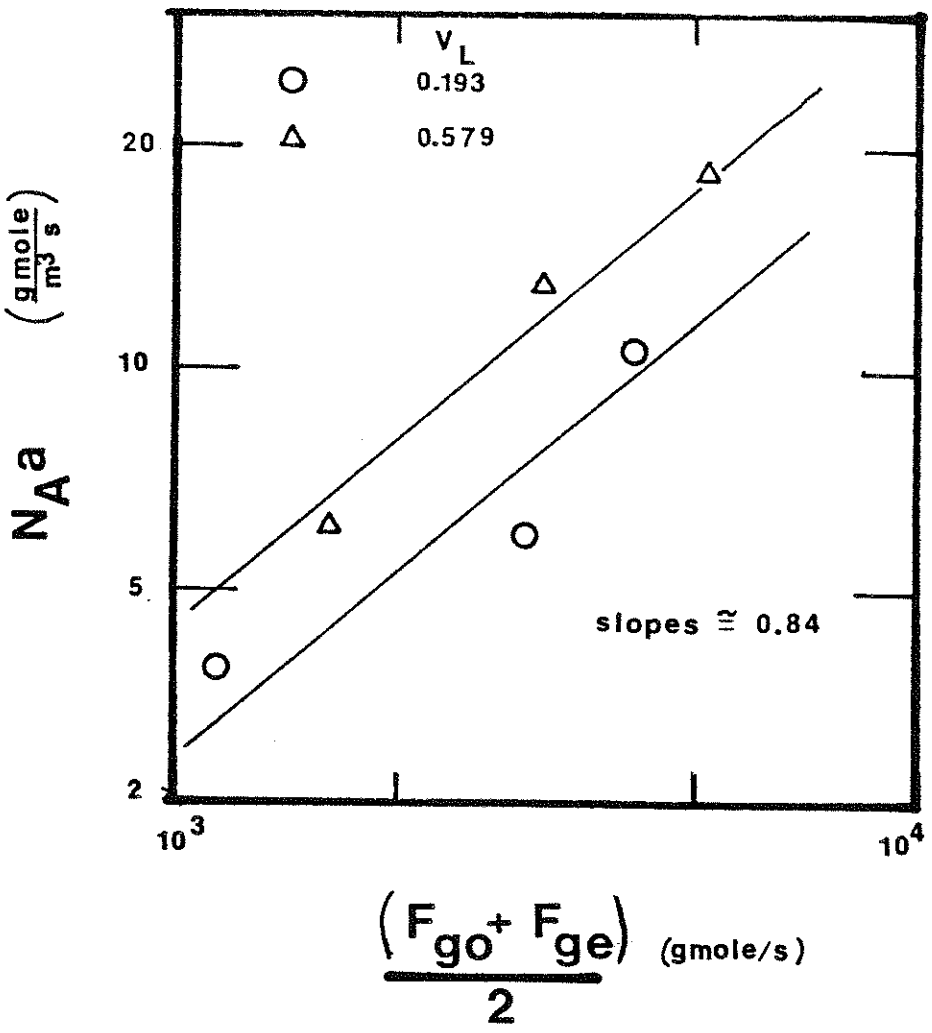

Figure 7.6.2 Relationship Between Rate of Absorption and Average Gas Flowrate in the Koch CY Mixer

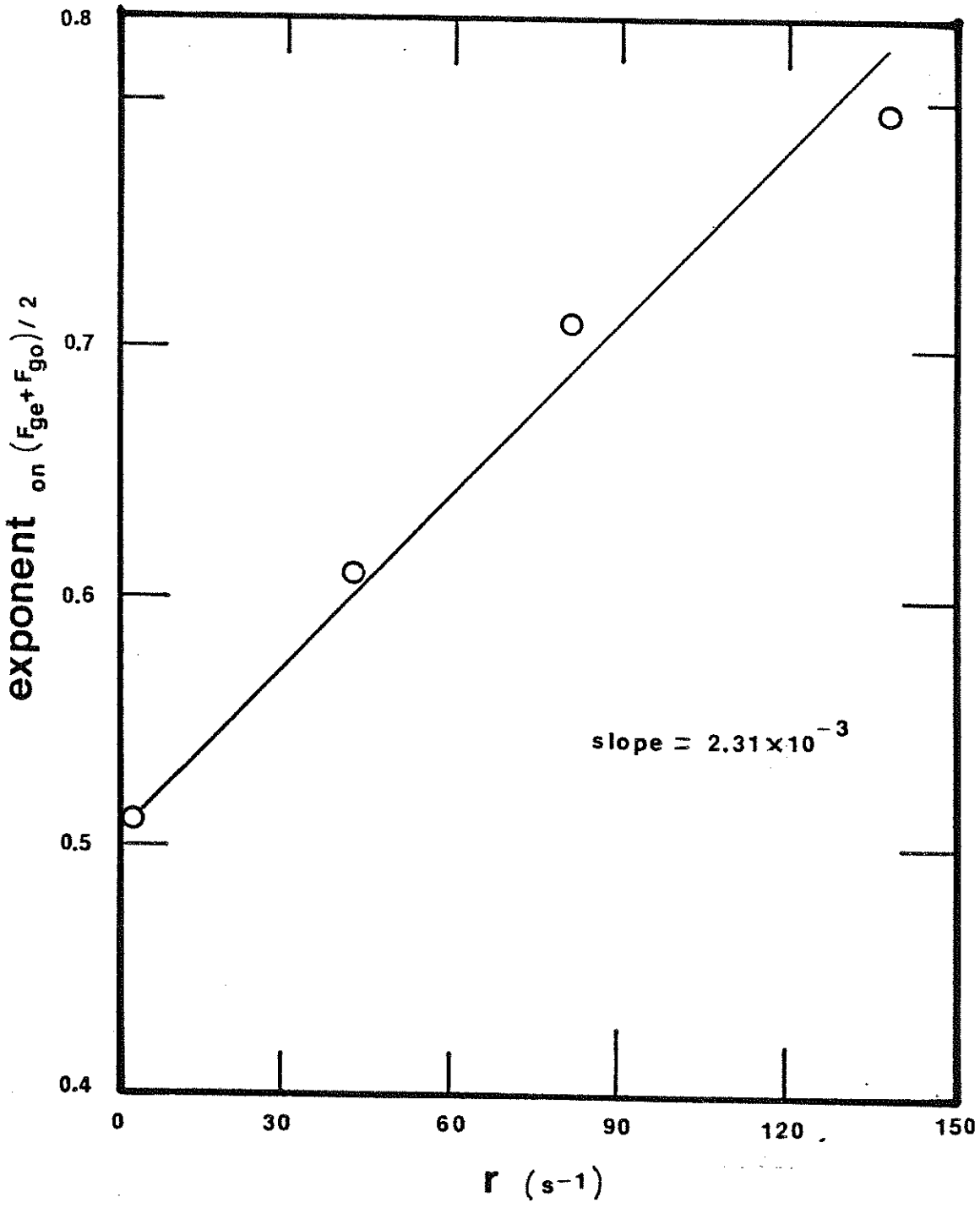

Figure 7.6.3 Varience of the Exponent on the Average Gas Flowrate as a Result of Changing Catalyst Concentrations

an approximation that does fail as $\frac{N_A \bar{a} V_R}{F_{go}}$ approaches unity. The smaller the gas uptake in the system, the better the assumption. Since the Koch mixer caused such a large reduction of gas at moderate catalyst concentrations, the accuracy of the correction was questioned. However zero catalyst concentration runs in the mixer only took up 50% of the gas so the approximation could be used for these points only.

After the evaluation was completed as shown in Chapter 4, an approximate value for n was determined. Table 7.6.1 shows the values for $(N_A a)^2$ evaluated from equation (108) and equation (94). Equation (108) consistently gave lower values, so that the final a values given in the body of the report are on the conservative side. Even so, the values are not that far apart and well within the titration errors.

Table 7.6.1

Comparison of Results from Two Gas Depletion Correction Schemes

Run	r	original	eq. (98)	eq. (104)
		$(N_A a)_T$	$(N_A a)_R$	$(N_A a)_R$
#	s^{-1}	gmole/cm^3s	gmole/cm^3s	gmole/cm^3s
		x 10^6	x 10^6	x 10^6
1	139.8	1.89	3.53	3.60
1	112.4	2.61	5.92	5.43
2	111.0	3.26	9.08	7.55
1	90.5	2.12	4.21	3.85
2	69.2	1.87	3.48	3.14
1	52.7	1.30	2.10	1.92
2	42.4	1.30	2.10	1.90
1	34.9	0.97	1.44	1.32
2	2.9	0.87	1.26	1.12

APPENDIX 7.7

Error Analysis Supplement

This appendix provides the data and figure from which an error analysis was done and explained in Section 4.5.4.

The error data was taken from a set of runs done early in the study and had maximal titration errors. These points along with their associated titration error bars were plotted on Figure 7.7.1 and three lines were drawn through them. From the slopes and intercepts of these lines, the respective values and deviations in interfacial area, a and mass transfer coefficients, k_L were calculated and presented in Table 7.7.1.

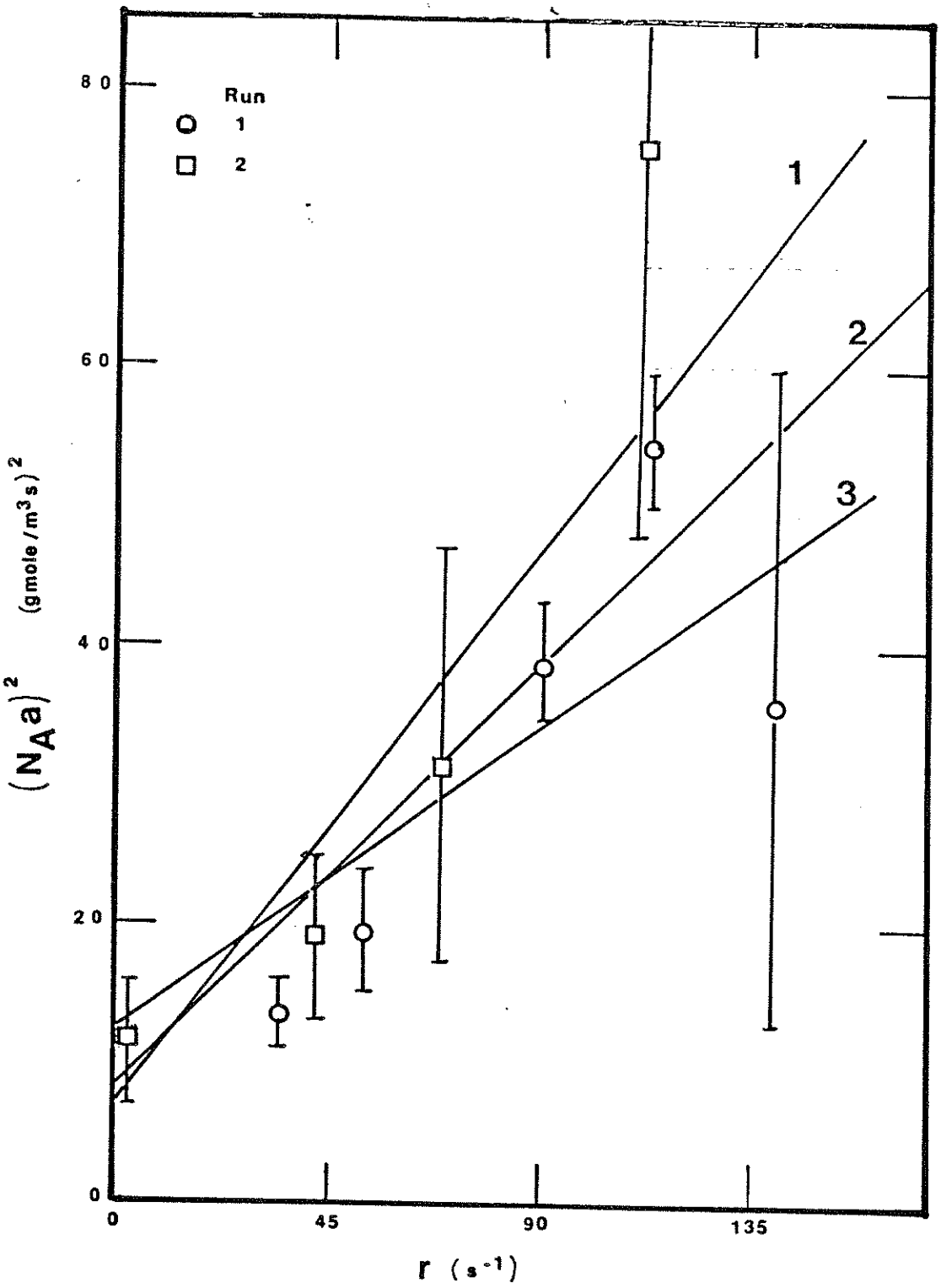

Figure 7.7.1 Figure Used for Evaluation of Errors in the Values of the Mass Transfer Coefficients and Interfacial Areas

Table 7.7.1

Maximal Magnitudes of Experimental Errors and Subsequent Errors in the Values of the Mass Transfer Coefficients and Interfacial Areas

r	$(N_A a) \times 10^6$	% titration error
s^{-1}	$gmole/cm^3 s$	
139.77	5.27	40
112.4	6.20	5
111.0	6.93	19
90.5	5.59	5
69.2	5.25	30
52.7	4.37	10
42.4	4.38	16
34.9	3.78	5
2.92	3.57	16

Line	Intercept	Slope	a	k_L
	$gmole^2/cm^6 s^2$	$gmole^2/cm^6 s$	m^{-1}	m/s
	$\times 10^6$	$\times 10^7$		$\times 10^4$
1	7.0	4.42	863	1.48
2	8.0	3.37	754	1.81
3	12.5	2.41	638	2.68
Average			751	1.99
% error			15%	31%

APPENDIX 7.8

Investigation of Appropriate Hatta Number Magnitude

In Appendix 7.1, the second boundary condition for the problem of unsteady state absorption and first order reaction stated that the concentration of gas A in the bulk of the liquid B was equal to zero. In order to assure that this boundary condition represents reality well, the Hatta number, which relates the relative speed of reaction and diffusion through the film, must be large. Linek (15) and many others suggest that $Ha >> 3$.

This appendix addresses the question whether such large values of the Hatta number are necessary in order for the form of the enhancement factor derived in Appendix 7.1 to hold.

Consider the absorption and subsequent irreversible first order reaction of gas A into liquid B across a liquid film into a bulk that is modeled by a continuously stirred tank. From Film Theory, the mass balance on A in the film gives:

$$D_A \frac{d^2 C_A}{d y^2} - r\, C_A = 0 \qquad (105a)$$

with boundary conditions:

$$y = 0 \qquad C_A = C_{A_i} \tag{105b}$$

$$y = \delta_L \qquad C_A = C_{A_b} \tag{105c}$$

A mass balance on A in the bulk is:

$$Q_L C_{A_b} + r\, C_{A_b}\, V_b + D_A \left.\frac{d\, C_A}{dy}\right|_{\delta_L} a\, V_b = 0 \tag{106}$$

The solution of equation (105)

$$C_A = C_{A_i} \exp\left(-\sqrt{\frac{r}{D_A}}\, y\right) +$$

$$\left[\frac{C_{A_b} - C_{A_i} \exp\left(-\sqrt{\frac{r}{D_A}}\, \delta_L\right)}{\exp\left(\sqrt{\frac{r}{D_A}}\, \delta_L\right) - \exp\left(-\sqrt{\frac{r}{D_A}}\, \delta_L\right)}\right] \times$$

$$\left[\exp\left(\sqrt{\frac{r}{D_A}}\, y\right) - \exp\left(-\sqrt{\frac{r}{D_A}}\, y\right)\right] \tag{107}$$

The derivative of C_A with respect to y at the film width, δ_L, can now be determined from the above equation and by using the definition of the Hatta number:

$$Ha = \frac{\sqrt{r \cdot D_A}}{k_L} \tag{17}$$

and film width:

$$\delta_L = \frac{D_A}{k_L} \tag{12}$$

can be written as follows:

$$\left.\frac{d\ C_A}{dy}\right|_{\delta_L} = \sqrt{\frac{r}{D_A}}\ (C_{A_b} \cdot \coth Ha - C_{A_i} \cdot (1 + \coth Ha)) \tag{108}$$

The bulk concentration of gas A, C_{A_b}, can now be solved by replacing equation (108) into equation (107) and is given as follows:

$$C_{A_b} = \frac{C_{A_i} \cdot k_L a \cdot Ha \cdot (\tanh Ha + 1)}{(1/\tau + r) \cdot \tanh Ha + k_L a H_a} \tag{109}$$

where τ = CSTR residence time, (s).

The molar flux across the interface is:

$$N_A = -D_A \cdot \left.\frac{d\ C_A}{dy}\right|_{y\ =\ 0} \tag{110}$$

Again using equation (107) by taking the derivative with respect to y and then setting y equal to zero, the molar flux can be written as follows:

$$N_A = \frac{\sqrt{r \cdot D_A} \cdot C_{A_i}}{\tanh Ha} \left[1 - \frac{C_{A_b}}{C_{A_i}} \frac{1}{\cosh Ha} \right] \tag{111}$$

The true enhancement factor is then defined by:

$$E_{L_{true}} = \frac{N_A}{k_L \cdot C_{A_i}} = \frac{Ha}{\tanh Ha} \left[1 - \frac{C_{A_b}}{C_{A_i}} \cdot \frac{1}{\cosh Ha} \right] \tag{112}$$

The approximate enhancement factor for this situation assume $C_{A_b} = 0$ as described in Appendix 7.1 and is given by Film Theory as:

$$E_L = \frac{Ha}{\tanh Ha} \tag{113}$$

The error resulting from the use of the approximate enhancement factor can then be written from equation (112) and (113) as:

$$1 - \frac{E_{L_{true}}}{E_L} = \frac{C_{A_b}}{C_{A_i}} \cdot \frac{1}{\cosh Ha} \tag{114}$$

which with the aid of equation (109) becomes:

$$1 - \frac{E_{L_{true}}}{E_L} = \frac{\tanh Ha + 1}{(\alpha \cdot \tanh Ha + 1) \cosh Ha} \qquad (115)$$

$$\text{where } \alpha = \frac{1/\tau + r}{k_L a \cdot Ha} \qquad (115b)$$

The errors associated with using the approximate enhancement factor with Ha numbers less than 3 can be determined for the conditions of our experiments by using the following quantities:

$1/\tau = 0$ for semi-batch operation

$2.2 < r < 130 \qquad (s^{-1})$

$k_L = 1.84 \times 10^{-4}$ (m/s)

$$C_{A_i} \sqrt{D_A} = 7.7 \times 10^{-4} \left(\frac{\text{mole}}{m^2 \, s^{1/2}} \right)$$

$$D_A = 1.38 \times 10^{-9} \left(\frac{m^2}{s} \right)$$

$300 < a < 1100 \quad (m^{-1})$

Table 7.8.1 presents some errors at select values of r and a. Most of the points on a Danckwerts' plot values

APPENDIX 7.9

Holdup Correlation

In Section 4.1, it was mentioned that the family of lines that resulted from a plot of the holdup ratios versus the superficial velocity ratios on log-log paper for the Koch and Kenics mixers could be correlated into one line. The type of correlation that was suggested was one similar to that proposed by Yung Hsu (24) for gas-lift reactors which was specifically presented as:

$$\frac{1-\epsilon}{\epsilon} = 10.14 \left(\frac{V_L}{V_G}\right)^{0.73} (Fr_{TP})^{0.26} (Re_{TP})^{0.0044} (We_{TP})^{0.42} \quad (116)$$

where (Fr_{TP}) = Froude No. = $M^2/d\,g\,\rho_H^2$; (117)

(We_{TP}) = Weber No. = $d\,M^2/g\,\rho_H\sigma$; (118)

(Re_{TP}) = Reynolds No. = $d\,M/\mu$; (119)

M = Total mass flow = $V_G\rho_G + V_L\rho_L$; (120)

and, ρ_H = Homogeneous density = $\left(\frac{\epsilon}{\rho_G} + \frac{\epsilon}{\rho_L}\right)^{-1}$ (121)

From equation (116), it is apparent that Reynolds number is not very important and that the Froude number and the Weber number contain nearly all the same parameters. Accordingly, without any data for systems with different surface tensions, and analysis containing both the Froude and Weber number would produce an infinite number of correlations. Therefore, the subsequent correlations contain only the Weber number, which is most often used for holdup correlations in the literature.

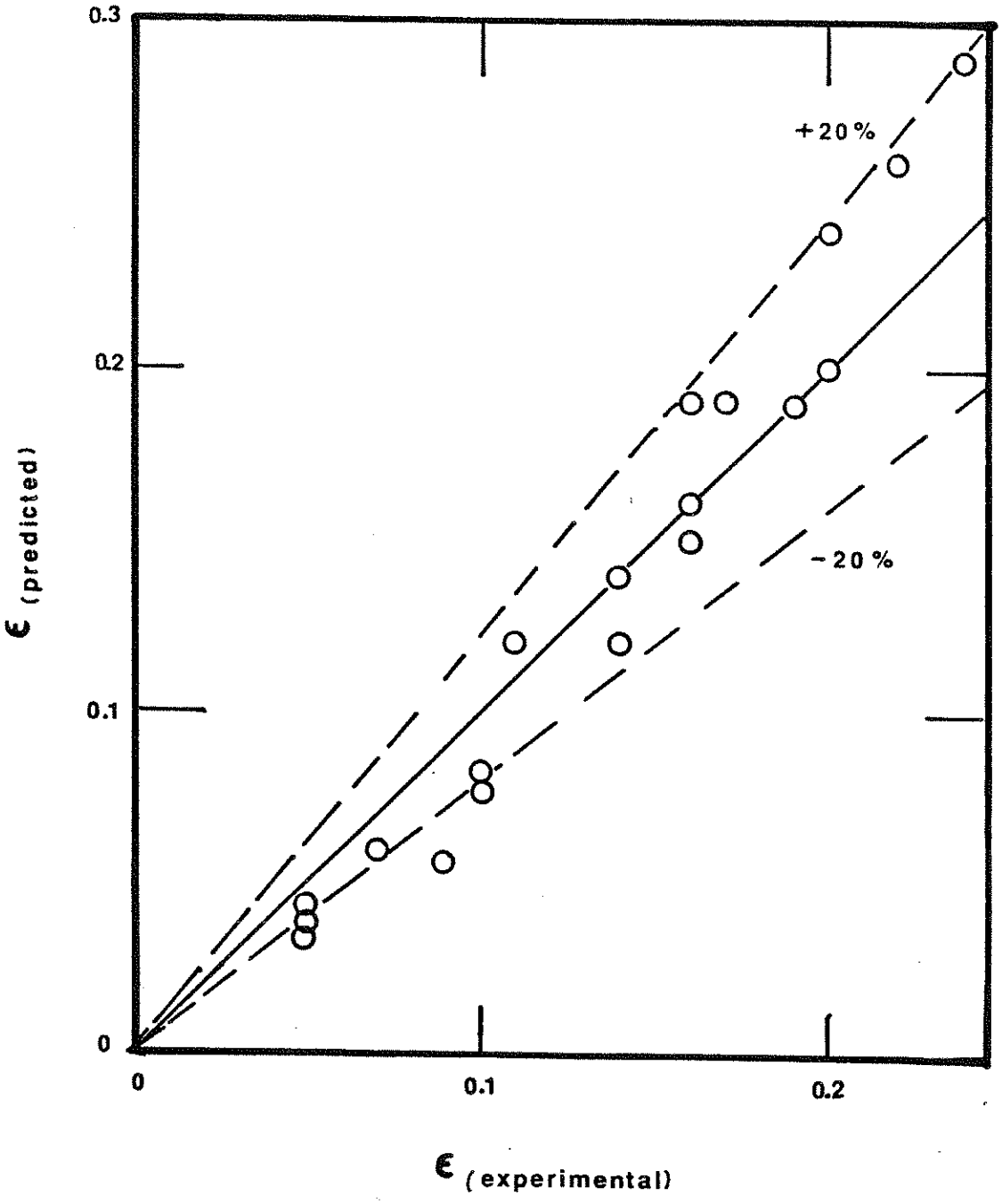

Figure 7.9.1 Experimental Gas Holdup Values Versus Predicted Gas Holdup Values from Equation (122) for the Kenics Mixer

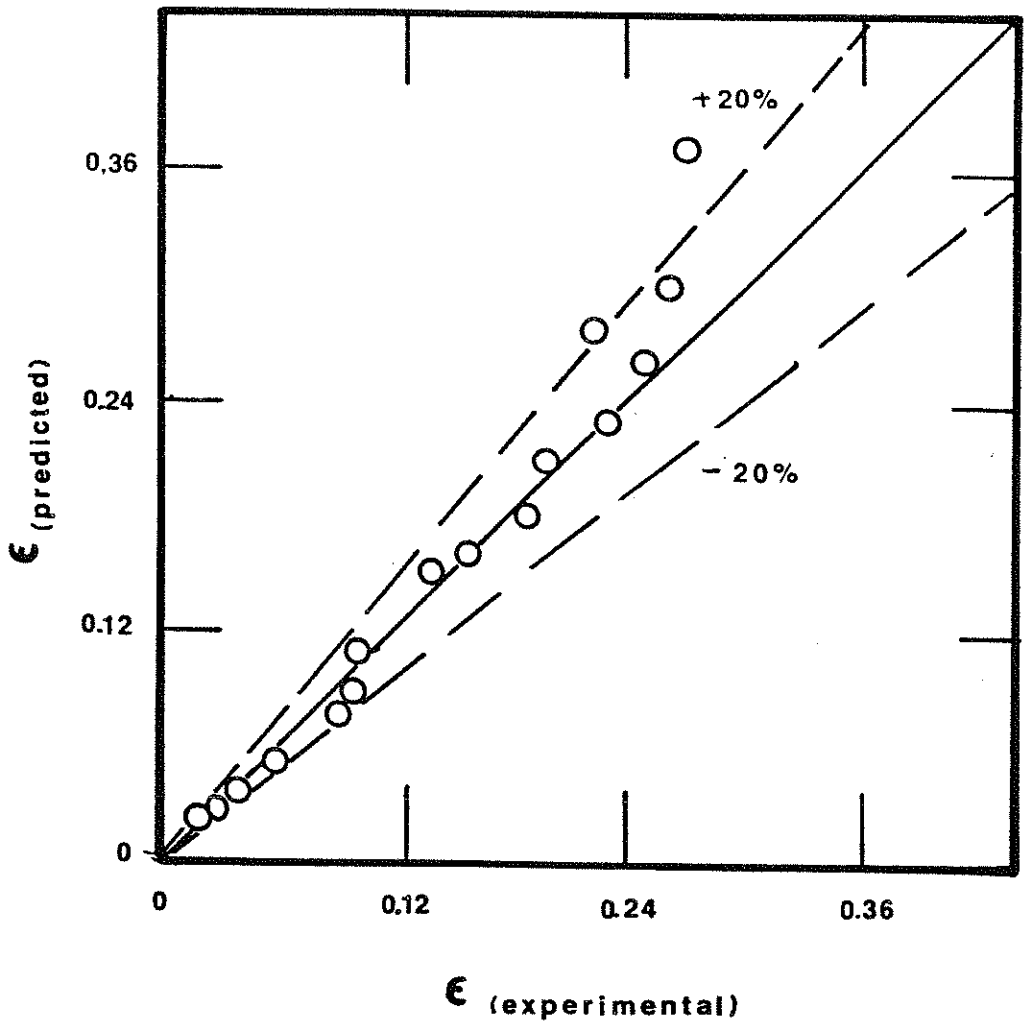

Figure 7.9.2 Experimental Gas Holdup Values Versus Predicted Gas Holdup Values from Equation (123) for the Koch CY Mixer

APPENDIX 7.10

Nomenclature

English

a = Interfacial area between gas and liquid per unit liquid volume, m^2/m^3, cm^2/cm^3.

A = Total interfacial area between the gas and liquid in the reactor, m^2, cm^2.

C_A = Concentration of gas A, $gmole/m^3$, $gmole/cm^3$.

C_{A_b} = Concentration of gas A in the liquid bulk, $gmole/m^3$, $gmole/cm^3$.

C_{A_i} = Concentration of gas A at the gas/liquid interface, $gmole/m^3$, $gmole/cm^3$.

C_B = Concentration of B in liquid, $gmole/m^3$.

C_{B_b} = Concentration of reactive substance B in the liquid bulk, $gmole/m^3$, $gmole/cm^3$.

d = Inside pipe diameter, m.

d_B = Sauter mean drop size, m.

d_h = Mixing element hydraulic diameter, m, inch.

D_A = Diffusivity of the gas A in the liquid phase, m^2/s, cm^2/s.

D_B = Diffusivity of reactive species B in the liquid phase, m^2/s, cm^2/s.

E = Power dissipation per unit reactor voidage, W/m^3.

E_i = Instantaneous enhancement factor, Equation (18), dimensionless.

E_L = Overall enhancement factor, dimensionless.

f_H = Homogeneous friction factor for pipe flow, dimensionless.

F = Molar flowrate of gas, gmole/s.

F_{ge} = Molar flowrate of gas at outlet, gmole/s.

F_{go} = Molar flowrate of gas at inlet, gmole/s.

Fr_{TP} = Two phase Froude number, equation (117), dimensionless.

g = Acceleration of gravity, m/s .

G_{in} = Volumetric flowrate of gas at inlet, m^3/s, cm^3/s.

G_{out} = Volumetric flowrate of gas at outlet, m^3/s, cm^3/s.

Ha = Hatta number, equation (17), dimensionless.

k_L = Liquid side mass transfer coefficient, m/s.

k_G = Gas side mass transfer coefficient, m/s.

L = Length along a reactor, m.

L_1 = Length between the two liquid manometer water levels, m.

L_2 = Distance between the two pressure taps, m.

M = Total mass flow, equation (120), kg/ m^2s.

M_w = Molecular weight, g/gmole.

N_A = Rate of absorption of A per unit interfacial surface area, gmole/m^3s, gmole/cm^3s.

P_w = Energy dissipation per unit volume of liquid in reactor, W/m^3.

Q_L = Volumetric flowrate of liquid, m^3/s, cm^3/s.

r' = Pseudo-first order reaction rate constant, s^{-1}.

r = Second order reaction rate constant, m^3/gmole s.

R_A = Rate of appearance of gas A from a reaction, gmole/m^3s.

Re = Liquid Reynolds number, dimensionless.

Re_{TP} = Two phase Reynolds number, equation (119), dimensionless.

s = Surface renewal frequency, s^{-1}.

t = Time, s or minutes.

V_b = Total volume of semi-batch liquid, m^3.

V_G = Superficial gas velocity in the reactor, m/s, cm/s.

V_H = Superficial velocity of a two phase mixture, m/s.

V_L = Superficial liquid velocity in the reactor, m/s, cm/s.

V_R = Volume of reactor voidage, m^3 or cm^3 .

V_S = Volume of separator and sparger, m^3 or cm^3.

V_T = Volume of the total reactor apparatus, m^3 or cm^3.

We = Liquid Weber number, dimensionless.

We_{TP} = Two phase Weber number, equation (118), dimensionless.

y = Distance away from gas/liquid interface, m.

z = Stoichiometric coefficient on reactant B, gmoles.

Z = Volume of liquid per volume of interface in a reactor, equation (19), dimensionless.

Greek

α = Assigned parameter, Equation (15b), dimensionless.

δ = Film thickness, m.

Δ = Titration volume difference, (ml).

ΔP_K = Pressure drop associated with loss in kinetic energy due to friction, N/m^2.

ΔP_S = Pressure drop associated with a static head or height difference, N/m^2.

ΔP_T = Total pressure drop, N/m^2.

ΔV = Slip velocity between two phase, equation (32), m/s.

ϵ = Fractional gas holdup in two phase flow, dimensionless.

Θ = Exposure time of a fluid element at the interface, s.

μ_L = Liquid viscosity, kg/s m.

ρ_G = Gas density, kg/m^3.

ρ_H = Homogeneous density of a gas/liquid mixture, kg/m^3.

ρ_L = Liquid density, kg/m^3.

σ = Surface tension , N/m.

τ = Residence time in reactor, s.

Other

[ ] = Concentration of species inside brackets, $gmole/m^3$, gmole/l, $gmole/cm^3$.

8. BIBLIOGRAPHY

1. Kenics Technical Literature, "Explosive Gas Mixing", Application Report E291-6, 1973.

2. Smith, J. M., "Two phase Gas Liquid Flow in Kenics Mixers", Technical Report, Delft University of Technology, August 16, 1978.

3. Middleton, J. C. , "Motionless Mixers as Gas-Liquid Contacting Devices, ICI Technical Report, October, 1978.

4. Pahl, M. H. and Muschelknautz, E., "Application and Design of Static Mixers", Chemical Engineering Technology, 51, pp. 347 - 364, 1979.

5. Mutsakis, M., "Static Mixing in the Chemical and Petrochemical Industies", Technical Report, Koch Engineering Company.

6. Chen, S. J. and Libby, D. R., "Gas-Liquid and Liquid-Liquid Dispersions in a Kenics Mixer", Technical Report, Kenics Corporation.

7. Streiff, F. A., "In-line Dispersion and Mass Transfer using Static Mixing Equipment", Sulzer Technical Review, 3, 1977.

8. Wang, K. B. and Fan, L. T., "Mass Transfer in Bubble Columns Packed with Motionless Mixers", Chemical Engineering Science, 33, 7, pp. 945-953, 1978.

9. Holmes, T. L. and Chen, G. K., "Gas-Liquid Contacting with Horizontal Static Mixing Systems", Koch Technical Report, Koch Engineering Company, Inc., June 2, 1981.

10. Landau, J., Boyle, J., Gomaa, H. G., and Al Taweel, A. M., "Comparison of Methods for Measuring Interfacial Areas in Gas-Liquid Dispersions" Canadian Journal of Chemical Engineering, 55, pp. 13-18, February, 1977.

11. Sharma, M. M. and Danckwerts, P. V., "Chemical Methods of Measuring Interfacial Area and Mass Transfer Coefficients in Two-Fluid Systems", British Chemical Engineering, 15, 4, pp. 522-528.

12. Danckwerts, P.V., Gas-Liquid Reactions, McGraw-Hill Co., New York, 1970.

13. Froment, G. F. and Bischoff, K. B., Chemical Reactor Analysis and Design, John Wiley and Sons Co., 1979.

14. Charpentier, J. C., "Mass Transfer Rates in Gas-Liquid Absorbers and Reactors, Advances in Chemical Engineering, Edition by Drew and Vermeulen, Academic Press, 11, pp. 2-133, 1980.

15. Linek, V. and Vacek, V., "Review Article Number 4: Chemical Engineering Use of Catalyzed Sulphite Oxidation Kinetics for the Determination of Mass Transfer Characteristics of Gas-Liquid Contactors", Chemical Engineering Science., 36, 11, pp. 1747-1768.

16. Roberts, D. and Danckwerts, P. V., "Kinetics of CO_2 Absorption in Alkaline Solutions - I", Chemical Engineering Science, 17, pp. 961-969, 1962.

17. Sharma, M. M. and Danckwerts, P. V., "Fast Reactions of CO in Alkaline Solutions - (a) Carbonate Buffers with Arsenite, Formaldehyde, and Hypochlorite as Catalysts (b) Aqueous Monoisopropanolamine (1-amino-2-propanol) Solution", Chemical Engineering Science, 18, pp. 729-735, 1963.

18. Vogel, A.I., Quantitative Inorganic Analysis, 2 edition, Logman, Green and Co., New York, pp. 248-253, 1951.

19. Fischer, R. B. and Peters, D. G., Introduction to Quantitative Chemical Analysis, W. B. Saunders Company, Philadelphia, Pa., p. 98, 1969.

20. Danckwerts, P.V. and Kennedy, A. M., "The Kinetics of Absorption of Carbon Dioxide into Neutral and Alkaline Solutions", Chemical Engineering Science, 18, pp. 1-15, 1958.

21. Wallis, G. B., One-Dimensional Two-Phase Flow, McGraw Hill, Inc., New York, 1969.

22. Butterworth, D., "A Comparison of Some Void-Fraction Relationships for Co-Current Gas-Liquid Flow", International Journal of Multiphase Flow, 1, p. 845, 1975.

23. Cichy, P. T., and Russell, T. W. F., "Two-Phase Reactor Design Tubular Reactors - Reactor Model Parameters", Industrial Engineering and Chemical Design and Development, 61, p. 14, 1969.

24. Hsu, Yung. C., "Gas Holdup and Liquid Recirculation in Gas-Lift Reactors", Doctoral Thesis, Washington University, St. Louis, Mo., 1978.

25. Calderbank, P. H. and Moo-Young, M. B., "The Continuous Phase Heat and Mass-Transfer Properties of Dispersions", Chemical Engineering Science, 16, p. 39, 1961.

26. Mangartz, K. H., and Pilhofer T. H., "Interpretation of Mass Transfer Measurements in Bubble Columns Considering Dispersion of Both Phases", Chemical Engineering Science, 36, pp. 1069-1077, 1981.

27. Hughmark G. H., "Holdup and Mass Transfer in Bubble Columns", Industrial Engineering Chemical Process Design and Development, 6, p. 218, 1967.

28. Higbie R., "The Rate of Absorption of a Pure Gas into a Still Liquid during Short Periods of Exposure", Transactions of American Institute of Chemical Engineers, 31, p. 365, 1935.

29. Nagel, O., Hegner, B. and Kurten, H., "Criteria for the Selection and Design of Gas/Liquid Reactors", International Chemical Engineering, 21, 2, pp. 161-171, April 1981.

30. Nagel, O., Kurten, H., and Sinn, R., Strofaustauschflache und Engergiedissipationsdichte als Auswahlkriterien fur Gas/Flussigkeits-Reaktoren", Chemical Engineering Technology, 44, pp. 899-903, 1972.

31. Alper E., "Measurement of Effective Interfacial Area in a Packed Column Absorber by Chemical Methods", Transactions of Institution of Chemical Engineers, 57, pp. 64-66, 1979.

32. Sahay, B. N. and Sharma, M. M., "Absorption in Packed Bubble Columns", Chemical Engineering Science, 28, 11, pp. 2245-2255, 1973.

33. Charpentier, J. C., "General Characteristics of Multiphase Gas-Liquid Reactors: Hydrodynamics and Mass Transfer", unpublished, Laboratoire des Sciences du Genie Chimique, Nancy, France, 1980.

34. Gokarn, A., Post-Doctoral Researcher with M. Dudukovic at Washington University, Personal Communication, 1982.

9. VITA

Biographical items on the author of the thesis, Mr. John W. Weston, as of May, 1982

1) Born December 10, 1957 in Everett, Washington.
2) Attended Nebraska Wesleyan University from September, 1975 to May, 1978. Received the degree of Bachelor of Science in Chemistry in May, 1979.
3) Attended Washington University from September, 1978 to May, 1980. Received the degree of Bachelor of Science in Chemical Engineering in May, 1980.
4) Began work toward the degree of Masters of Science in Chemical Engineering in September, 1980.
5) Membership in Honor Socities: Phi Kappa Phi, Sigma Pi Sigma and Tau Beta Pi.